FMUC FACULDADE DE MEDICINA
UNIVERSIDADE DE COIMBRA

LOCAL ANESTHETICS AS A NEW THERAPEUTIC APPROACH IN ORAL SQUAMOUS CELL CARCINOMA – AN *IN VITRO* STUDY.

Ana Isabel de Almeida Lopes Ribeiro
Coimbra, 2016

[Dissertação apresentada à Faculdade de Medicina da Universidade de Coimbra para prestação de provas de Mestrado em Patologia Experimental, sob a orientação científica da Professora Doutora Marília Dourado (Faculdade de Medicina da Universidade de Coimbra) e da Drª Ana Bernardino (Centro Hospitalar e Universitário de Coimbra).]

À minha filha,

"The important thing is not to stop questioning. Curiosity has its own reason for existing."

Albert Einstein

AKNOWLEDGMENTS

My deep gratitude to Professor Marília Dourado, for the opportunity I was given to conduct my research, for her guidance and understanding which supported me in the preparation of this work.

My special thanks to Dr. Ana Bernardino for the encouragement and constant example of professionalism and scientific update in anesthesiology.

To Professor Ana Bela Sarmento Ribeiro (Laboratory of Oncobiology and Hematology, Faculty of Medicine, University of Coimbra), for the support and knowledge that enriched the work presented.

A sincere acknowledgement to Dr. Cátia Domingues for her immense dedication and collaboration in the realization of the experimental work.

To Dr. Sílvia Neves for the support in the implementation of this research and the assistance in the interpretation of the experimental results.

To Dr. Ana Cristina Gonçalves for her support in the interpretation of the experimental results and statistical treatment of the work.

To Dr. Raquel Alves for her support in the interpretation of the work and to Dr. Paulo Matafome for having applied the essential technique of western blot.

To Professor Raquel Seiça (Laboratory of Physiology, Faculty of Medicine, University of Coimbra) and Professor Filomena Botelho (Institute of Biophysics, Faculty of Medicine, University of Coimbra) and their team for their contribution for experimental work.

To GAI (Gabinete de Apoio à Investigação) for funding this research project.

To my Family, for all the love, encouragement, solidarity and patience that motivated me and gave me confidence to write this thesis.

TABLE OF CONTENTS

ABSTRACT

Oral squamous cell carcinoma (OSCC) represents the most frequent malignant neoplasia that affects the oral cavity, accounting for more than 90% of cases. The etiology of OSCC is multifactorial and involves intrinsic and extrinsic factors, namely tobacco and alcohol. Besides the new and advanced therapeutic strategies, patients with OSCC show poor survival rates.

Local anesthetics are usually used to control pain in patients with head and neck tumors, but recent reports have been shown that also can inhibit cancer cell proliferation, invasion and migration.

In this work, we proposed to evaluate the potential therapeutic efficacy of the local anesthetics, Lidocaine and Mepivacaine, in *in situ* and metastatic OSCC cell lines, alone and in combination with conventional treatment (Cisplatin, 5-Fluorouracil) and studied the underlying mechanisms, namely their role in cancer invasion and metastization.

For these proposes, two OSCC cell lines were maintained in culture, the HSC-3 (metastatic) and BICR-10 (*in situ*) cells, in absence and in presence of different concentrations of Lidocaine or Mepivacaine in monotherapy (daily or single dose administration) or in association with conventional chemotherapeutic drugs (Cisplatin or 5-Fluorouracil). Cell viability was assessed by the rezasurin assay and cell death by optical microscopy (May-Grünwald-Giemsa staining) and flow cytometry using the Annexin V/Propidium Iodide double staining. The influence of these compounds in cell cycle (Propidium Iodide incorporation), mitochondrial membrane potential (JC-1 probe), caspases (Apostat kit), reactive oxygen species production (hydrogen peroxide and superoxide anion were evaluated by 2,7-Diclorofluorescein and Dihidroetidium, respectively) and in the level of the antioxidant defense reduced glutathione (using Mercury Orange) were performed by flow cytometry. Cell adhesion was evaluated by measure E-chaderin expression, by flow cytometry, and β1-Integrin and β-Catenin expression, by western blot. Cell migration evaluation was realized by measuring basal

expression of matrix metalloproteinases 2 and 9 by flow cytometry, and their proteolytic activity by zymography assay, and, posteriorly, performing the wound healing assay. Results were statistically analyzed.

Our study showed that local anesthetics in monotherapy and in combination with conventional chemotherapy inhibited cell proliferation and migration, and induced cell death mainly by later apoptosis/necrosis in both cell lines in a dose, time, administration schedule and cell type dependent manner, being the HSC-3 the most sensitive relatively to BICR-10. At 48 hours, the IC_{50} of both local anesthetics, in HSC-3 cells, was reached at 4.5 mM, while in BICR-10 cells the IC_{50} was reached with 5,5 mM of Lidocaine and 10 mM of Mepivacaine. These results may be related with the increased in caspases and superoxide anion levels and decreased mitochondrial membrane potential, suggesting the involvement of mitochondria in cell death. The high sensitivity of HSC-3 cells to local anesthetics may be related with the lowest reduced glutathione levels when compared to BICR-10 cells. The pre-G1 peak observed in cell cycle analysis with Lidocaine and Mepivacaine at IC_{50} doses confirms apoptosis. The association of both local anesthetics with chemotherapeutic drugs induced an anti-proliferative effect with blockade of cell cycle, predominantly in S phase. Cell adhesion was not affected significantly by local anesthetics, although we observed a tendency to increase E-cadherin expression levels. Local anesthetics and its association with Cisplatin and 5-Fluorouracil also inhibits cell migration as we observed a decrease in matrix metalloproteinases proteolytic activity (more prominent in metastatic cell line), and a gap in wound healing assay after treatment comparing with the non-treated condition after 24 hours of scratch.

As conclusion, our *in vitro* results showed that Lidocaine and Mepivacaine alone or in combination with conventional chemotherapeutic treatment may constitute a new complementary therapeutic approach in OSCC, namely in metastatic cancer.

Keywords: local anesthetics, oral cancer, cytotoxicity, anti-proliferative effect, migration inhibition, treatment.

RESUMO

O carcinoma espinho-celular é a neoplasia mais frequente da cavidade oral, representando mais de 90% dos casos. A etiologia do carcinoma espinho-celular da cavidade oral (CECCO) é multifatorial, envolvendo fatores intrínsecos e extrínsecos, nomeadamente o consumo de tabaco e álcool. Apesar das novas estratégias terapêuticas, os doentes com CECCO apresentam uma baixa sobrevivência.

Os anestésicos locais são usados para controlo da dor em doentes com cancro da cabeça e pescoço. Estudos recentes mostram que estes também podem inibir a proliferação, invasão e migração de células neoplásicas.

Neste trabalho, propusemo-nos avaliar a eficácia terapêutica dos anestésicos locais (Lidocaína e Mepivacaína) e seus mecanismos, em linhas celulares de CECCO *in situ* e metastático, quer em monoterapia, quer em combinação com quimioterápicos de uso convencional (Cisplatina e 5-Fluorouracilo).

Para cumprir estes objetivos, foram mantidas em cultura duas linhas celulares de CECCO, HSC-3 (metastático) e BICR-10 (*in situ*), na ausência e presença de diferentes concentrações de Lidocaína e Mepivacaína em monoterapia (administração única e diária) e em associação com fármacos quimioterápicos convencionais (Cisplatina e 5-Fluorouracilo). A viabilidade celular foi avaliada pelo teste da resazurina e a morte celular por microscopia ótica (coloração de May-Grünwald-Giemsa) e por citometria de fluxo usando dupla marcação com Anexina V/Iodeto de Propídeo. A influência destes fármacos no ciclo celular (incorporação com Iodeto de Propídeo), no potencial de membrana mitocondrial (sonda JC-1), na expressão de caspases (Apostat kit), na produção de espécies reativas de oxigénio (peróxido de hidrogénio e anião superóxido, através das sondas 2,7-Diclorofluoresceína e Dihidroetideo, respetivamente) e na expressão de glutationa reduzida (pelo Alaranjado de Mercúrio) foi realizada por citometria de fluxo. A adesão celular foi avaliada pela medição da expressão de E-Caderina, por citometria de fluxo, e ainda da expressão das β1-Integrina e β-Catenina, por

western blot. O estudo da migração celular foi realizado pela avaliação da expressão de metaloproteinases da matriz 2 e 9 por citometria de fluxo, e da sua atividade proteolítica por zimografia de gelatina. Posteriormente, foi ainda realizado o teste de *scratch*. Os resultados foram analisados estatisticamente.

O nosso estudo mostrou que os anestésicos locais em monoterapia e em combinação com a terapêutica quimioterápica convencional inibiram a proliferação e migração celulares e induziram morte celular principalmente por apoptose tardia/necrose em ambas as linhas celulares estudadas de uma forma dose, tempo, tipo de administração e tipo celular dependente. As células HSC-3 mostraram-se mais sensíveis a estes efeitos que as células BICR-10. Às 48 horas, os CI_{50} nas células HSC-3 foi de 4,5 mM para ambos os anestésicos locais, enquanto as células BICR-10 atingiram o CI_{50} na concentração de 5,5 mM de Lidocaína e 10 mM de Mepivacaína. Estes resultados podem estar relacionados com o aumento da expressão de caspases e anião superóxido e com a redução do potencial de membrana observados, sugerindo o envolvimento da via mitocondrial da apoptose. A maior sensibilidade das células HSC-3 aos anestésicos locais pode estar relacionada com os níveis mais baixos de glutationa reduzida quando comparada com as células BICR-10. Nas células tratadas com Lidocaína e Mepivacaína na dose de CI_{50}, o pico pré-G1 observado na análise do ciclo celular confirma a indução de morte por apoptose. A associação dos anestésicos locais com os fármacos quimioterápicos induziu um efeito antiproliferativo, com bloqueio do ciclo celular, predominantemente em fase S. Apesar de visível uma tendência para o aumento da expressão de E-Caderina, os anestésicos locais não alteraram significativamente a expressão das moléculas de adesão estudadas. No estudo da migração celular foi verificado que, os anestésicos locais em monoterapia e em combinação com a Cisplatina e 5-Fluorouracilo, levaram a uma redução da atividade proteolítica das metaloproteinases da matriz (efeito mais marcado na linha celular metastática). Foi ainda observado, no teste de *scratch*, uma inibição da migração celular das células tratadas

com os anestésicos locais e sua combinação com quimioterápicos convencionais após 24 horas de incubação.

Como conclusão, podemos referir que o nosso estudo *in vitro* mostrou que tanto a Lidocaína como a Mepivacaína, em monoterapia e em combinação com os fármacos usados na quimioterapia convencional, podem apresentar-se como uma terapêutica nova e complementar no CECCO, nomeadamente no CECCO metastático.

Palavras-chave: anestésicos locais, cancro da cavidade oral, citotoxicidade, efeito antiproliferativo, inibição da migração, tratamento.

FIGURE AND TABLE INDEX

FIGURES

TABLES

ACRONYMS AND ABBREVIATIONS LIST

4EBP1, 4E-binding protein 1

5-FU, 5-Fluorouracil

A, Aggregates

AKT, Protein kinase B

AKTS1, V-akt murine thymoma viral oncogene homolog 1

Anti-hMMP, Anti-human matrix metalloproteinase

AP-1, Activator protein 1

Apaf-1, Apoptotic protease activating factor 1

Apf-1, ATP-dependent proteolysis factor 1

AV, Annexin V

BAD, Bcl-2 antagonist of cell death

BAK, Bcl-2 homologous antagonist/killer

BAX, Bcl-2 associated X protein

BCA, Bicinchoninic

BCL-2, B-cell leukemia/lymphom

BCL-xl, B-cell leukemia extra large

BID, BH3 interacting domain death agonist

BSA, Bovine Serum Albumin

Ca^{2+}, Calcium

$CaCl_2$, Calcium Chloride

CAFs, Tumor-associated fibroblasts

CD95, Cluster differentiation

CDK, Cyclin-dependent kinases

CDKN2A, Cyclin-dependent kinase inhibitor

CECCO, Carcinoma espinho-celular da cavidade oral

CI_{50}, Metade da concentração inibitória máxima

CIS, Cisplatin

COX, Cyclooxygenase

CTL, Control

CXCL1, Chemokine [CXC motif] ligand 1

CXCL8, Chemokine [CXC motif] ligand 8

DCF, Dichlorofluorescein

DHE, Dihydroeidine

DISC, Death-inducing signaling complex

DMEM, Dulbecco´s Modified Eagle´s Medium

DMSO, Dimethyl Sulfoxide

DNA, Deoxyribonucleic acid

E^+, Ethidium

E2F, E2 factor

ECL, Enhanced Chemiluminescence

ECM, Extracellular matrix

EDTA, Ácido etilenodiamino tetra-acético

EGFR, Epidermal growth factor receptor

eIF4E, Eukaryotic translation initiation factor 4E

EMT, Epithelium mesenchymal transition

ERK, Extracellular regulated kinase

FADD, FAS-associated death domain

FAS, Tumor necrosis factor receptor superfamily member 6

FasL, Fas ligand

FBS, Fetal Bovine Serum

FGF, Fibroblast growth factor

FITC, Fluorescein isothiocyanate

G0/G1 phase, Gap 0/Gap 1

G2/M phase, Gap 2/mitotic phase

GDP, Guanine diphosphate

GMCSF, Granulocye-macrophage colony-stimulating factor

Grb2, Growth-factor receptor bound protein 2

GSH, Reduced gluthathione

GTP, Guanine triphosphate

H_2DCF-DA, 2´, 7´- dichlorodihydrofluorescein diacetate

H_2O_2, Peroxides

HIF, Hypoxia-inducible factor

HNC, Head and neck cancers

HtrA2/Omi, High temperature requirement protein A2

IAPs, Inhibitor of Apoptosis Proteins

IC_{50}, Half maximal inhibitory concentration

IL, Inteleukin

Int, Intensity

JC-1, 5,5´, 6, 6´- tethracloro-1, 1´, 3, 3´- tetraethylbenzimidazolcarbocyanine iodide

LA, Local anesthetics

LIDO, Lidocaine

LOH, Loss of heterozygosity genes

LST8, Lethal with Sec Thirteen 8

M, Monomer

M/A, Ratio monomers/aggregates

MAPK, Mitogen Activated Protein Kinases

MEK, MAPK ERK kinase

MEPI, Mepivacaine

Mercury Orange, 1-(4-Chloromercuryphenyl-azo)-2-naphthol

MFI, Mean fluorescence intensity

MMP, Matrix metalloproteinase

MNK, MAPK-interacting kinase

mRNA, Messenger ribonucleic acid

MSK, Mitogen- and stress-activated protein kinase

MT1-MMP, Membrane type 1-matrix metalloproteinase

mTOR, Mammalian target of Rapamycin (mTOR)

mTORC2, Mammalian target of Rapamycin complex 2

Na^+ , Sodium

NaCl, Sodium Chloride

NF-κB, Factor nuclear kappa B

NOTCH1, Notch homolog 1

O_2^-, Superoxide anion

OSCC, Oral squamous cell carcinoma

P, Phosphorus

PBS, Phosphate-Buffered Saline

PDGF, Platelet-derived growth factor

PDK, Phosphoinositide-dependent kinase

PE, Phycoerythrin

PI, Propidium Iodide

PI3K, Phosphatidylinositol-4,5-bisphosphate 3-kinase

PPARɣ, Peroxisome proliferator activated receptors ɣ

pRB, Retinoblastoma protein

PS, Phosphatidylserine

PTEN, Phosphatase and Tensin homolog

PVDF, Nitrocellulose

RAF, Ras function

RAS, Rat sarcoma

Rb, Retinoblastoma

RIPA, Radioimmuno Precipitation Assay

RNA, Ribonucleic acid

RNAse, Ribonuclease

ROS, Reactive oxygen species

RSK, MAPKAP-K1 ou MAPK-activated protein kinase-1

S phase, Synthesis phase

S6K1, Ribosomal protein S6 kinase beta-1

SDS, Sodium dodecyl sulfate

SEM, Standard error of mean

SMAC/DIABLO, Second Mitochondria-Derived Activator of Caspases (Smac)/Direct IAP Binding Protein with low isoelectric point (DIABLO)

SOS, Son of sevenless

STAT, Signal transducer and activator of transcription

TBS-T, Trisbuffered Saline Tween-20

TEMED, 1,2-Bis(dimethylamino)ethane

TGF-β, Transforming growth factor-β

TNF, Tumor necrosis factor

TNFR1, Type 1 TNF receptor

TNF-α, Tumor necrosis factor-α

TP53, Tumor protein p53

TRADD, TNF receptor-associated death domain

TRAIL, TNF related apoptosis inducing ligand

Tris, 2-amino-2-hydroxymethylpropane-1,3-diol

TSC, Tuberous sclerosis complex

VEGF, Vascular endothelial growth factor

α-SMA, α-smooth muscle actin

$\Delta\psi_{mit}$, Mitochondrial membrane potential

1. INTRODUCTION

1.1. Origin of cancer

Cancer is the leading cause of death in economically developed countries and the second leading cause of death in developing countries (Jemal A *et al.*, 2011).

The origin of cancer relies on cancer cell acquired characteristics that enable tumor growth and metastatic dissemination, described by Hanahan D *et al.*, in 2000. These cancer characteristics, resumed in Figure 1, are known as the six hallmarks of cancer: (1) ability to sustain chronic proliferation by promoting proliferative signaling, (2) ability to circumvent powerful programs that negatively regulate cell proliferation, promoting evasion from growth suppressors, (3) ability to resist to cell death, by evolve a variety of strategies to limit or circumvent apoptosis or gaining an advantage by tolerating some degree of necrotic cell death, (4) ability to replicate unlimitedly, leading to immortality, (5) ability to induce angiogenesis, helping sustain expanding neoplastic growths and (6) ability to activate a multistep process of invasion and metastasis (Hanahan D *et al.*, 2000; Hanahan D *et al.*, 2011).

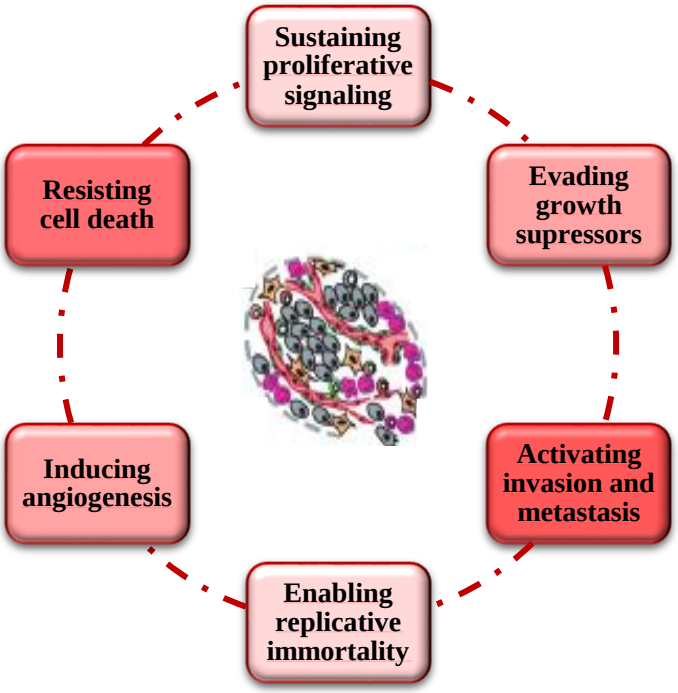

Figure 1 – The six hallmarks of cancer. These hallmarks are proposed by Douglas Hanahan *et al.*, in 2000. (*in* and adapted from Douglas Hanahan *et al.*, 2000, 2011)

In 2011, the same authors suggest that the capability of cell cancer to reprogram cellular metabolism in order to most effectively support neoplastic proliferation and its capability to evade immunological destruction are emerging hallmarks characteristics of cancer cells. Additionally, they proposed that two consequential characteristics of neoplasia facilitate acquisition of all hallmarks: genome instability and mutation and tumor-promoting inflammation (Figure 2) (Hanahan D *et al.*, 2011).

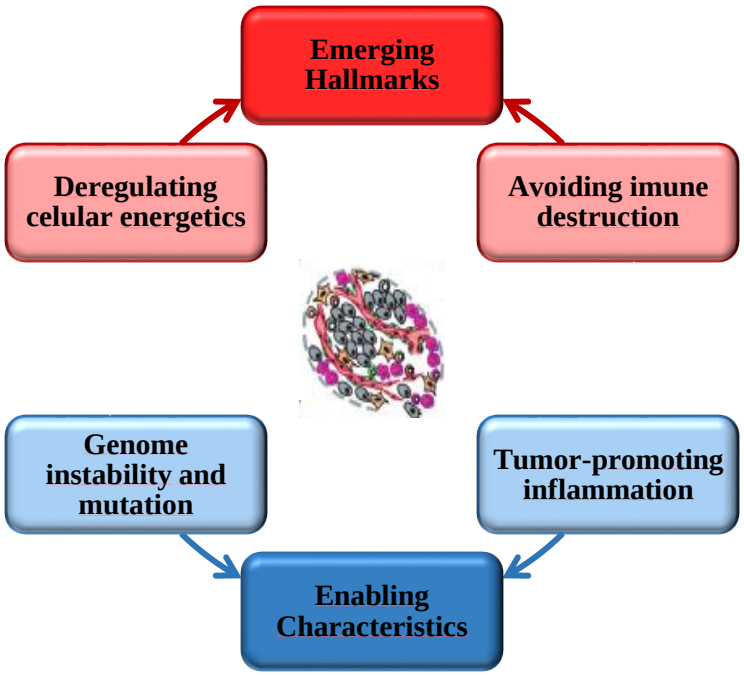

Figure 2 – Emerging hallmarks and enabling characteristics of cancer. These new hallmarks are proposed by Hanahan D *et al.*, in 2011. (*in* and *adapted* from Hanahan D *et al.*, 2011)

Besides cancer cells, the tumor microenvironment has been recognized as an important and complex part of tumorigenesis. Cancer cells are among a heterogeneous set of cell types known to contribute in important ways to the biology of many tumors and to regulatory signaling that controls their individual and collective functions. Some of cell types that intervene in tumor microenvironment are cancer stem cells, endothelial cells, pericytes, immune inflammatory cells, cancer-associated fibroblasts, and stem and progenitor cells of the tumor stroma (Figure 3) (Hanahan D et al., 2011).

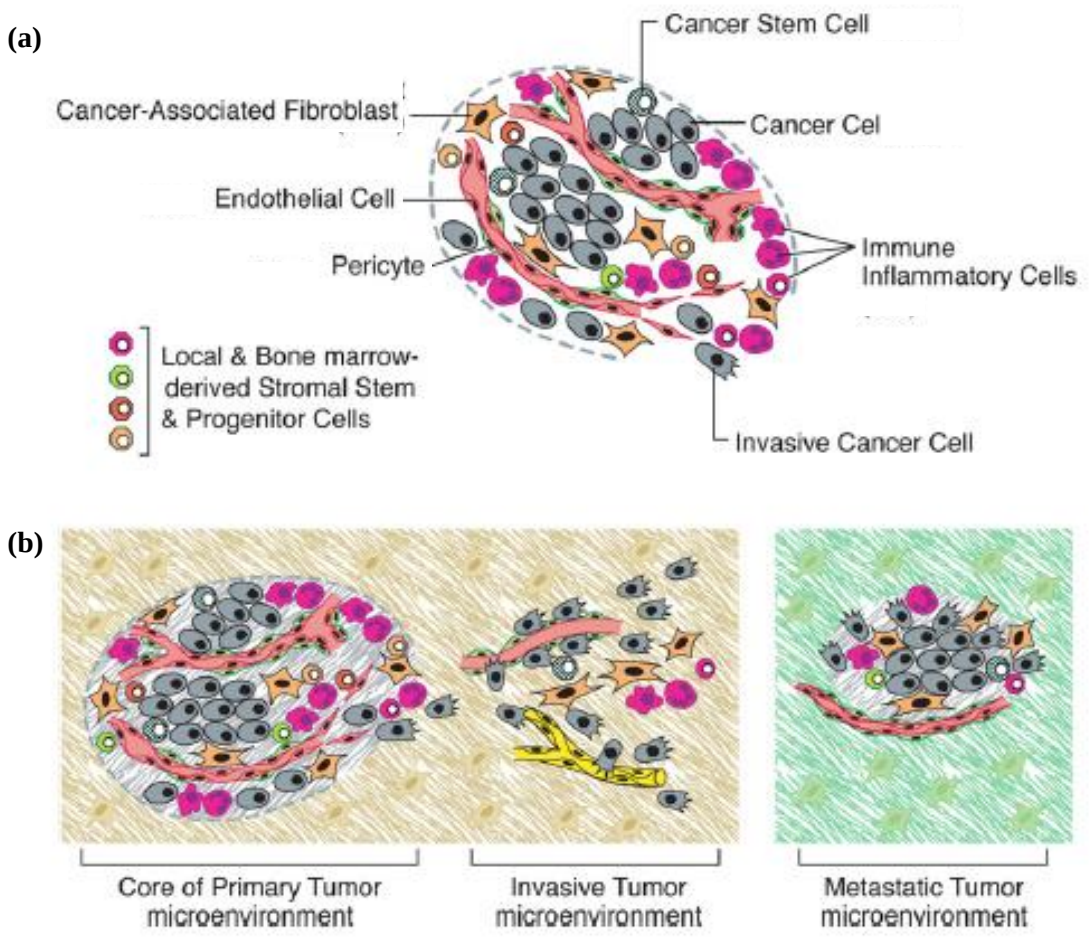

Figure 3 – The cells of the Tumor Microenvironment. (a) Parenchyma and stroma of tumors contain different cell types and subtypes that collectively enable tumor growth and progression. The immune inflammatory cells present in tumors can include both tumor-promoting as well as tumor-killing subclasses. **(b)** The multiple stromal cell types create a succession of tumor microenvironments that change as tumors invade normal tissue, seed and colonize distant tissues. The abundance, histologic organization, and phenotypic characteristics of the stromal cell types, as well as of the extracellular matrix (hatched background), evolve during progression, enabling metastization. (in and adapted from Hanahan D et al., 2011)

1.2. Oral cancer – epidemiology and physiopathology

Oral cancer is a subgroup of head and neck cancers (HNC) that develop at the lips, tongue, salivary glands, gingiva, floor of the mouth, oropharynx, buccal surfaces and other intra-oral locations, according to the International Classification of Diseases (Ram H *et al.*, 2011; Tsantoulis PK *et al.*, 2007). An estimated 263,900 new cases and 128,000 deaths from oral cavity cancer occurred in 2008 (Jemal A *et al.*, 2011), being the sixth most common cancer worldwide (Figure 4) (Ram H *et al.*, 2011).

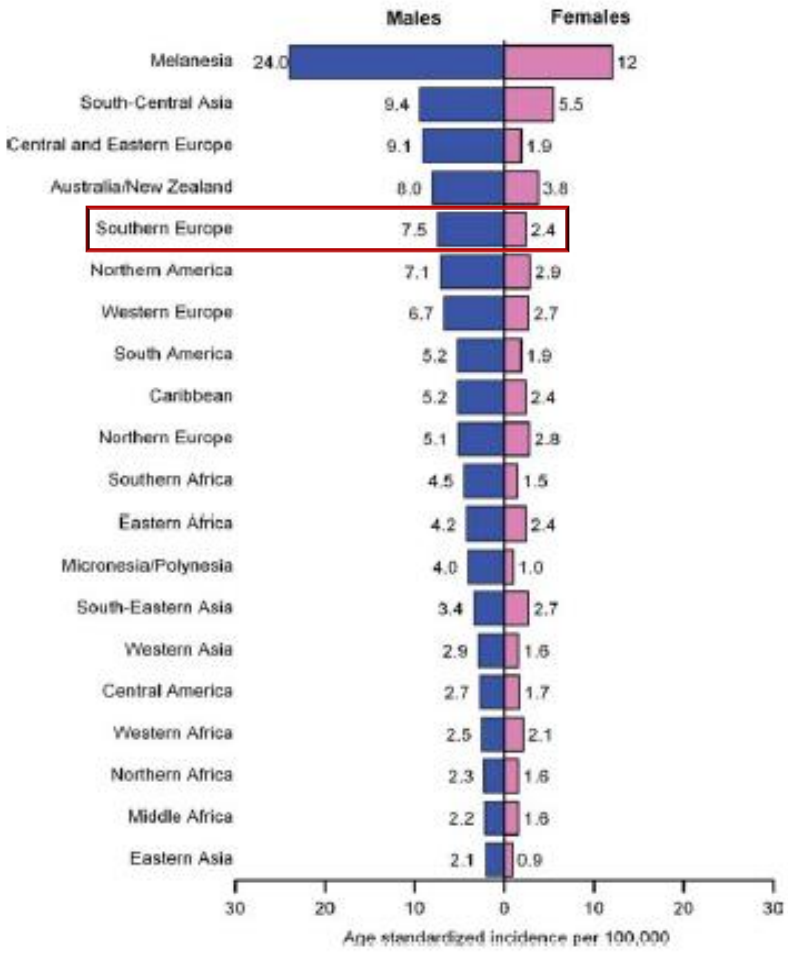

Figure 4 – Age–standardized oral cavity cancer incidence rates by sex and world area. Source: GLOBOCAN 2008. (*in* and adapted from Jemal A *et al.*, 2011)

Oral squamous cell carcinoma (OSCC) is the most common HNC, accounting for more than 90% of all malignant presentations (Ram H *et al.*, 2011; Tsantoulis PK *et al.*, 2007; Lippman SM *et al.*, 2005). OSCC causes great morbidity, and despite therapeutic advances, five-year overall survival rate remains less than 50% in the past 30 years (Lippman SM *et al.*, 2005; Ziober BL *et al.*, 2001).

Tobacco, alcohol, human papillomavirus infections, and ultraviolet radiation are the major risk factors for oral cavity cancer, with tobacco and alcohol having synergistic effects (Rivera C, 2015; Jemal A *et al.*, 2011; Ram H *et al.*, 2011; Tsantoulis PK *et al.*, 2007; Vecchia CL *et al.*, 1997).

Oral carcinogenesis is a complex process that evolves through a multistep process of genetic and epigenetic changes leading to alterations in cell proliferation, adhesion, invasion and metastization pathways (Ram H *et al.*, 2011; Chiang AC *et al.*, 2008; Lippman SM *et al.*, 2005).

Clinical natural history of OSCC development usually involves normal oral mucosa changing to benign hyperplasia, to dysplasia, to carcinoma *in situ* and advanced cancer due to chronical exposition to risk factors, which lead to genetic or epigenetic alterations, with consequent alteration in cell cycle, DNA repair mechanisms, cell differentiation and apoptosis. Genetic alterations occur in *TP53*, NOTCH1 (Notch homolog 1, translocation-associated [Drosophila]), *EGFR* (epidermal growth factor receptor), *CDKN2A* (cyclin-dependent kinase inhibitor 2a), *STAT 3* (signal transducer and activator of transcription 3), *Cyclin D1*, *Rb* (retinoblastoma) and *LOH* (loss of heterozygosity) genes. These alterations culminates in loss of cellular control, allowing acquisition of phenotypic characteristics of invasive cancer cells (showing advantages of adaptability, survival and proliferation above normal oral mucosa cells), and a substantial risk of biologically aggressive cancer (Rivera C, 2015; Tsantoulis PK *et al.*, 2007; Lippman SM *et al.*, 2005). Oncogenic changes contribute to microenvironmental

alterations such as reactive oxygen species (ROS) accumulation, overproduction of cytokines and epithelial mesenchymal transition. Inflammation and hypoxia induces angiogenesis and altered metabolism, with OSCC cell lines using glycolytic and oxidative metabolism to survive and proliferate. Biophysical and biochemical signs of tumor-associated into the extracellular matrix influence the essential characteristics of cancer and are essential for malignancy (Rivera C, 2015).

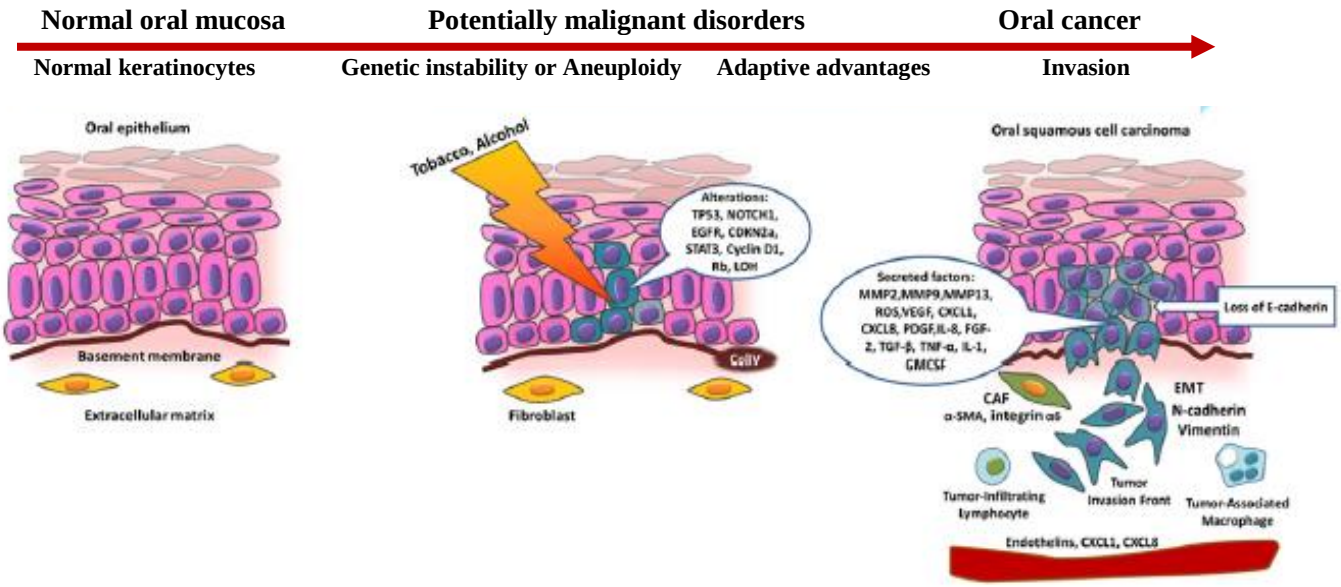

Figure 5 – OSCC multistep carcinogenesis. Normal oral mucosal keratinocytes are chronically exposed to risk factors, which generate genetic instability. Key genetic alterations occurring in *TP53*, *NOTCH1*, *EGFR*, *CDKN2A*, *STAT3*, *Cyclin D1*, *Rb* plus *LOH*. The proliferation and uncontrolled growth, along with adaptive advantages over the surrounding cells, promote local invasion and orchestrate a collaboration of the surrounding stromal cells. Some of the factors secreted by tumor cells are MMP (matrix metalloproteinase)-2, MMP-9, MMP-13, ROS (reactive oxygen species), VEGF (vascular endothelial growth factor), CXCL1 (chemokine [CXC motif] ligand 1), CXCL8 (chemokine [CXC motif] ligand 8), PDGF (platelet-derived growth factor), IL-8 (inteleukin 8), FGF-2 (fibroblast growth factor 2), TGF-β (transforming growth factor-β), TNF-α (tumor necrosis factor-α), IL-1 (inteleukin 1), GMCSF (granulocye-macrophage colony-stimulating factor). This microenvironment promotes cell adhesion loss (ex. E-cadherin) and facilitates epithelium mesenchymal transition (EMT). CAFs (tumor-associated fibroblasts) markers are α-SMA (α-smooth muscle actin) and integrin α6. Endothelins can contribute to pro-migratory paracrine signaling between CAFs and oral cancer cells. It also promotes CXCL1 and CXCL8 endothelial cell proliferation and survival. Endothelial cells produce factors like EGF, which increase migration. (*in* and adapted from from Rivera C, 2015)

1.2.1. Signal transduction pathways and oral cancer

The disruption of several cell signalling pathways involved in cell survival and growth, as the MAPK/RAS/RAF and PI3K/AKT/mTOR pathways, contribute to the development and progression of HNC, in particular oral cancer. These pathways are associated with enhanced expression and activity of EGFR and culminate in cell cycle deregulation as represented in Figure 6 (Safdari Y *et al.*, 2014).

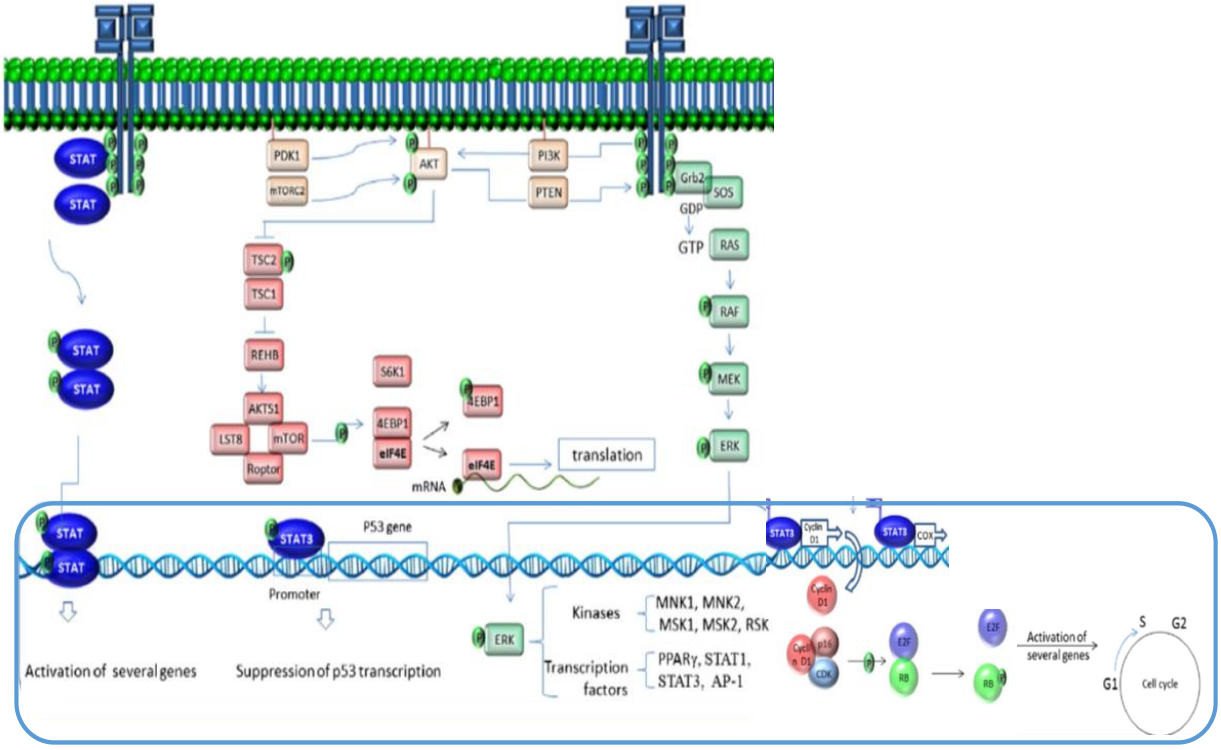

Figure 6 – The MAPK/RAS/RAF and PI3K/AKT/mTOR cell signalling pathways. The activation of these cell signalling pathways leads to phosphorylation of several kinases and activation of a number of transcription factors as eIF4E and STATs. After phosphorylation, STATs are dimerized and translocate into the nucleus, where it activates the expression of several genes mostly involved in cell proliferation. The activation of cyclin D1 and inactivation of RB by phosphorylation leads to E2F activation and cell cycle progression from G1 to S phase. (Adapted from Safdari Y *et al*., 2014)

1.2.2. Apoptosis and oral cancer

During tumor development, uncontrolled cell proliferation is aided by the disablement of cell death responses triggered by specific oncogenes, including evasion of apoptotic cell death (Jain MV *et al.*, 2013; Wong RSY, 2011; Bruin EC *et al.*, 2008). These acquired mutations and associated alterations in signaling pathways in tumor cells that cause increased resistance to cell death are relevant therapeutic targets to treat cancer (Jain MV *et al.*, 2013). Furthermore, apoptosis evasion could contribute to resistance to anti-cancer therapies (Bruin EC *et al.*, 2008).

Apoptosis is an active, specialized and tightly regulated form of cell death, also frequently called programmed cell death, well-orchestrated by a set of hierarchical molecular events (Chaabane W *et al.*, 2013; Jain .MV *et al*, 2013; Wong RSY, 2011; Bruin EC *et al.*, 2008). It can be initiated by two different types of signals: intracellular stress signals (growth factor withdrawal, DNA damage, oxidative stress, and oncogene activation) and extracellular ligands (such as FAS ligand, TNFα or TRAIL) (Bruin EC *et al.*, 2008).

Biochemical changes observed in apoptosis, recognized by phagocytic cells, are activation of caspases, DNA and protein breakdown, and membrane changes (Wong RSY, 2011).

Caspases are a group of enzymes belonging to the cysteine protease family, central to the mechanism of apoptosis as initiators and executioners (Jain MV *et al.*, 2013; Wong RSY, 2011). Activated caspases cleave many vital cellular proteins and break up the nuclear scaffold and cytoskeleton. They also activate DNAases, which further degrade nuclear DNA (Wong RSY, 2011).

There are two main pathways by which caspases can be activated: intrinsic (or mitochondrial), and extrinsic (or death receptor) pathways. They lead to a common pathway that is the executioner phase of apoptosis (Figure 7) (Wong RSY, 2011).

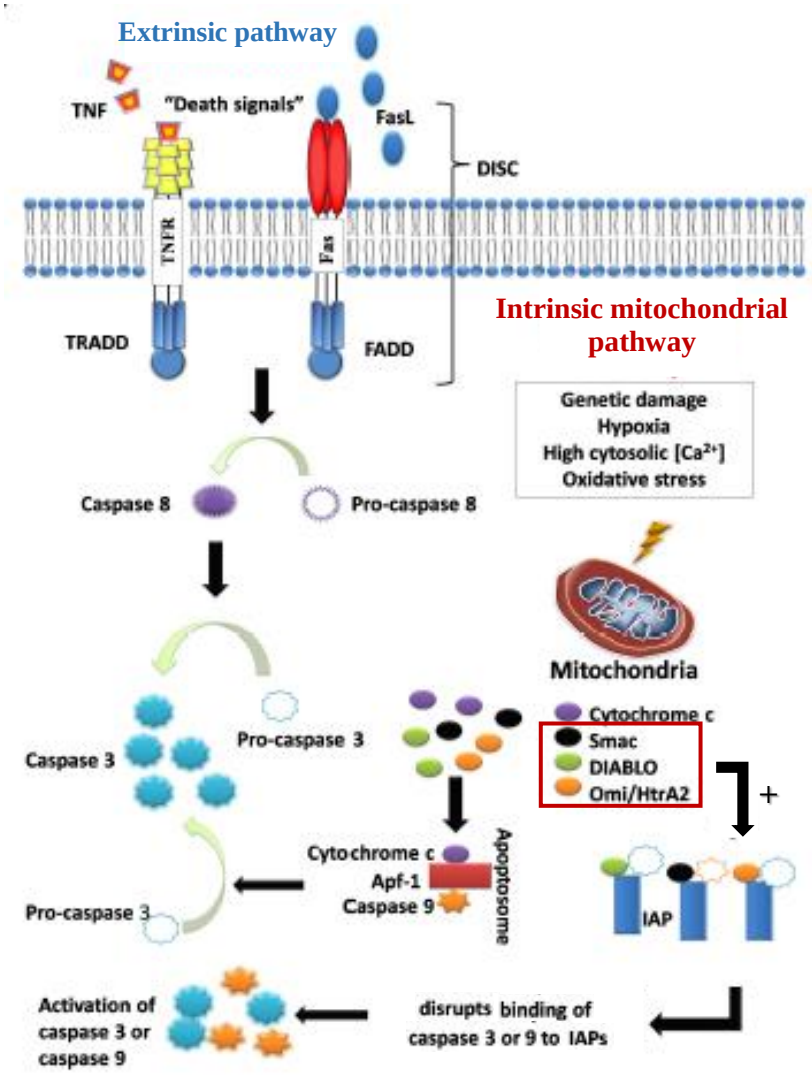

Figure 7 - The intrinsic and extrinsic pathways of apoptosis. (*in* and adapted from Wong RSY, 2011)

The extrinsic death receptor pathway begins when death ligands bind to a death receptors and transmit apoptotic signals (Jain MV *et al.*, 2013; Wong RSY, 2011). Death

receptors are the type 1 TNF receptor (TNFR1) and a related protein called FAS (CD95) and their ligands are called TNF and Fas ligand (FasL), respectively (Wong RSY, 2011). These death receptors have an intracellular death domain that recruits adapter proteins such as TNF receptor-associated death domain (TRADD) and FAS-associated death domain (FADD), as well as cysteine proteases like caspase 8 (Jain MV *et al.*, 2013; Wong RY, 2011; Bruin EC *et al.*, 2008). Binding of the death ligand to death receptor results in the formation of a binding site for an adaptor protein and the whole ligand-receptor-adaptor protein complex is known as the death-inducing signaling complex (DISC) (Wong RSY, 2011; Bruin EC *et al.*, 2008). DISC then initiates the assembly and activation of pro-caspase 8 (Chaabane W *et al.*, 2013; Wong RSY, 2011). The activated form of the enzyme, caspase 8 is an initiator caspase, which initiates apoptosis by cleaving other downstream or executioners caspases, like caspase-3 (Chaabane W *et al.*, 2013; Wong RSY, 2011; Bruin EC *et al.*, 2008; Hsu S *et al.*, 2004).

The intrinsic pathway is initiated within the cell, resulting from an increase in mitochondrial permeability and release of pro-apoptotic molecules, such as cytochrome *c*, into the cytoplasm. This pathway is closely regulated by a group of proteins belonging to the BCL-2 family. There are two main groups of the BCL-2 proteins, namely the pro-apoptotic proteins (e.g. BAX, BAK, BAD, BID) and the anti-apoptotic proteins (e.g. BCL-2, BCL-XL) (Wong RSY, 2011). While the anti-apoptotic proteins regulate apoptosis by blocking the mitochondrial release of cytochrome *c*, the pro-apoptotic proteins act by promoting such release (Wong RSY, 2011; Bruin EC *et al.*, 2008). The multidomain of the proapoptotic BAX and BAK proteins are essential to induce mitochondrial permeabilization by forming pores (Bruin EC *et al.*, 2008). Cytoplasmic release of cytochrome *c* activates caspase-3 via the formation of a complex known as apoptosome which is made up of cytochrome *c*, Apaf-1 and caspase-9 (Wong RSY, 2011).

Both apoptotic pathways lead to activation of the executioner's caspases, -3, -6 and -7, which are the main proteases that degrade the cell. Their activity is kept in check by Inhibitor

of Apoptosis Proteins (IAPs). IAPs themselves are inhibited by the proteins SMAC/DIABLO and the serine protease HtrA2/Omi. These proteins are also released from the mitochondria, possibly simultaneously with cytochrome *c* to alleviate the inhibitory signal and to enhance the apoptotic signal (Bruin EC *et al.*, 2008).

When cells undergo the typical process of apoptosis, morphological alterations can be observed such as chromatin condensation, phosphatidylserine translocation with its exposure on the cell surface, cytoplasmic shrinkage and membrane blebbing, and finally the formation of apoptotic bodies (Bruin EC *et al.*, 2008; Hsu S *et al.*, 2004).

In OSCC, approximately 50% of tumors exhibited dysfunctional p53, leading to the incapacity of cells with damaged genomes to undergo apoptosis, allowing the defective genome to persist and replicate. Chromosomal aberrations and accumulation of mutations in many genes encoding crucial proteins or oncoproteins that control cell growth and apoptosis may also induce neoplastic formation. These genes include those coding for cell cycle regulators (cyclins, cyclin-dependent kinases, CDK, cyclin and CDK inhibitors, p53 and pRB, the retinoblastoma tumor suppressor protein), pro-survival regulators (telomerase, growth factors or their receptors, inhibitors of apoptotic proteins, NF-κB, BCL-2 and BCL-xl), and pro-apoptotic regulators (caspases, BAX, BAK, BID, FAS, TNFα and TRAIL death receptors) (Hsu S *et al.*, 2004).

1.2.3. Angiogenesis and metastization in oral cancer

When primary tumor grows to a certain size, their survival is threatened because nutrients supply by diffusion is inadequate. At this step, tumor cells promote angiogenesis (Lee SY *et al.*, 2011).

Angiogenesis is the formation of new vessels from preexisting ones. It is a crucial step in tumor growth, progression and metastization. Regulation of angiogenesis *in vivo* is complex and is controlled by a variety of factors, as hypoxic stimulus (Chiang AC *et al.*, 2008; Tsautoulis PK *et al.*, 2007). Tumor cells hypoxia results in production of hypoxia-inducible factor (HIF), which causes changes in anaerobic metabolism, angiogenesis, invasion, and survival (Chiang AC *et al.*, 2008). HIF increases VEGF (vascular endothelial growth factor) expression, which plays a dominant role in angiogenesis. VEGF enhanced expression in OSCC promotes its progression by up-regulating microvessel density (Tsautoulis PK *et al.*, 2007).

Primary tumors consist of heterogeneous populations of cells with genetic alterations that allows them to surmount physical boundaries, disseminate, and colonize a distant organ. Metastasis is a succession of these individual processes: invasion of the surrounding tissue, enter in the microvasculature of the lymph and blood systems, survival and translocation through the bloodstream to microvessels of distant tissues, exit from the bloodstream, survival in the microenvironment of distant tissues, and finally adapt to the foreign microenvironment of these tissues in ways that facilitate cell proliferation and formation of a macroscopic secondary tumor (Chaffer CL *et al.*, 2011; Chiang AC *et al.*, 2008).

Cancer cells that evade normal tissue organization become exposed to environmental stresses: lack of oxygen and nutrients, low pH, reactive oxygen species, and mediators of the inflammatory response. For example, HIF expression leads to enhanced cell-matrix adhesion

and invasion related with elevated lysyl oxidase expression, which correlate with shorter metastasis-free survival and with poor prognosis of HNC (Chiang AC *et al.*, 2008).

Cadherins are transmembrane glycoproteins that play the principal role in maintaining physical cell-cell contact, being direct mediators of cell-cell adhesive interactions (Figure 8) (Chiang AC *et al.*, 2008; Thomas GJ *et* al., 2001). To exhibit functional adhesion activity they form complexes with cytoplasmic proteins called catenins (α-, β- and ɣ-catenins). The cadherins and catenins form a single functioning unit, and loss or mutation of any one of the proteins may result in loss of function and perturbation of cell-cell adhesion (Thomas GJ *et al.*, 2001).

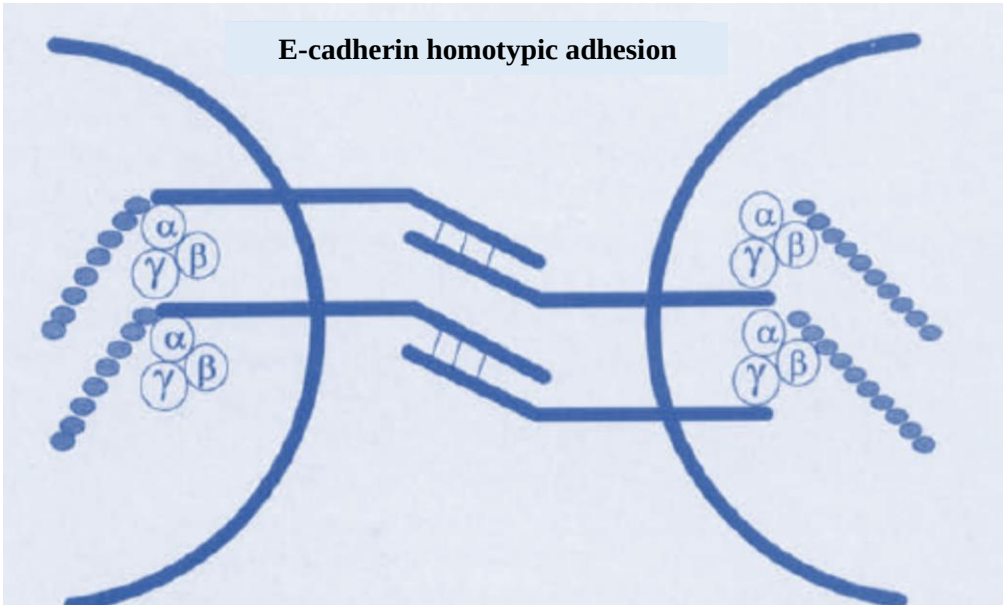

Figure 8 - E-Cadherin function. Cadherin mainly exhibit homotypic adhesion and are responsible in oral epithelium for maintaining contact between keratinocytes. To exhibit functional adhesion activity, cadherins must form complexes with cytoplasmic proteins called catenins (α-, β- and ɣ). (*in* Thomas GJ *et al.*, 2001)

E-cadherin mediates interconnection of epithelial cells and maintenance of the integrity of stratified epithelium (Thomas GJ *et al.*, 2001).

In many tumors with invasive properties, intercellular adhesion is reduced, often because of a loss of E-cadherin. Disruption of the expression of E-cadherin lead to early

invasion and metastasis. Various mechanisms can cause loss of E-cadherin: mutations (inactive protein), gene silencing (methylation), and down-regulation (e.g. by growth factor receptors). It loss contributes to epithelial-to-mesenchymal transition, a process whereby epithelial cells switch to a mesenchymal progenitor-cell phenotype, enabling detachment and reorganization of epithelial-cell sheets during tumor invasion and metastasis (Chiang AC *et al.*, 2008).

In several reports, OSCC show loss of epithelial cell cohesion, and this is often associated with a reduction in E-cadherin expression or function (Thomas GJ *et al.*, 2001). Tumor cells may temporarily uncouple cadherins, thereby permitting distant metastasis to occur. Dysfunction of cadherin-catenin complexes allow dissociation of the invasive cells following stimulation by effectors like integrin-extracellular matrix (ECM) interaction and/or activation by cytokines (Ziober BL *et al.*, 2001).

The ECM serves as a support along which cells attach and move by contacts between cell-surface receptors called integrins and ECM components such as fibronectin, collagen, and laminin (Chiang AC *et al.*, 2008).

Integrins are a family of transmembrane glycoproteins and are the largest family of ECM-adhesion receptors. They are formed by an α and a β subunit which associate in a non-covalent manner to form functional heterodimers (Thomas GJ *et al.*, 2001). They provide a linkage between the cell cytoskeleton and the extracellular environment – having adhesive functions, and are involved in many cell-signaling pathways regulating dynamic processes such as cell growth, apoptosis, angiogenesis, protease production, migration, differentiation, and gene expression – all properties involved in malignant conversion and invasion (Chiang AC *et al.*, 2008; Thomas GJ *et al.*, 2001; Ziober BL *et al.*, 2001).

Often, oral carcinomas show reduced or loss integrin expression, founded in normal epithelium (such as β1, β4 and αv families) and demonstrate *de novo* expression of the αvβ6 integrin in oral dysplasia and cancer, suggesting that this integrin may be important in

promoting a malignant phenotype, include matrix metalloproteinase production, increased cell migration, and increased invasion (Thomas GJ *et al.*, 2001).

Various members of the matrix metalloproteinases (MMP) family are also implicated in cancer-cell invasion (Chiang AC *et al.*, 2008).

The MMP are a family of zinc-dependent endopeptidases, proteolytic enzymes that can decompose ECM components, as collagen, gelatin, elastin, fibronectin, and proteoglycans (Lee SY *et al*., 2011). Their action is crucial during the progression of cancer since they allow the remodelling of the surrounding healthy tissues (basement membranes, vessel or lymphatic duct epithelium) and enable local invasion and metastasis (Lee SY *et al*., 2011; Tsantoulis PK *et al.*, 2007).

It has been demonstrated that gelatinases (MMP-2 and -9), stromelysins (MMP-3, -10 and -11), collagenases (MMP-1 and -13) and membrane-bound MMPs (MT1-MMP) are expressed in OSCC and contributes functionally to its progression (Lee SY *et al*., 2011; Tsantoulis PK *et al.*, 2007).

1.3. New therapies in oral cancer – the role of local anesthetics

Classical treatment of oral cancer relies on surgery, radiation, and chemotherapy or a combination of these methods (Hsu S *et al.*, 2004) and it is not always satisfactory (Tsantoulis PK *et al.*, 2007). Chemotherapeutic drugs, 5-Fluorouracil and Cisplatin, are currently being used for HNC treatment and found to induce specific apoptotic pathways. Drug induced cell damage does not inevitably lead to tumor cell death, in part due to evasion of apoptosis by cancer cells. OSCC cells resistant to one drug may be susceptible to a combination of drugs, due to alternate apoptotic pathways activation (Hsu S *et al.*, 2004). However, they could also develop multidrug resistance. To improve the outcomes of patients it is important to develop new therapeutic targets.

Local anesthetics (LA) had its origin in South America, by natives of Peru, who chewed the leaves of an indigenous plant called *Erythroxylon coca* (Figure 9) (Cox B *et al.*, 2003).

Figure 9 – *Erythroxylon coca*. *(in* http://www.herbmuseum.ca/files/images)

In 1860, the chemist Nieman isolates the active principal of the leaves, resulting an alkaloid named Cocaine. In 1884, Koller reported its successful use for topical anesthesia of the eye. Einhorn reported in 1904 the synthesis of Procaine (aminoester compound) (Figure 10), appearing for the first time in 1905 in an article published by Professor Heinrich Braun.

Although considered to have a good safety profile, some patients and health professionals proved to be highly allergic to it (Calatayud J *et al.*, 2003; Cox B *et al.*, 2003).

In 1943, Nils Löfgren and Bengt Lundquist developed Lidocaine (Figure 10), which was as safety as Procaine, and had stronger effect and less allergic profile. It was introduced in 1948, being the prototype of the amide class of LA. (Hadzic *et al.*, 2012; Cox B *et al.*, 2003) Since Lidocaine´ synthesis, amide-type anesthetic drugs began to be developed, like Mepivacaine synthesized in 1957 by Bo af Ekenstam. (Hadzic *et al.*, 2012; Calatayud J *et al.*, 2003))

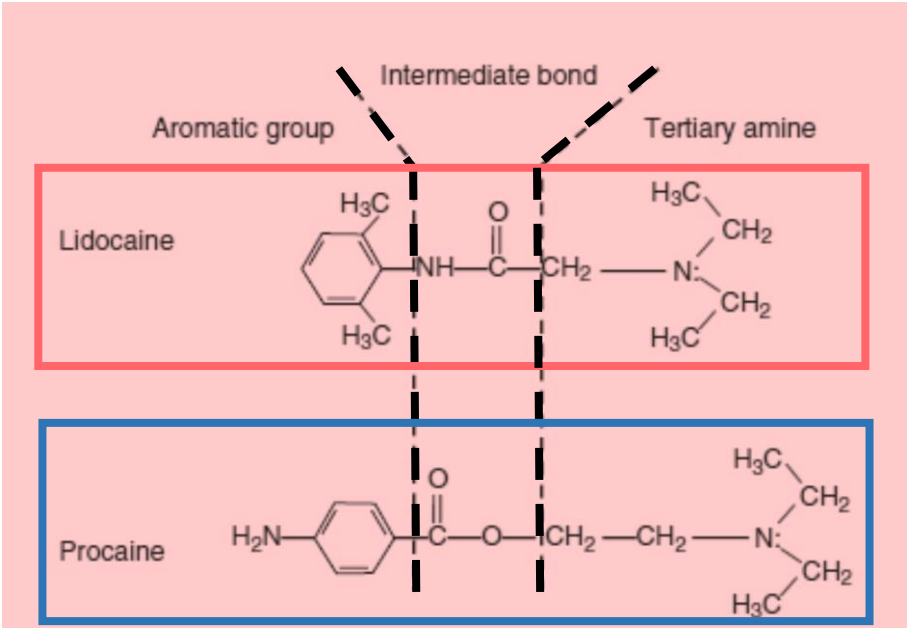

Figure 10 – Structures of two local anesthetics: the aminoamide Lidocaine and the aminoester Procaine. In both groups, a hydrophobic aromatic group is joined to a more hydrophilic base, the tertiary amine, by an intermediate amide or ester bond. (*in* and adapted from Miller *et al.*, 2015)

LA prevent or relieve pain, their principal clinical use, by interrupting nerve conduction (Hadzic *e*t al., 2012). They penetrate as free drug molecules on nerve´s axon membranes and accumulate within the axoplasm (Miller *et al.*, 2015). Binding of LA α subunit of voltage-gated Na^+ channels prevents opening of the channels and influx of Na^+ into the cell by inhibiting the

conformational changes that underlie channel activation, halting the transmission of the advancing wave of depolarization down the length of the nerve (Miller *et al.*, 2015; Hadzic *et al.*, 2012).

Lidocaine is the prototype of the amide class of LA, as mentioned (Figures 10 and 11). It has an intermediate duration (Hadzic *et al.*, 2012). The site of injection influences the absolute amount, as with other agents, but maximum doses of 300mg or 4-5mg/Kg are considered safe (Cox B *et al.*, 2003).

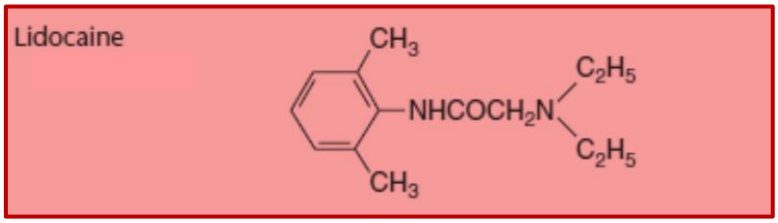

Figure 11 – Chemical structure of Lidocaine. (*in* and adapted from Miller *et al.*, 2015)

Mepivacaine is an intermediate-duration amino amide LA (Figure 12). Its pharmacologic properties are similar to those of Lidocaine (Hadzic *et al.*, 2012). Pharmacological features of Mepivacaine are: its amide structure; its rapid metabolism, which takes place in the liver; and its rapid excretion via the kidneys. Clinically, Mepivacaine shows: short onset time (very similar to that of Lidocaine); intermediate duration and low toxicity. Suggested maximum doses are 300mg or 4-5mg/Kg (Cox B *et al.*, 2003).

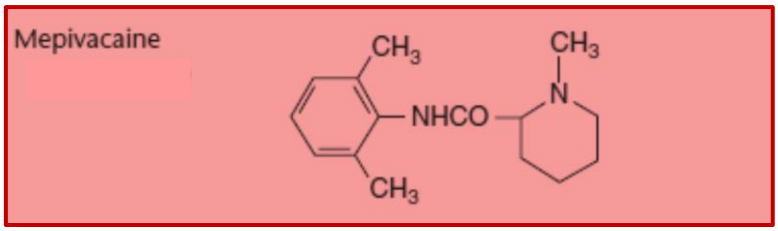

Figure 12 – Chemical structure of Mepivacaine. (*in* and adapted from Miller *et al.*, 2015)

The use of LA for the treatment of pain and cardiac arrhythmias is well established. Several studies have demonstrated that LA are able to interfere with other receptors. These had led to the administration of LA in different settings including postoperative ileus, neuroprotection, decompression sickness, cerebral air embolism, cancer recurrence, and various types of inflammation (Borgeat A *et al.*, 2010).

Decades after the introduction of LA for perioperative analgesia, there are still emerging properties and applications for this class of drugs, namely in cancer (Borgeat A *et al.*, 2010).

1.3.1. Local anesthetics and cancer

Surgical removal is the mainstay treatment of solid tumors (Mao L *et al.*, 2013; Deegan CA *et al.*, 2010; Snyder GL *et al.*, 2010; Yeager MP *et al.*, 2010). However, it is well known that tumor manipulation during surgical resection is associated with increased number of cancer cells in vascular and lymphatic circulations, leading to metastatic spread of the disease (Lirk P *et al.*, 2014; Mao L *et al.*, 2013; Deegan CA *et al.*, 2010; Snyder GL *et al.*, 2010; Yeager MP *et al.*, 2010). Recent studies suggest that perioperative period is a possible therapeutic window for the eradication of micrometastatic cancer (Mao L *et al.*, 2013; Yeager MP *et al.*, 2010).

LA are used for analgesia and local anesthesia in the perioperative period in patients submitted to cancer surgery, including HNC surgery (Kobayashi K *et al.*, 2012; Sakagushi M *et al.*, 2006). In the last years, there are several reports suggesting that LA might have a positive role in cancer treatment by their capacity to inhibit cancer cells proliferation, invasion and migration (Chang YC, Hsu YC *et al.*, 2014; Chang YC, Liu CL *et al.*, 2014; Snyder GL *et al.*, 2010). These effects appear unrelated to their modulation of sodium channels (Chang YC, Hsu YC *et al.*, 2014; Chang YC, Liu CL *et al.*, 2014). So, there is emerging evidence that LA administered in the perioperative period may prevent tumor dissemination during cancer surgery (Lucchinetti E *et al.*, 2012). Many experiments show that LA have antiproliferative or cytotoxic effects on several tumor cells (Chang YC, Liu CL *et al.*, 2014; Chang YC, Hsu YC *et al.*, 2014; Snyder GL *et al.*, 2010; Boselli E *et al.*, 2003) and inhibits invasion of tumor cells (Mammoto T *et al.*, 2002).

Besides, there are evidence of the antiproliferative and cytotoxic properties of local anesthetics in *in vitro* experiments using oral cancer cells (Kobayashi K *et al.*, 2012; Sakagushi M *et al.*, 2006), the therapeutic role of LA in OSCC is not well clarified.

1.4. Aims

This work pretends to evaluate the potential antitumoral effect of lidocaine and mepivacaine, two LA frequently used in anesthetic practice, in OSCC cell lines and their therapeutic effect in association with conventional therapeutic drugs, Cisplatin and 5-Fluorouracil. Although, it pretends also to study the underlying mechanisms behind LA antitumoral effect, namely their role in cancer invasion and metastization.

2. MATERIAL AND METHODS

2.1. Reagents

For culture of the OSCC cell lines were used: Cisplatin (Sigma-Aldrich); Dulbecco´s Modified Eagle´s Medium (DMEM) with 4500 mg/L Glucose, L-Glutamine, Sodium Pyruvate and 25 mM HEPES plus 10% (v/v) Fetal Bovine Serum (FBS) and 1% of Penicillin/Streptomycin (all Biowest products) Solution; 5-Fluorouracil (Sigma-Aldrich); Hydrocortisone (Sigma-Aldrich); Lidocaine Hydrochloride (B|Braun); Mepivacaine Hydrochloride (B|Braun); Phosphate-Buffered Saline (PBS) (Sigma-Aldrich); Trypsin-EDTA Solution (Biowest).

For OSCC cell lines studies the following reagents were used: Acetic Acid (Sigma-Aldrich); Acetone (Sigma-Aldrich); Acid Sodium Dodecyl Sulfate (SDS) (Sigma-Aldrich); Annexin V conjugated with Fluorescein isothiocyanate (FITC) (Immunostep); Anti-hMMP-2-FITC (R&D Systems); Anti-hMMP-9-PE (Phycoerythrin) (R&D Systems); Anti- Human E-Cadherin C-terminal Recombinant protein (BD Pharmingen); Anti-goat Antibody (1:5000, Invitrogen); Anti-mouse Antibody (1:5000, Bio-Rad); ApoStat kit (R&D Systems); β-Catenin (1:1000, BD transduction laboratories); β1-Integrin (1:1000, BD transduction laboratories); Bovine Serum Albumin (BSA) (Sigma-Aldrich); Bromophenol Blue (Sigma-Aldrich); $CaCl_2$ (Sigma-Aldrich); Calnexin (1:1000, SICGEN); ClorAcrylamide (Sigma-Aldrich); Comassie Brilliant Blue (Sigma-Aldrich); Dihydroeidine (DHE) (Invitrogen); Dimethylformamide (Sigma-Aldrich); Dimethyl Sulfoxide (DMSO) (Sigma-Aldrich); Enhanced Chemiluminescence (ECL) Substrate (Bio-Rad); Fixation and Permeabilization Solutions Intracellular Kit (Immunostep); Gelatin from porcine skin Type A (Sigma-Aldrich); Giemsa solution (Sigma-Aldrich); Hydrochloric (Sigma-Aldrich); May-Grünwald solution (Sigma-Aldrich); Propidium Iodide (Immunostep); Propidium Iodide/RNAse solution (Immunostep); Radioimmuno Precipitation Assay (RIPA) Buffer supplemented with complete Mini and

PhosSTOP (Roche, Sigma-Aldrich); Resazurin salt (Sigma-Aldrich); Trisbuffered Saline Tween-20 (TBS-T) (Sigma-Aldrich); Triton X-100 (Merck Millipore); 1,2-Bis(dimethylamino)ethane (TEMED) (Sigma-Aldrich); 1-(4-Chloromercuryphenyl-azo)-2-naphthol (Mercury Orange) (Sigma-Aldrich); 2-Acrylamido-2-methyl-1-propanesulfonic Acid Sodium Salt Solution (AMPS) (Sigma-Aldrich); 2-amino-2-hydroxymethylpropane-1,3-diol (Tris) base (Sigma-Aldrich); 2´, 7´- dichlorodihydrofluorescein diacetate (H_2DCF-DA) (Invitrogen); 5,5´, 6, 6´- tethracloro-1, 1´, 3, 3´- tetraethylbenzimidazolcarbocyanine iodide (JC-1) (Invitrogen).

2.2. Cell line culture conditions

The human HSC-3 cell line was offered by PhD Maria Conceição Pedroso Lima (Center of Neuroscience and Cell Biology, University of Coimbra, Portugal). It was obtained from tongue squamous cell carcinoma of a 64 year-old man, and it has a high metastatic potential, with lymphatic invasion.

HSC-3 cell line were maintained in High-Glucose - DMEM supplemented with 10% FBS (v/v), L-glutamine 2mM, HEPES 25 mM, and penicillin 100U/mL and streptomycin 100µg/mL, at 37ºC in a humidified incubator containing 5% CO_2.

The human cell line BICR-10 was acquired from European Collection of Cell Cultures (ECACC). It was obtained from an oral mucosae in situ squamous cell carcinoma from a Caucasian female.

BICR-10 cell line was maintained in High-Glucose - DMEM supplemented with 10% FBS (v/v), L-glutamine 2mM, HEPES 25 mM, hydrocortisone 0,4 µg/mL and penicillin 100U/mL and streptomycin 100µg/mL at 37ºC in a humidified incubator containing 5% CO_2.

For subsequent studies, cells were washed with PBS and detached with trypsin-EDTA solution for 5 to10 minutes at 37ºC. Detached cells were transferred into a centrifuge tube and harvested by centrifuging at 100 xg for 5 minutes and resuspended in growth medium. Cells were grown in 5% of CO_2 concentration atmosphere and at a temperature of 37ºC at an initial density of 75000 cells/cm^2.

2.2.1. Cell line culture with local anesthetics and conventional chemotherapeutic drugs

The OSCC cell lines, HSC-3 and BICR-10, were maintained in culture as previously described, in absence and in presence of increasing concentrations of local anesthetics (LA), Lidocaine or Mepivacaine in monotherapy (single dose vs daily dose administrations) and in association with conventional chemotherapeutic drugs (Cisplatin or 5-Fluorouracil) for 72 hours, as seen in **Table 1**.

Table 1 – Drug treatment conditions of BICR-10 and HSC-3 cell lines for 72 hours.

LOCAL ANESTHETICS MONOTHERAPY - SINGLE DOSE ADMINISTRATION -		
	BICR-10 cell line	**HSC-3 cell line**
LIDO (mM)	0 to 8	0 to 5
MEPI (mM)	0 to 10	0 to 5
LOCAL ANESTHETICS MONOTHERAPY - DAILY DOSE ADMINISTRATION -		
	BICR-10 cell line	**HSC-3 cell line**
LIDO (mM)	2 (cumulative)* 2 (medium extraction)'	2 (cumulative)* 2 (medium extraction)'
MEPI (mM)	2 (cumulative)* 2 (medium extraction)'	2 (cumulative)* 2 (medium extraction)'
LOCAL ANESTHETICS ASSOCIATED WITH CONVENTIONAL CHEMOTHERAPEUTIC DRUGS		
	BICR-10 cell line	**HSC-3 cell line**
LIDO (mM)	2	2
MEPI (mM)	2	2
CIS (µM)	10	2,5
5-FU (µM)	50	2,5
LIDO (mM) + CIS (µM)	2 + 10	2 + 2,5
MEPI (mM) + CIS (µM)	2 + 10	2 + 2,5
LIDO (mM) + 5-FU (µM)	2 + 50	2 + 2,5
MEPI (mM) + 5-FU (µM)	2 + 50	2 + 2,5

*,administration of Lidocaine/Mepivacaine at 2mM each day without medium extraction; ‘, administration of Lidocaine/Mepivacaine 2mM each day with daily medium extraction; LIDO, Lidocaine; MEPI, Mepivacaine; CIS, Cisplatin; 5-FU, 5-Fluorouracil.

2.3. Cell viability evaluation by Resazurin Assay

Cell viability was assessed by resazurin assay each 24h, during 72h and the IC_{50} (drug inhibition concentration to attaint 50% of cell viability) was calculated.

Alamar blue is a colorimetric/fluorimetric assay that quantifies indirectly *in vitro* cell viability by determination of metabolic activity. When resazurin (oxidized form of Alamar Blue) is added to the cell culture, viable cells reduce resazurin into resofurin (reduced form of Alamar Blue) changing color from non-fluorescent indigo blue to fluorescent pink (Perrot S *et al*, 2003; Gonçalves AC, Barbosa-Ribeiro A *et al*, 2013).

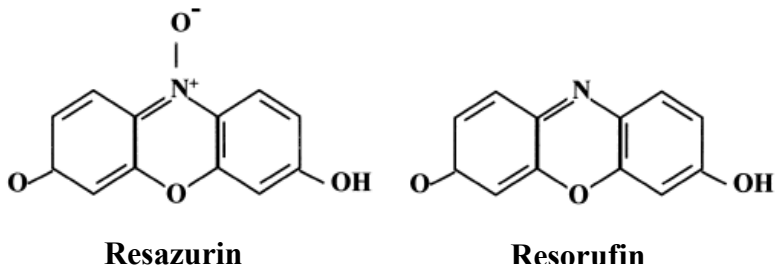

Resazurin Resorufin

Figure 13 – Resazurin and resorufin chemical structures. Resazurin (non-fluorescent indigo blue) is converted in resorufin (fluorescent pink) by acceptance of electrons. (Adapted from O´Brien J *et al*, 2000)

Resazurin salt (0,1mg/ml in PBS) was diluted to 10% (v/v) in DMEM and this solution was added to the cells and one well was used for a negative control. After incubation for 2 hours at 37°C in a humidified atmosphere with 5% CO_2, withdraw from 100 µL of each well to a 96-well plate proceeded to the reading of absorbance in a spectrophotometer at the wavelength of 570 nm and 600 nm (BioTek). Cell viability is determined as a percentage relative to control cells (untreated cells) using the formula:

$$\frac{[(A_{570} - A_{600})Sample] - [(A_{570} - A_{600})Blank]}{[(A_{570} - A_{600})Control] - [(A_{570} - A_{600})Blank]} \text{ X } 100$$

Results were expressed as percentage of cell viability.

2.4. Cell death evaluation

BICR-10 and HSC-3 cell death was assessed under the conditions described above by optical microscopy, using May-Grünwald-Giemsa staining for morphologic characteristics evaluation, and by flow cytometry using Annexin V and Propidium Iodide double staining. Also, cell death mechanisms characterization was performed by the evaluation of caspase activity, mitochondrial membrane potential, reactive oxygen species production and reduced glutathione levels using flow cytometry.

2.4.1. Evaluation of type of cell death by Optical Microscopy and Flow Cytometry

2.4.1.1. Optical Microscopy

May-Grünwald-Giemsa stain method was used to assess morphologic characteristics of cell lines by optical microscopy (Houwen B, 2000), identifying the different nuclear and membrane alterations of the cell death type.

Smears were prepared from BICR-10 and HSC-3 cell lines, previously incubated for 48 hours under conditions described above. 5x10^4 cells were centrifuged at 300 xg for 5 minutes, washed with PBS and re-suspended with FBS for smears preparation (Dacie J *et* al, 1995; Houwen B, 2000). For May-Grünwald-Giemsa stain, previously obtained smears were stained with May-Grünwald solution (prepared with 0.3% of methanol and diluted to 1:1 with distilled water) for 3 minutes. Then Giemsa solution (1 g Giemsa stain dissolved in 66 mL of glycerol and 66 mL of methanol; diluted to 1:8 with distilled water) was added during 15 minutes. After that, smears were washed with distilled water and dried. Cellular morphology were analyzed by optical microscopy and photographed. Equipment used was a Nixon Eclipse 80i equipped with a Nikon Digital Camera DXm 1200F.

2.4.1.2. Flow Cytometry

The morphological changes typical of apoptosis, loss of integrity of the plasma membrane and breakdown of nuclear DNA, provide several features that permit recognition of apoptotic cell death that are associated with changes in distribution of plasma membrane phospholipids. In live cells, plasma membrane phospholipids are asymmetrically distributed between inner and outer leaflets of the plasma membrane and phosphatidylserine (PS) is almost

exclusively observed on the inner surface of the membrane. Early in apoptosis there is a breakdown of this asymmetry and PS undergoes translocation to the external leaflet of the plasma membrane. Annexin V (AV), a Ca^{2+}-dependent anticoagulant protein, has high affinity for negatively charged PS and when conjugated with a fluorochrome can be used as a marker to identify apoptosis. On the other hand, Propidium Iodide (PI) (red fluorescence), enters membrane permeable cells and intercalate in DNA, emitting fluorescence. Viable cells are AV negative and PI negative, early apoptotic cells are AV positive but PI negative, and late apoptotic cells as well as necrotic cells are positive for both AV and PI.

After drug treatments in the above conditions, BICR-10 and HSC-3 cells were stained simultaneously with AV, labelled with the fluorescent probe FITC and with PI using the manufacturer´s recommended protocol. Therefore, incubated cells were collected and washed twice with ice-cold PBS (centrifuged at 500 xg for 5 minutes), after which were resuspended in 100 µL of binding buffer (AV - binding buffer) and incubated with 5µl of AV-APC solution and 2µL of PI solution for 15 minutes in the dark. After incubation time, cells were diluted in 400 µL of ice-cold binding buffer, and analyzed by flow cytometry (Gonçalves AC, Alves V *et al*, 2013; Gonçalves AC, Barbosa-Ribeiro A *et al*, 2013, Dourado M *et al*, 2007). Flow cytometry analyses were performed using a FACSCalibur™ flow cytometer (Becton Dickinson) equipped with an argon ion laser emitting at 488 nm. The fluorescence of AV-FITC and PI was evaluated at 530 and 610 nm, respectively.

For each assay, $1x10^{\wedge 6}$ cells were used and at least 10.000 events were collected by acquisition using *CellQuest* software (Becton Dickinson) and analyzed using a *Paint-a-Gate* software (Becton Dickinson). The results as percentage of viable, apoptotic and necrotic cells.

2.4.2. Analysis of cell death mechanisms by Flow Cytometry

2.4.2.1. Caspases expression levels by Flow Cytometry

The expression levels of caspases were evaluated by ApoStat kit (R&D Systems) that detects intracellular caspases. After drug treatments in the above conditions, BICR-10 and HCS-3 cells were washed, resuspended in 1 mL PBS and incubated for 15 minutes at room temperature with 5 µL ApoStat. Then, cells were washed in 2 mL PBS (centrifuged at 1000 xg for 5 minutes) and resuspended in 400 µL of the same buffer.

Caspase expression detection were assessed by flow cytometry, using equipment described above, at an emission wavelength of 519 nm and excited wavelength of 488 nm, using argon laser. At least 10.000 events were collected by acquisition using *CellQuest* software (Becton Dickinson) and analyzed using a *Paint-a-Gate* software (Becton Dickinson). Results were expressed in mean fluorescence intensity (MFI) for basal caspase expression in both OSCC cell lines, and normalized to control when comparing caspase expression levels in cells incubated with drugs cited above.

2.4.2.2. Reactive oxygen species intracellular production by Flow Cytometry

Production of reactive oxygen species is one of the mechanisms implicated in anti-proliferative effect induced by local anesthetics (Eliana Lucchinetti *et* al, 2012). Reactive oxygen species (ROS) production was determined by oxidation of 2´, 7´-dichlorodihydrofluorescein diacetate (H_2DCF-DA), for analysis of intracellular expression of peroxides (H_2O_2), and dihydroeidine (DHE), for analysis of intracellular expression of superoxide anion (O_2^-) (Mendes F *et al*, 2015).

H_2DCF-DA probe enter cells and accumulates in the cytosol, where it is deacetylated by esterases to dichlorofluorescin (DCFH). This nonfluorescent product is converted by ROS into de-esterified dichlorofluorescein (DCF) that has strong fluorescence at 525nm when excited at 488nm (Halliwell B *et al*, 2004).

BICR-10 and HSC-3 cells cultured with drugs as described above, were incubated with 5 µM of H_2DCF-DA for 30 minutes, at 37ºC in the dark. Cells were then washed with PBS by centrifugation for 5 minutes at 300 xg, resuspended in 400 µL of PBS and fluorescence was detected by flow cytometer FACSCalibur™ (Becton Dickinson) equipped with argon laser and an excitation wavelength of 525nm was used. At least 50.000 cells were collected by acquisition using *CellQuest* software (Becton Dickinson) and analyzed using a *Paint-a-Gate* software (Becton Dickinson).

DHE passes through cell membranes, where it is oxidized by O_2^- originating ethidium (E^+), which is retained in the nucleus, mixing with the DNA. E^+ is a fluorescent compound with emission wavelength of 610 nm and excitation wavelength of 520 nm (Gomes A *et al*, 2005).

OSCC cell lines were treated with drugs as described earlier. Then they were incubated with 2 µM of DHE (diluted previously with DMSO) during 15 minutes, at 37ºC in the dark. Cells were then washed with PBS by centrifugation for 5 minutes at 300 xg, resuspended in 400 µL of PBS and fluorescence was detected by flow cytometer FACSCalibur™ (Becton Dickinson) equipped with argon laser and an excitation wavelength of 610nm was used. At least 50.000 cells were collected by acquisition using *CellQuest* software (Becton Dickinson) and analyzed using a *Paint-a-Gate* software (Becton Dickinson).

Results of ROS analysis were expressed in MFI for basal expression in both BICR-10 and HSC-3 cell lines, and normalized to control when comparing effect on ROS production in cells incubated with LA and chemotherapeutic drugs.

2.4.2.3. Reduced glutathione levels by Flow Cytometry

For analysis of Gluthathione (GSH) levels was used fluorescent compound mercury orange. Mercury orange reacts faster with GSH than with sulfhydryl groups of proteins, emitting intense red fluorescence when excited at a wavelength of 488 nm with an argon laser, making it suitable for flow cytometric determination of GSH (O´Connor JE *et al*, 1988; Hedley DW *et al*, 1994).

After drug treatment as described before, OSCC cell line were washed by centrifugation with PBS for 5 minutes at 300 xg, being then resuspended in 1 mL of same buffer. Cells were incubated with 40 µM of mercury orange (diluted previously with acetone) for 15 minutes, at 37ºC, and at dark. After incubation, cells were washed with PBS (centrifuged at 300 xg for 5 minutes) and resuspended in 400 µL of the same buffer. Fluorescence was detected by flow cytometry at an excitation wavelength of 620 nm, using equipment described previously. Results are expressed in MFI for basal expression of GSH in both OSCC cell lines, and normalized to control when comparing effects on GSH expression in cells incubated with drugs referred above.

2.4.2.4. Mitochondrial membrane potential evaluation by Flow Cytometry

A decrease in mitochondrial membrane potential is one of the earliest events in apoptosis (Yuan-Ching Chang, Yi-Chiung Liu *et al*, 2014). Mitochondrial membrane potential ($\Delta\psi_{mit}$) integrity was evaluated using fluorescent probe JC-1, a lipophilic cationic dye (Mendes F *et al*, 2015), which accumulates inside mitochondria. When mitochondrial membrane was depolarized (reduction of $\Delta\psi_{mit}$), JC-1 probe stays at cytosol as monomer (M) emitting green-

fluorescence at wavelength of 525nm. When $\Delta\psi_{mit}$ increases, JC-1 monomers enter in mitochondria forming aggregates (A) that emit red-fluorescence at wavelength of 590 nm. The ratio between green and red fluorescence, ratio monomers/aggregates (M/A), provides an estimate of $\Delta\psi_{mit}$ (Yao L *et al*, 2008; Gonçalves AC, Alves V *et al*, 2013). After drug treatment, as described above, at least $5x10^{\wedge 5}$ cells were washed with PBS (centrifugation at 300 xg during 5 minutes) and resuspended in 1 mL of the same solution. Resuspended cells were incubated, at 37ºC for 15 minutes, with 5µg/ml JC-1 (prepared previously with DMSO). Then, cells were washed with PBS (centrifugation at 300 xg for 5 minutes), resuspended in 400 µL of PBS and analyzed by flow cytometry. The results were expressed as JC-1 M/A MFI ratio for basal expression in both OSCC cell lines, and normalized to control when comparing cells incubated with drugs previously referred.

2.5. Cell cycle analysis by Flow Cytometry

To evaluate the anti-proliferative effect of cells cultured with LA and chemotherapeutic drugs, we evaluated the cell cycle by the DNA quantification, identifying the different cell cycles phases – G0/G1, S and G2/M. PI, a fluorogenic compound that binds to nucleic acids, being fluorescence emission proportional to the DNA content of a cell (Riccardi C *et* al, 2006). Quiescent and G1 cells have one copy of DNA and therefore have 1X fluorescence intensity. Cells in G2/M phase of the cell cycle have two copies of DNA and accordingly have 2X intensity. Since the cells in S phase are synthesizing DNA their fluorescence values are between 1X and 2X populations. This technique also identify apoptotic cells. They display a broad hypo diploid (sub-G1) peak, which is discriminated from narrow peak of cells with normal (diploid) content in the red fluorescent channels. Necrotic cells can also display some degrees of DNA fragmentation, resulting in hypo diploid nuclei (Riccardi C *et al*., 2006).

The cells were plated into six well culture plates and maintained in culture with local anesthetics in monotherapy and in association with conventional chemotherapeutic drugs for 48 hours. After the incubation period, cells were detached using a scraper and centrifuged at 300 xg during 5 minutes. Thereafter, the ethanol 70% were added to fix the cells for 30 minutes at 4°C and washed two times with PBS 1x. Then, 200 µL of PI/RNAse solution was added to the cells and analyzed in flow cytometry at 640 nm wavelength. The cells were analyzed using Modfit DNA analysis software. The results were expressed in % of cells in different cell cycle phases.

2.6. Analysis of cell adhesion by Western Blot Assay and Flow Cytometry

2.6.1. Expression of E-Cadherin by Flow Cytometry

E-cadherin expression were analyzed in OSCC cell lines cultured at conditions described above. Basal and after drug treatment levels of E-Cadherin in both cells populations was determined by flow cytometry using Intracell kit (Immunostep) as described before. The monoclonal antibody used was 5 µL of anti-E-Cadherin-PE. Cells were washed twice with PBS, resuspended in the same solution and fluorescence was analyzed by FACSCalibur™ (Becton Dickinson) flow cytometer equipped with argon laser. The emission and excitation wavelength used were, respectively, 578 and 480 nm. 10.000 cells were acquired with *CellQuest* software (Becton Dickinson) and results were analyzed with *Paint-a-Gate* software (Becton Dickinson). Results are expressed in MFI for basal expression of E-Cadherin analysis in both OSCC cell lines, and normalized to control when comparing effects of drugs referred above in E-cadherin expression in BICR-10 and HSC-3 cell lines.

2.6.2. Expression of β1-Integrine and β-Catenin by Western Blot Assay

To determine the expression of Integrin β1 and β-Catenin in BICR-10 and HSC-3 cell lines, the cells were cultured as described above for 48 hours.

Protein extracts were prepared on ice using a solution of RIPA buffer supplemented with complete Mini and PhosSTOP. After sonication and centrifugation at 14000 g, samples were kept at −80 °C prior use. Supernatants were collected, centrifuged and protein concentration was determined using the bicinchoninic (BCA) method (Pierce). 40 µg of each protein samples were separated by SDS-PAGE and electrotransferred to nitrocellulose (PVDF) membranes (Santos K *et al.*, 2014). Membranes were blocked with TBS-T solution (25 mM Tris-HCl, 150 mM NaCl, 0.1% Tween, pH 1⁄4 7.6) supplemented with 5% BSA. Membranes were incubated overnight at 4º C with the respective primary antibodies β-Catenin (1:1000); β1-Integrin (1:1000); Calnexin (1:1000) and during 2 hours at room temperature with the secondary antibodies anti-mouse (1:5000) and anti-goat (1:5000). Membranes were incubated with enhanced chemiluminescence (ECL) substrate and revealed using the VersaDoc system (Bio-Rad). Membrane analysis was performed using the *Image Quant* software (Molecular Dynamics). The results are expressed in percentage of β1-Integrine and β-catenin expression relative to control.

2.7. Cell migration evaluation

2.7.1. Basal expression of matrix metalloproteinases (MMP-2 and MMP-9) by Flow Cytometry

MMP-2 and MMP-9 basal expression levels in OSCC cell lines were analyzed by flow cytometry, using monoclonal antibodies labelled with fluorescent probes. For MMP-2 was used anti-hMMP-2-FITC and for MMP-9 the anti-hMMP-9-PE. For each OSCC cell line, $5x10^{\wedge 5}$ cells were washed with PBS by centrifugation at 300 xg for 5 minutes. 100 µL of fixative solution (Solution A, Immunostep Intracellular Kit) were added to the cell pellet, and cells were incubated for 15 minutes, at dark, and at 37ºC. Then, cells were washed with PBS (centrifuged during 5 minutes at 300xg) and incubated for 15 minutes, in dark at 37ºC with 100µL permeabilization solution (Solution B, Immunostep Intracellular Kit). Cells were washed again with PBS and centrifuged. Posteriorly, it was added to cell pellet 5 µL of anti-hMMP-2-FITC and 5 µL of anti-hMMP-9-PE. Cells were washed twice with PBS, resuspended in the same solution and fluorescence was analyzed by FACSCalibur™ flow cytometer equipped with argon laser. The emission and excitation wavelength used were 519 and 495 nm, for antibodies conjugated with FITC. For antibodies conjugated with PE, emission and excitation wavelength used were, respectively, 578 and 480 nm. 10.000 cells were acquired with *CellQuest* software and results were analyzed with *Paint-a-Gate* software. Results are expressed in MFI.

2.7.2. Matrix metalloproteinases proteolytic activity by Zymography Assay

Proteolytic activity of MMP-2 and MMP-9 were analyzed by gelatin zymography.

MMP-2 and MMP-9 are both gelatinases (a group of MMP family) that are extremely efficient in hydrolyzing denatured collagen I (gelatin). This characteristic led to development of a technique to detect their presence in biological samples, gelatin zymography. This technique identifies gelatinolytic activity in biological samples (Hu X *et al.*, 2010; Toth M *et al.*, 2001).

Solutions containing MMPs are loaded into a polyacrylamide gel containing sodium dodecyl sulfate (SDS) and gelatin. The sample buffer increase sample viscosity, provide a tracking dye (bromophenol blue – monitor of sample migration), provide denaturing molecules and control pH of the sample (Hu X *et al.*, 2010). The electrophoresis of the samples are done under nonreducing conditions to maintain enzymatic activity (Toth M *et al.*, 2001). The proteins distance of migration is inversely correlated with their molecular weight. SDS is removed from the gel by Triton X-100 (Hu X *et al.*, 2010). Samples are incubated with a calcium-containing buffer and partially renatured enzymes can now degrade the gelatin leaving a cleared zone that can be detected after staining the gel (Toth M *et al.*, 2001). The clearer the band, the more concentrated proteases (MMP-2 and MMP-9) it contains. Band staining intensity can then be determined by densitometry, allowing samples comparison (Hu X *et al.*, 2010).

OSCC cell lines were seeded in 6 well plates and were grown in complete medium as described previously for 24 hours until cells formed a confluent monolayer. Then, the medium was removed and the cell monolayer was washed twice with PBS. After, a new conditioned culture medium without FBS was added with different concentrations of LA and conventional chemotherapeutic drugs, alone and/or in association, and were incubated. Supernatant of each sample was collected and kept at −80 °C prior use. Samples were eluted in 1:1 of 1×

nonreducing SDS loading buffer. Samples were subjected to SDS-PAGE in 8% polyacrylamide gels containing 0.1% gelatin. Following electrophoresis at 4ºC, gels were washed in renaturation buffer (2.5% Triton X-100 in 50 mM Tris–HCl (pH 7.5), 150 mM of NaCl, 5 mM of $CaCl_2$) for 1 h in an orbital shaker. Then the zymograms were incubated for at 37°C during 24 and 48 hours for BICR-10 and HSC-3 cells, respectively, in incubation buffer (50 mM Tris–HCl (pH 7.5), 150 mM of NaCl, 5 mM of $CaCl_2$). Gels were then stained with Coomassie blue (Comassie Brilliant Blue at 0,25%, Methanol at 50% and Acetic Acid at 10%), and agitated for 15 minutes. Then, gel was washed with bidistilled water and added to destaining solution (Methanol at 25%, Acetic Acid at 5%). Areas of enzymatic activity appeared as clear bands over the dark background. The gel was analyzed by Gel Doc, in *Quantity One* software (Bio-Rad). Results were expressed in Intensity (Int)/mm^2 and were control normalized.

2.7.3. Cell migration by Wound Healing Assay

Cell migration was studied by scratch assay. On a confluent cell monolayer is created an artificial gap, "scratch". The cells on the edge of the gap will move toward the opening to close the "scratch" until new cell-cell contacts are again established. Images are captured at the beginning and during cell migration, and then compared to determine the rate of cell migration (Liang CC *et al.*, 2007).

For this wound assay, BICR-10 and HSC-3 cells were seeded in 24 well plate and were grown for 24 hours until cells formed a confluent monolayer. Then, the cell monolayer was scraped with a sterile p200 pipet tip. Debris were removed by washing cells twice with PBS. Then, a new culture medium was added with different concentrations of LA and conventional chemotherapeutic drugs, alone and/or in association, and were incubated. Wound healing (images of the scratched areas under each condition) was documented by photography immediately after scratch creation (time 0 hours), at 8, 12 and 24 hours. For images analysis of percentage of scratched open area, it was used *TScratch* software (developed by Koumoutsakos group, CSE Lab at ETH Zurich) (Gebäck T *et al.*, 2008). Results were expressed as percentage of scratch open area and normalized to control.

2.8. Statistical analysis

Results were expressed in mean ± standard error of mean (SEM). Statistical analysis was performed using *GraphPad Prism 7* software. Groups were compared by analysis of variance (ANOVA) with Dunnett´s (to compare every mean to a control mean) and Tukey´s (to compare every mean with every other mean) *post hoc* tests to compensate for multiple comparisons. Statistical significance was set at $p < 0,05$, $p < 0,01$, $p < 0,001$, and $p < 0,0001$.

3. RESULTS

3.1. Evaluation of cell viability of BICR-10 and HSC-3 cell lines treated with local anesthetics

To study Lidocaine and Mepivacaine effects in BICR-10 and HSC-3 cell lines viability and proliferation, we proceeded to resazurine assay, as described in material and methods section.

The Figures 14 and 15 show that both local anesthetics (LA) induced a cytotoxic effect in OSCC cell lines, dependent on the dose, time, cell type and schedule of drug administration.

The HSC-3 cells showed a higher sensitivity to both LA, being the IC_{50} (dose to attain 50% of viability reduction) at 48 hours around 4,5 mM for both Lidocaine and Mepivacaine, and at 72 hours around 3 mM for the same local anesthetics (Figure 14-b). Otherwise, BICR-10 cells presented a reduction in 50% of their viability at 48 hours around 5,5 mM for Lidocaine, and 10 mM for Mepivacaine. At 72 hours, in BICR-10 cells, the IC_{50} was obtained for Lidocaine at 4,5 mM, and Mepivacaine at 9 mM (Figure 14-a).

To study if different administrations schemes interfere with cytotoxic effect of Lidocaine and Mepivacaine in both OSCC cell lines, we incubated BICR-10 and HSC-3 cells with both local anesthetics at lower doses (2 mM), administrated each 24 hours. In one set of experiments, we removed the medium, and in another, we maintained it. The results were presented in Figure 15.

We observed that, in BICR-10 cells daily administration of Lidocaine or Mepivacaine with medium removal led to a cell proliferation, more pronounced with Lidocaine. On the other hand, the daily administration of 2 mM of Lidocaine without medium removal led to a decrease in cell viability about 10% at 72 hours of incubation, with no benefit relative to Lidocaine at 6 mM in single administration that presented a decrease in 75% of cell viability. When cells were treated with Mepivacaine we assisted to a slightly proliferation of BICR-10 cells relative to control, more pronounced at 48 hours, and no cytotoxic effect (Figure 15-a).

In HSC-3 cells we observed that administration of low doses of LA without medium removal induced a more cytotoxic effect than when medium was removed. The cytotoxic effect of 2 mM daily administration of both LA, Lidocaine and Mepivacaine, demonstrated to be inferior at 48 hours of incubation (about 20% of reduction in cell viability) when compared with single administration of 4 mM of both LA, where we saw a reduction in cell viability about 45% (Figure 15-b).

To evaluate if there is a synergistic effect between LA and drugs used in conventional chemotherapy we tested the association of low doses of Lidocaine and Mepivacaine (2 mM) with Cisplatin and 5-Fluorouracil at doses less than those used in monotherapy. As presented in Figure 16-b, in HSC-3 cells, all associations of LA with chemotherapeutic drugs show a synergistic effect, as we observed a more pronounced cytotoxic effect when cells are treated with the drugs in combination compared with chemotherapeutic drugs alone. In BICR-10 cells (Figure 16-a), the same was seen for associations of Lidocaine with Cisplatin and 5-Fluorouracil, but not for associations where Mepivacaine were present. In contrary, in the association of Mepivacaine with Cisplatin a proliferative effect is observed in BICR-10 cells (Figure 16-a).

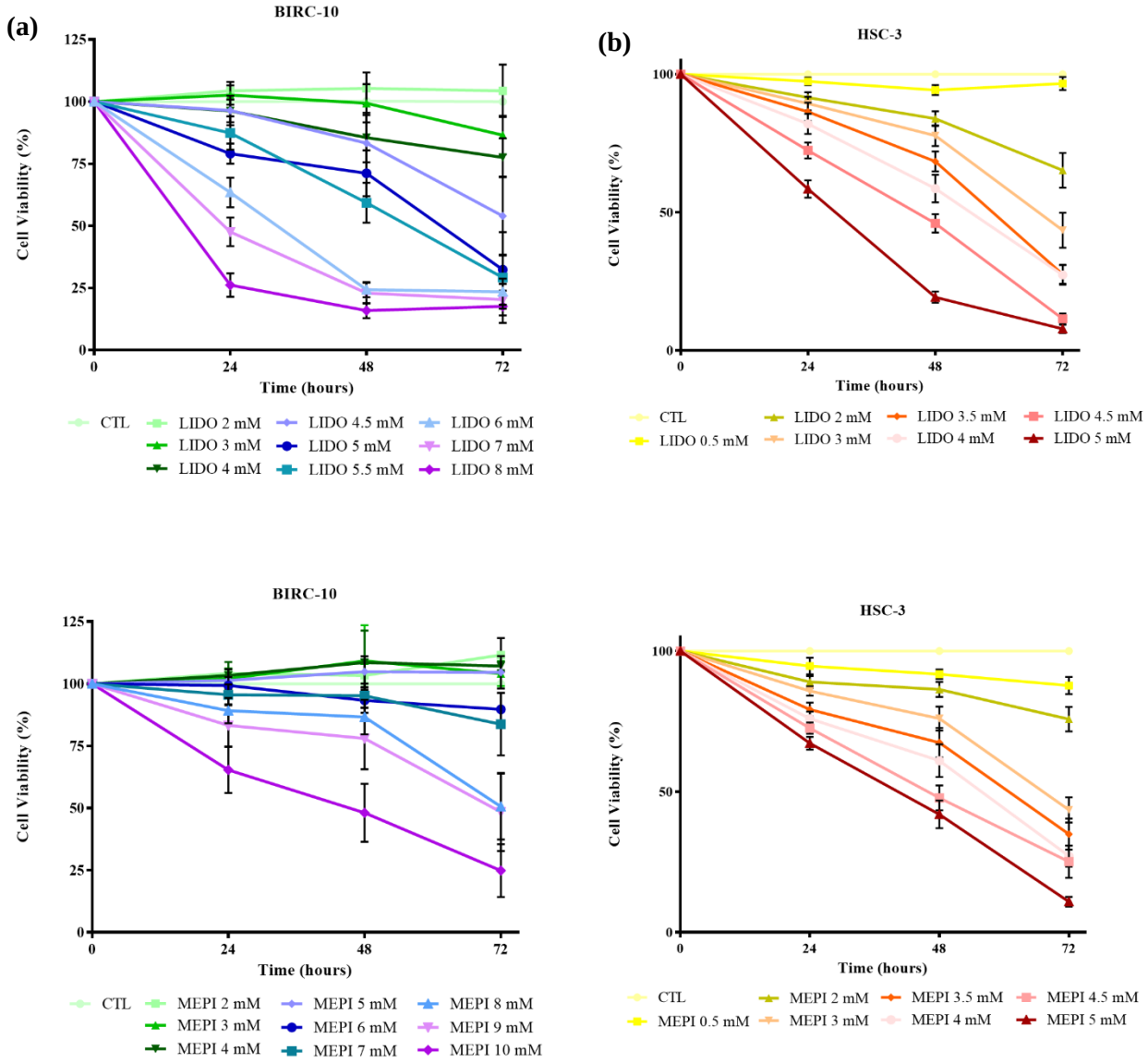

Figure 14 – Effect of Lidocaine and Mepivacaine in (a) BICR-10 and (b) HSC-3 cell lines viability. Cells were incubated with different doses of local anesthetics for 72 hours as represented in the Figure. At each 24 hours of incubation, cells were collected and viability were evaluated with resazurine assay, as described in material and methods section. Results are expressed as percentage of cells, and represented mean ± SEM of 2 to 12 independent experiments. CTL, Control; LIDO, Lidocaine; MEPI, Mepivacaine.

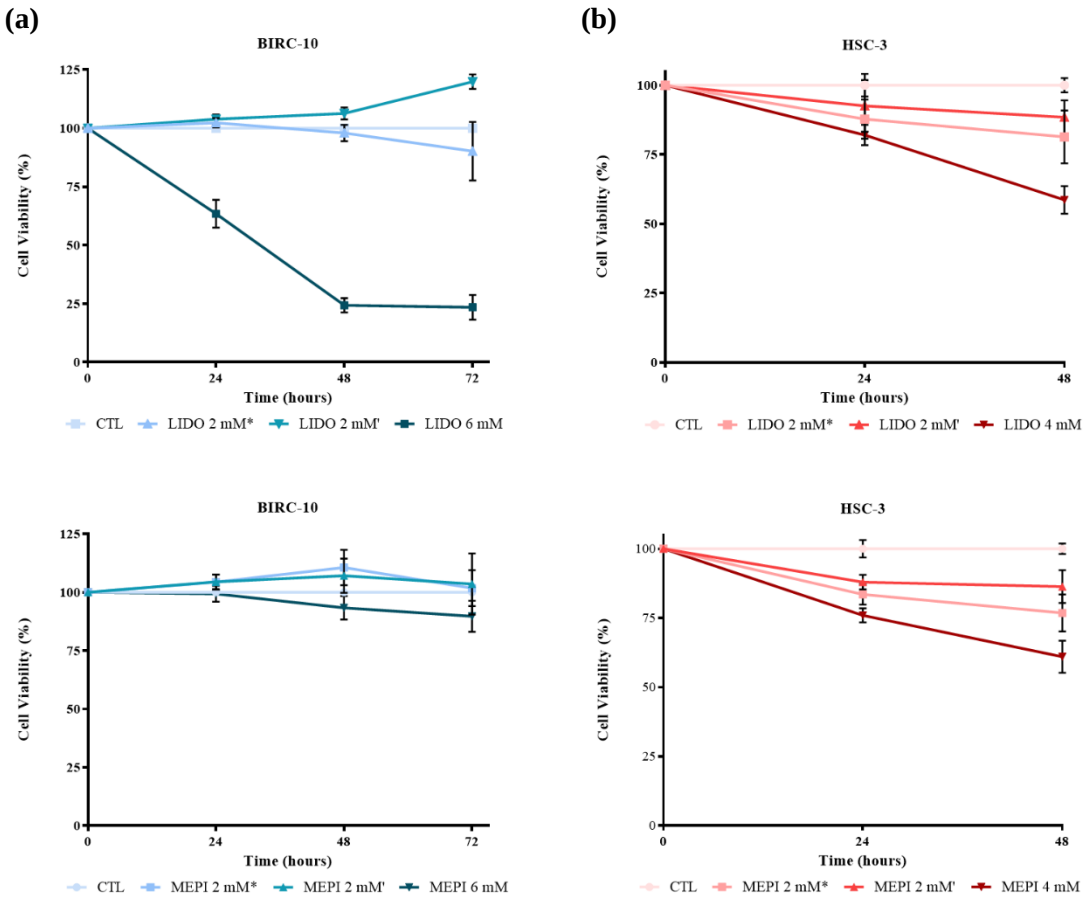

Figure 15 – Effect of daily administration of Lidocaine and Mepivacaine in (a) BICR-10 and (b) HSC-3 cell lines viability. BICR-10 cells were incubated for 72 hours, and HSC-3 cells for 48 hours with local anesthetics at concentrations referred in the legends, representing * without medium removal, and ‘ with medium removal. Each 24 hours of incubation, cells were collected and viability analyzed by the resazurine assay, as described in material and methods section. Results are expressed in percentage of cells, and represented mean ± SEM of 2 to 12 independent experiments. CTL, Control; LIDO, Lidocaine; MEPI, Mepivacaine.

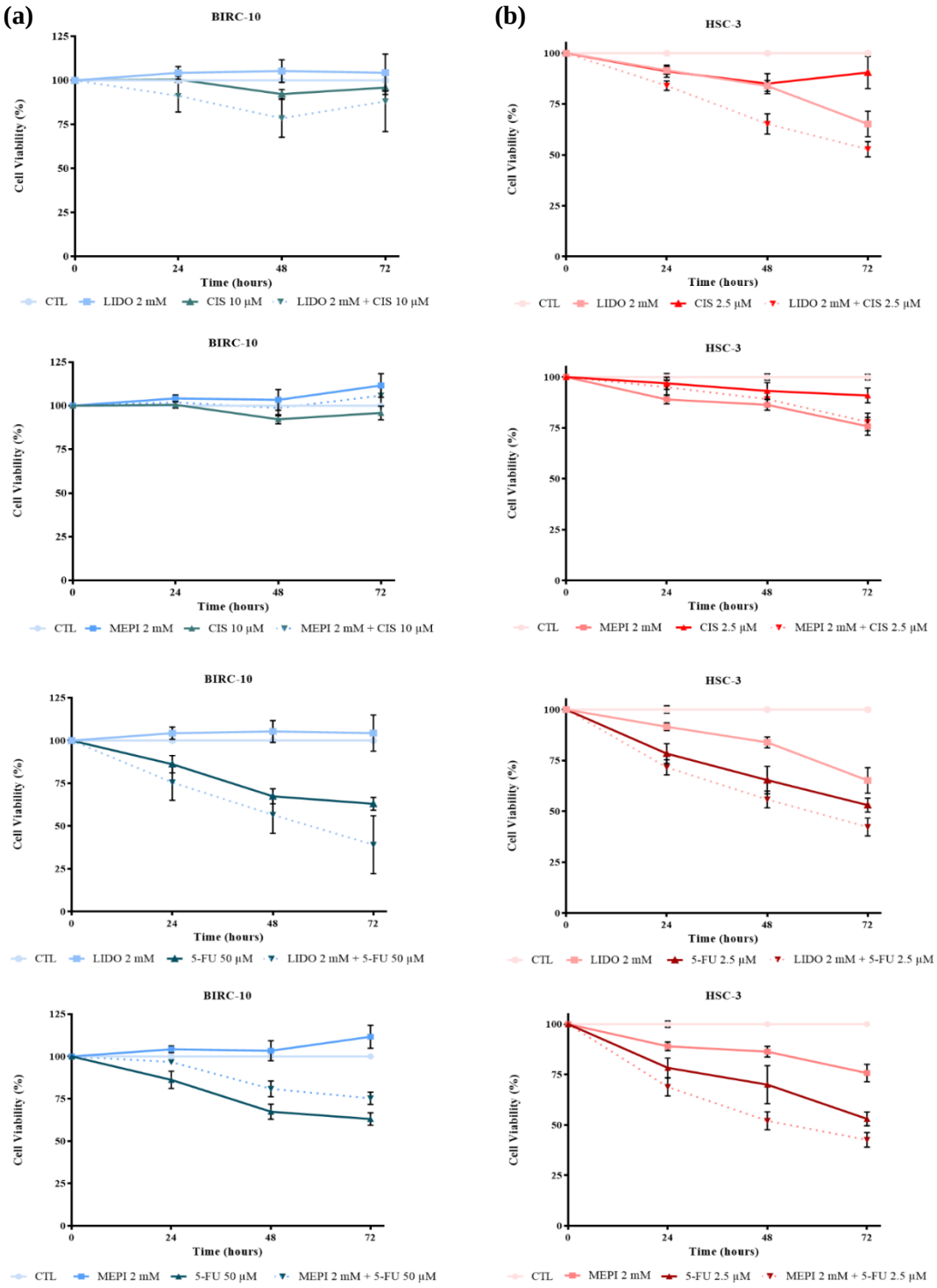

Figure 16 – Effect of the associations of Lidocaine and Mepivacaine with Cisplatin and 5-Fluorouracil in (a) BICR-10 and (b) HSC-3 cell lines viability. Cells were incubated for 72 hours with drugs in the combinations and concentrations referred in the legends. Each 24 hours of incubation, cells were collected and cell viability were analyzed by the resazurine assay, as described in material and methods section. Results are expressed in percentage of cells, and represented mean ± SEM of 2 to 12 independent experiments. CTL, Control; LIDO, Lidocaine; MEPI, Mepivacaine; CIS, Cisplatin; 5-FU, 5-Fluorouracil.

3.2. Evaluation of cell death induced by local anesthetics in BICR-10 and HSC-3 cell lines

The type of cell death induced by local anesthetics, Lidocaine and Mepivacaine, in monotherapy and in association with Cisplatin and 5-Fluorouracil (conditions described earlier at material and methods section), in OSCC cell lines were analyzed by flow cytometry and confirmed by optical microscopy.

Flow cytometry

The cytotoxic effect of local anesthetics in different conditions specified above, were analyzed by flow cytometry using Annexin V (AV) and Propidium Iodide (PI) double staining (Figure 17). This method distinguish viable from death cells and identifies the type of cell death induced by a drug, apoptosis and/or necrosis. Figure 17 represents the effects in cell viability and type of cell death in BICR-10 cells incubated for 48 hours with Lidocaine at 5,5 mM and Mepivacaine at 9 mM, in monotherapy and with the same local anesthetics at 2 mM in association with Cisplatin at 10 µM and 5-Fluorouracil at 50 µM.

The results showed that there is a reduction in cell viability after incubation with all represented conditions relative to control. However, only in BICR-10 cells treated with Mepivacaine 9 mM (viable cells: 67,69 ± 9,875) and Mepivacaine associated with Cisplatin (viable cells: 69,62 ± 8,277), the results are statically significant ($p < 0,01$). The association of Mepivacaine and Cisplatin (viable cells: 69,62 ± 8,277) showed more cytotoxic effect than Cisplatin alone (viable cells: 80,81 ± 3,782). The associations of both Lidocaine and Mepivacaine with 5-Fluorouracil showing no benefit as these drug combinations (viable cells of 82,69 ± 2,028, $n = 3$; and 83,17 ± 1,498, respectively) had less cytotoxic effect than 5-Flourouracil alone (viable cells: 79,78 ± 1,535).

In the conditions referred above, the decrease in cell viability is accompanied by an increase in cell death, predominantly by late apoptosis/necrosis. The effect is dose dependent. Mepivacaine at 9 mM showed the higher percentage of cells in late apoptosis/necrosis of all conditions relative to control ($p < 0,05$).

Although, the type of cell death in BICR-10 cells remained predominantly by late apoptosis/necrosis, the association of local anesthetics with Cisplatin and 5-Fluorouracil, also induce an increase in cells in necrosis when compared with chemotherapeutic drugs alone (Figure 17).

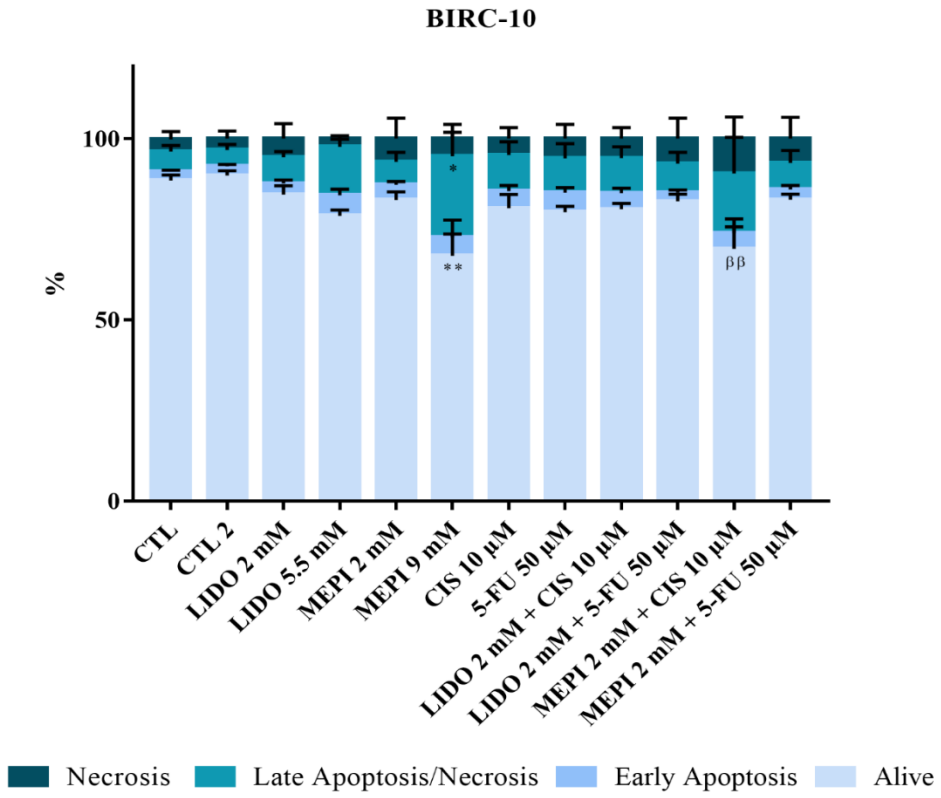

Figure 17 – Evaluation of cell death induced by local anesthetics in BICR-10 cell line by flow cytometry. Cells were incubated for 48 hours, with Lidocaine and Mepivacaine, in monotherapy (at IC_{50} doses) and in association with conventional chemotherapeutic drugs, Cisplatin and 5-Fluorouracil. Viability and cell death were evaluated by double stained with AV-FITC and PI, according with described in material and methods section. The results are expressed in percentage and represents the mean ± SEM of 3 to 5 independent experiments. CTL, Control; CTL 2, Control 2 (Sodium Chloride + Dimethyl Sulfoxide, NaCl + DMSO); LIDO, Lidocaine; MEPI, Mepivacaine; CIS, Cisplatin; 5-FU, 5-Fluorouracil. *, Statistical difference relative to Control (* $p < 0,05$, ** $p < 0,01$)

In Figure 18 is represented the effect of local anesthetics in monotherapy and in association with conventional chemotherapeutic drugs, in HSC-3 cells viability and the type of cell death induced after 48 hours of incubation.

All conditions showed a reduction in HSC-3 cells viability, accompanied by an increase in late apoptosis/necrosis, except in cells treated with Mepivacaine at 4,5 mM (IC_{50} dose), where the percentage of viable cells are similar to control. This result has to be clarified posteriorly, since Mepivacaine at 2 mM showed a cytotoxic effect in HSC-3 cells, with lesser percentage of cell viability (78,05 ± 3,458) relatively to control (83,54 ± 1,929). Lidocaine at 4,5 mM (IC_{50} dose) (56,27 ± 7,794) induces the highest decrease in cell viability, about 22% relatively to control, and an increase in apoptosis (about 21%). Although, Mepivacaine at 2 mM didn´t show any significant effect, when in association with Cisplatin at 2,5 µM, a decrease in cell viability and an increase in cell death is detected (Figure 18) ($p < 0,0001$, and $p < 0,001$, respectively). The associations of both local anesthetics with Cisplatin showed a higher cytotoxic effect in HSC-3 cells when compared with Cisplatin alone (51,54 ± 5,884 *vs* 75,66 ± 4,455), being the association with Mepivacaine statistically significant ($p < 0,05$). The association of both local anesthetics with 5-Fluorouracil did not modified the percentage of cell viability relative to 5-Fluorouracil alone.

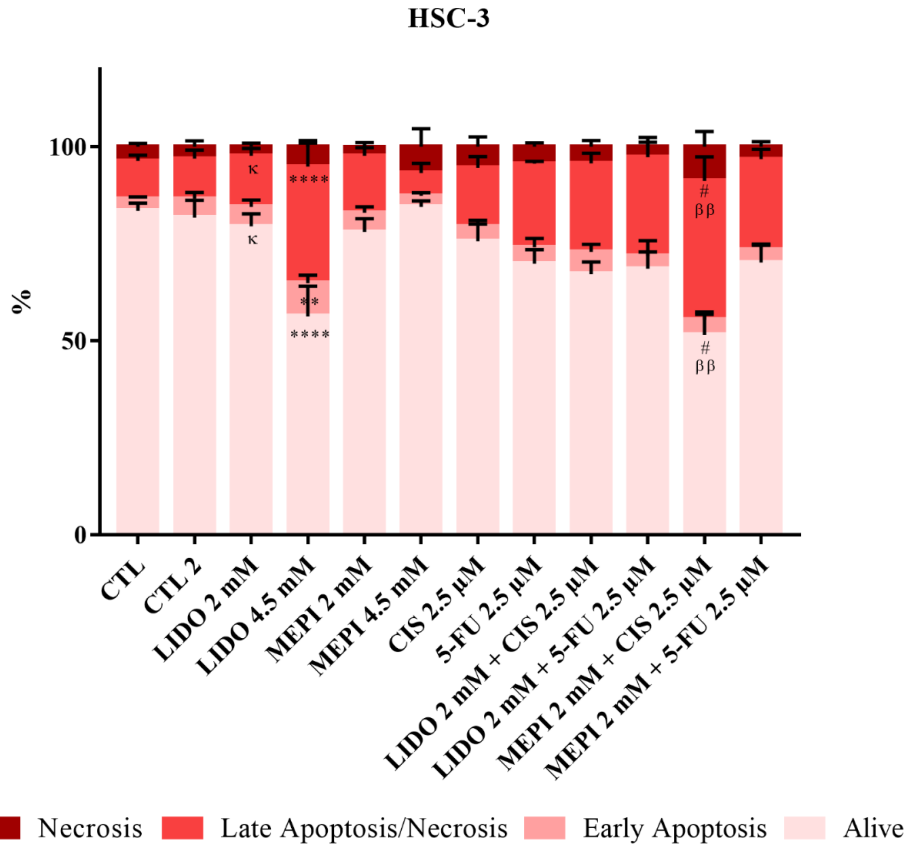

Figure 18 – Evaluation of cell death induced by local anesthetics in HSC-3 cell line by flow cytometry. Cells were incubated for 48 hours with Lidocaine and Mepivacaine, in monotherapy (at IC_{50} doses) and in association with conventional chemotherapeutic drugs, Cisplatin and 5-Fluorouracil, in conditions specified in the figure, and then double stained with AV-FITC and PI, according with material and methods section. The results are expressed in percentage and represent the mean ± SEM of 3 to 12 independent experiments. CTL, Control; CTL 2, Control 2 (Sodium Chloride + Dimethyl Sulfoxide, NaCl + DMSO); LIDO, Lidocaine; MEPI, Mepivacaine; CIS, Cisplatin; 5-FU, 5-Fluorouracil. *, Statistical difference relative to Control (* $p < 0,05$, ** $p < 0,01$, *** $p < 0,001$, **** $p < 0,0001$); #, Statistical difference relative to Cisplatin at 2,5 µM (# $p < 0,05$); κ, Statistical difference relative to Lidocaine at 4,5 mM (κ $p < 0,05$).

Figure 19 shows *Dot plots* representative of OSCC cell lines viability and death induced by Lidocaine at IC_{50} dose, evaluated by flow cytometry.

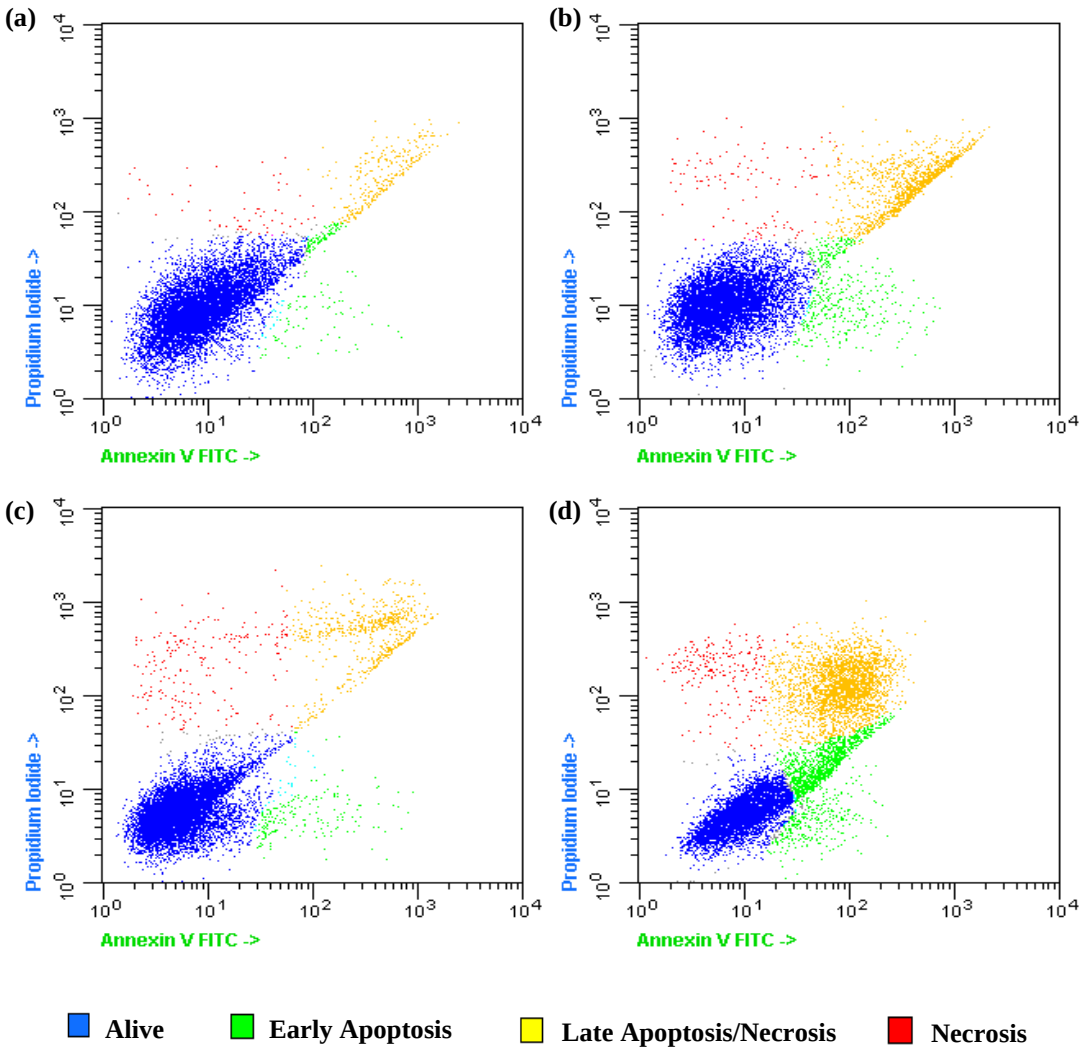

Figure 19 – *Dot plots* representative of OSCC cell lines viability and death induced by Lidocaine at IC_{50} dose, by flow cytometry. BICR-10 and HSC-3 cells were incubated for 48 hours with Lidocaine at 5,5 mM for BICR-10 cells and Lidocaine at 4,5 mM for HSC-3 cells, and then stained with AV-FITC and PI, as described in material and method section. **(a)** BICR-10 cells control; **(b)** BICR-10 cells incubated with Lidocaine at 5,5 mM; **(c)** HSC-3 cells control; **(d)** HSC-3 cells incubated with Lidocaine at 4,5 mM.

Optical Microscopy

To confirm the type of cell death induced by LA in OSCC cell lines we observed the morphological characteristics by optical microscopy after stained the cells with May-Grünwald-Giemsa (Figures 20 and 21). In generally, in cells treated with LA, in particular HSC-3 cells (Figure 21), we observed cellular retraction, membrane blebbing and nuclear fragmentation, all characteristics of apoptosis.

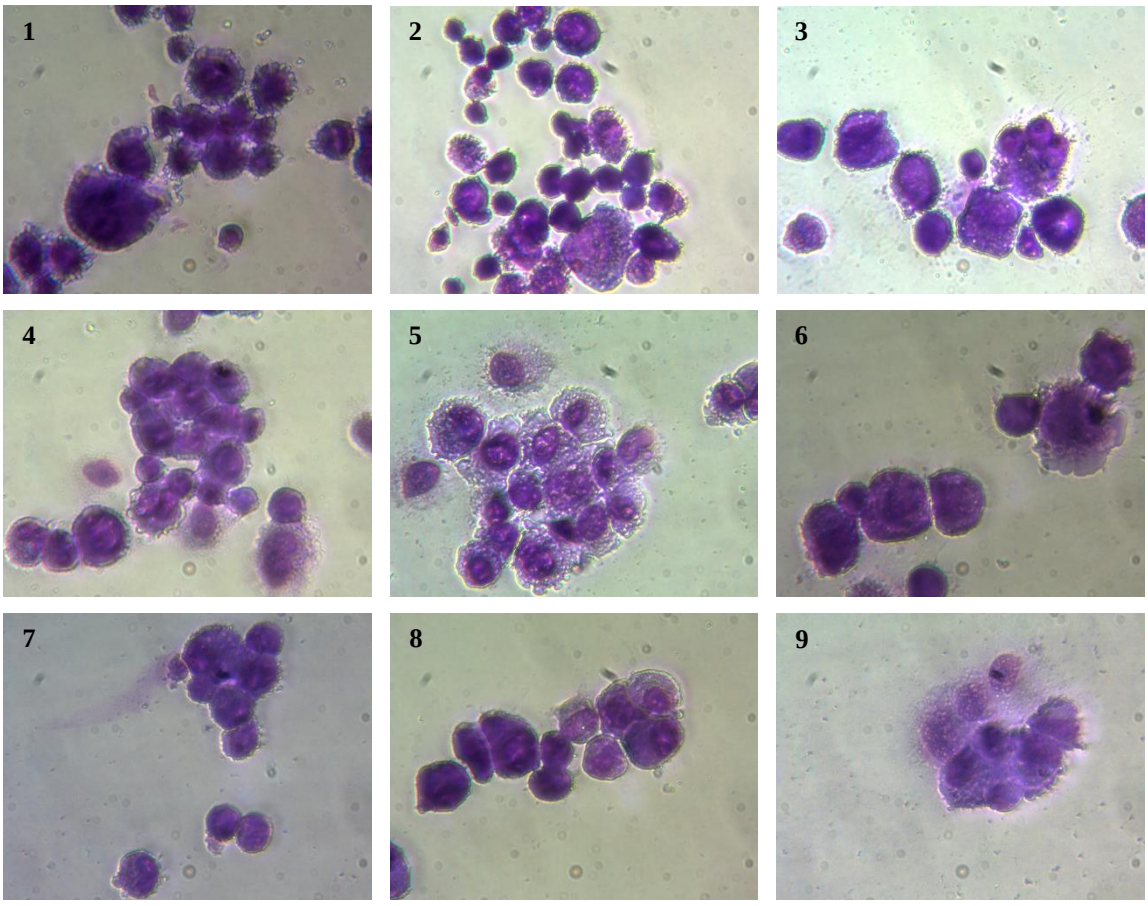

Figure 20 – Morphologic characteristics of BICR-10 cells before and after treatment with local anesthetics in monotherapy and in association with chemotherapeutic drugs. The morphological characteristics of BICR-10 cells without treatment **(1)**, treated with LIDO at 5,5 mM **(2)**, MEPI at 9 mM **(3)**, CIS at 10 µM **(4)**, LIDO at 2 mM + CIS at 10 µM **(5)**, MEPI at 2 mM + CIS at 10 µM **(6)**, 5-FU at 50 µM **(7)**, LIDO at 2 mM + 5-FU at 50 µM **(8)**, and MEPI at 2 mM + 5-FU at 50 µM **(9)**. Cells were incubated for 48 hours with drugs and concentrations referred above. After realization of smears, cells were stained with May-Grunwald-Giemsa, as described in material and methods section. Cells were observed at optical microscope with an amplification of 400x. LIDO, Lidocaine; MEPI, Mepivacaine; CIS, Cisplatin; 5-FU, 5-Fluorouracil.

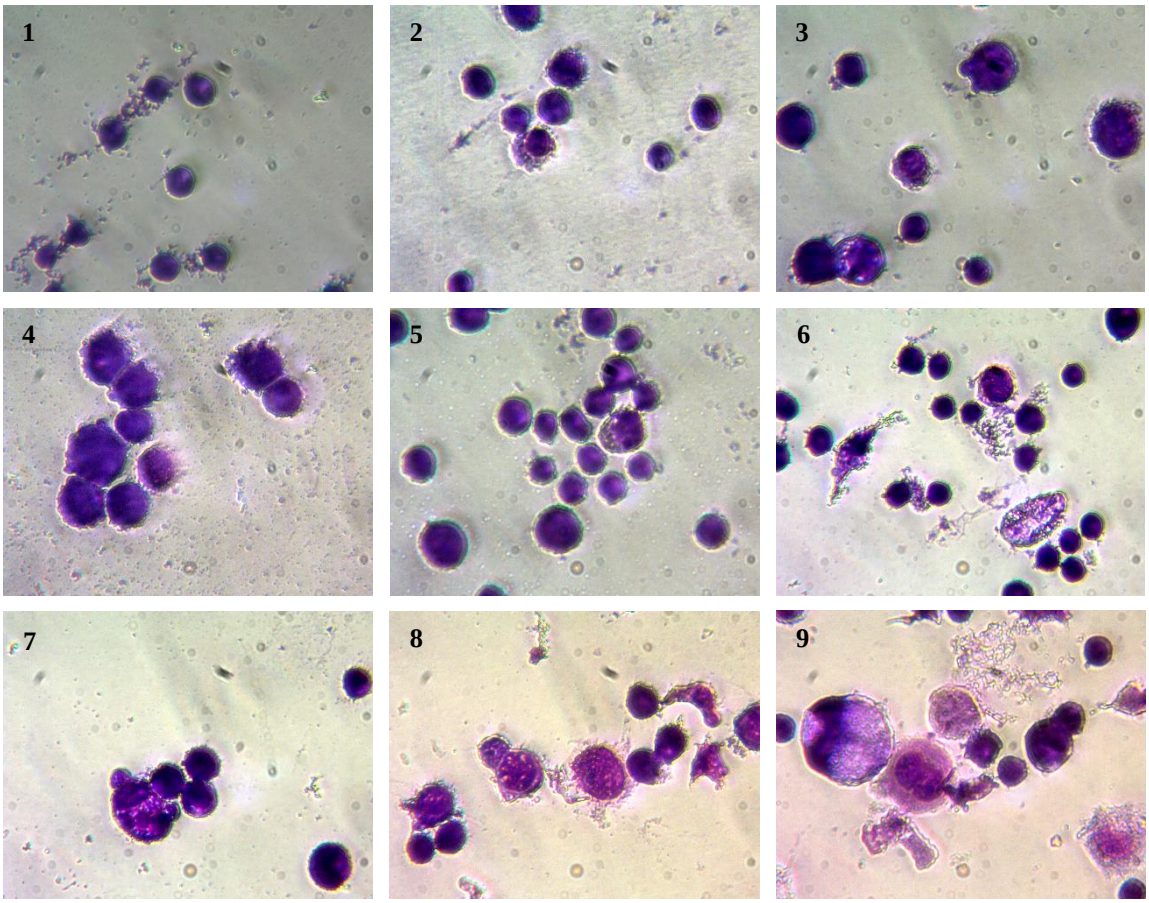

Figure 21 – Morphologic characteristics of HSC-3 cells before and after treatment with LA in monotherapy and in association with chemotherapeutic drugs. The morphological characteristics of HSC-3 cells without treatment **(1)**, treated with LIDO at 4,5 mM **(2)**, MEPI at 4,5 mM **(3)**, CIS at 2,5 µM **(4)**, LIDO at 2 mM + CIS at 2,5 µM **(5)**, MEPI at 2 mM + CIS at 2,5 µM **(6)**, 5-FU at 2,5 µM **(7)**, LIDO at 2 mM + 5-FU at 2,5 µM **(8)**, and MEPI at 2 mM + 5-FU at 2,5 µM **(9)**. Cells were incubated for 48 hours with drugs and concentrations referred above. After realization of smears, cells were stained with May-Grunwald-Giemsa, as described in material and methods section. Cells were observed at optical microscope with an amplification of 400x. LIDO, Lidocaine; MEPI, Mepivacaine; CIS, Cisplatin; 5-FU, 5-Fluorouracil.

3.2.1. Analysis of cell death mechanisms induced by local anesthetics by Flow Cytometry

Flow cytometry was performed to determine mechanisms of death observed in BICR-10 and HSC-3 cell lines when these cells are incubated with Lidocaine and Mepivacaine at IC_{50} concentratations, and in association with chemotherapeutic drugs, Cisplatin and 5-Fluorouracil for 48 hours. In these context, we evaluated caspase activity, reactive oxygen species production, reduced glutathione levels and mitochondrial membrane potential.

3.2.1.1. Evaluation of caspases expression levels

To clarify and confirm the type of death predominantly observed in OSCC cell lines by flow cytometry and optical microscopy, we measured the basal intracellular caspase expression levels in BICR-10 and HSC-3 cells and after treat these cells with conditions referred above. The results are represented in Figures 22 and 23, respectively. The intracellular caspase expression levels were evaluated by flow cytometry and the results expressed in mean fluorescence intensity (MFI). As can be seen in Figure 22, HSC-3 cells expressed higher basal caspases levels than BICR-10 cells (50,19 ± 1,966 MFI *vs* 38,48 ± 7,57 MFI, respectively). However this difference is not statistically significant.

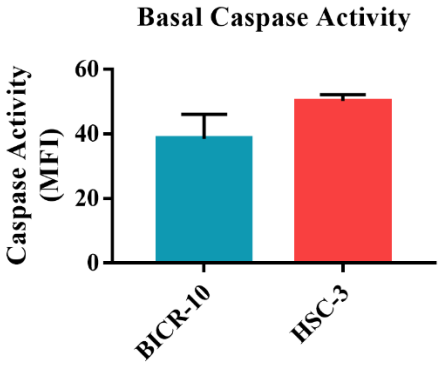

Figure 22 – Basal caspase expression levels in BICR-10 and HSC-3 cell lines. The basal activity of caspases was determined by flow cytometry, using Apostat Kit, as described in material and methods section. The results represent the mean ± SEM of 3 to 4 independent experiments, and are expressed in MFI, which is directly proportional to the total of antibodies associated to target in two OSCC cells populations. MFI, Mean Fluorescence intensity.

When cells are incubated with LA in IC_{50} concentrations, we observed, in generally, an increase in caspases levels, more evident in HSC3 cells (Figure 23). In fact, as we observed in Figure 23, in BICR-10 cell line, we observed an increase in caspases activity about 1,44x and 1,4x, when cells are treated, respectively, with Lidocaine at 5,5 mM (1,437 ± 0,287) and Mepivacaine at 9 mM (1,396 ± 0,38) relatively to control cells (Figure 23-a). We verified that these effect induced by LA in caspase levels was dose-dependent, since Lidocaine and Mepivacaine at 2 mM also presented an increase in caspase activity relative to control, but that increment was lesser when compared with local anesthetics at IC_{50} doses. In cells incubated with the association of Lidocaine and Mepivacaine with Cisplatin we also observed an increase in caspases levels relative to Cisplatin alone (1,211x and 1,135x, respectively, *vs* 0,887x ± 0,105). When LA are combined with 5-Fluorouracil, the association with Mepivacaine, but not with Lidocaine, presented a higher caspases levels (1,31x) compared with 5-Fluorouracil alone (1,142 ± 0,097), However, there are in progress new experiments to confirm this results obtained to BICR-10 cell line.

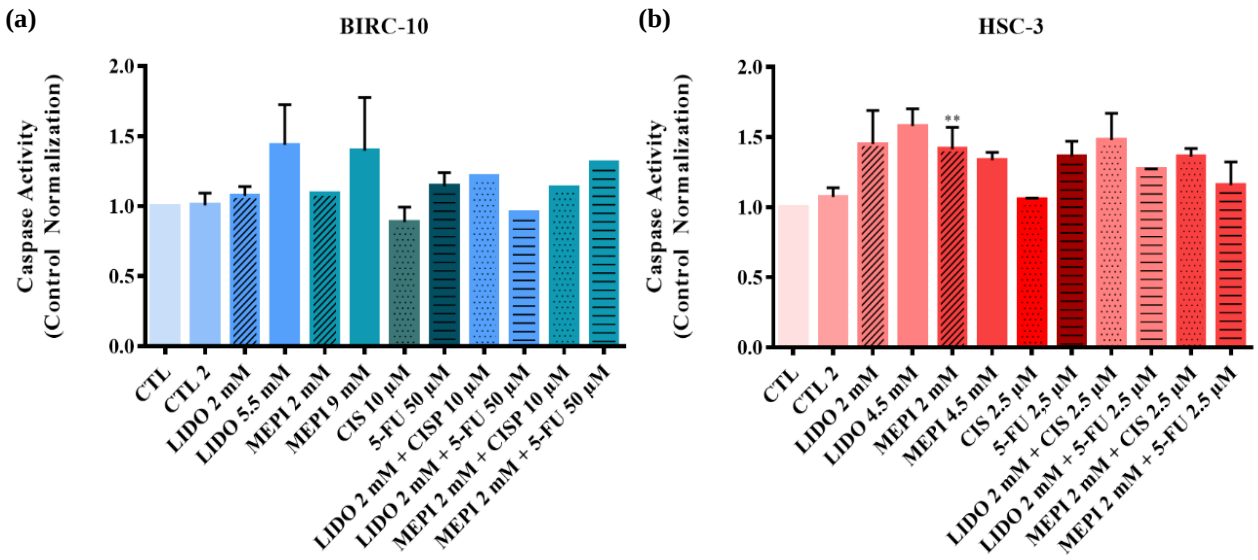

Figure 23 – Caspase expression levels in (a) BICR-10 and (b) HSC-3 cell lines incubated with Lidocaine and Mepivacaine, in monotherapy and in combination with Cisplatin and 5-Fluorouracil. The caspase expression levels was determined by flow cytometry using the Apostat Kit, as described in material and methods section. The results represent mean ± SEM of 1 to 2 independent experiments in BICR-10 cells and 2 to 5 independent experiments in HSC-3 cells. They are expressed normalized to control. CTL, Control; CTL 2, Control 2 (Sodium Chloride + Dimethyl Sulfoxide, NaCl + DMSO); LIDO, Lidocaine; MEPI, Mepivacaine; CIS, Cisplatin; 5-FU, 5-Fluorouracil. *, Statistical difference relative to Control (** $p < 0,01$).

In HSC-3 cell line, represented in Figure 23-b, the caspase levels was higher for all conditions previously referred, relatively to control, with exception of cells treated with Cisplatin alone, which remained similar to control. In cells treated with Lidocaine at 4,5 mM we observed the higher increase in caspases levels (1,58x ± 0,12) compared with those observed in cells incubated with Mepivacaine at 4,5 mM (1,34x ± 0,055), or not treated (control cells), Lidocaine ($p < 0,01$). For Lidocaine, we verified a dose-dependent increase in caspase activity, since Lidocaine at 2 mM had less effect than Lidocaine at 4,5 mM. This dose-dependent increase in caspase levels was not verified for Mepivacaine. The association of both LA with Cisplatin showed a higher level of caspase activity (Lidocaine: 1,48x ± 0,191; Mepivacaine: 1,36x ± 0,058) when compared with Cisplatin alone (1,056x ± 0,01). The association of both

local anesthetics with 5-Fluorouracil induced a decrease in caspase activity relative to 5-Fluorouracil alone. The conditions where Lidocaine was present seemed to have a higher effect in increase caspase activity than conditions with Mepivacaine, in HSC-3 cell line.

Control 2 (1,308 ± 0,238, n = 3) condition, in HSC-3 cells, induced an increase in caspase activity relative to control. Thus, conditions that had as vehicle DMSO (conditions were Cisplatin and 5-Fluorouracil were present), since this is the most probable compound to induce this effect, were compared to control 2 condition and not to control.

3.2.1.2. Evaluation of intracellular reactive oxygen species production and reduced glutathione levels

To verify if LA induced cell death mediated by oxidative stress we evaluated in both OSCC cell lines incubated with drugs, as described before, the levels of reactive oxygen species (ROS) production (peroxides and superoxide anion) and reduced glutathione (GSH), by flow cytometry. H_2DCF-DA was used for analysis of intracellular expression of peroxides (H_2O_2), and DHE for analysis of intracellular expression of superoxide anion (O_2^-). These compounds when inside the cells produce fluorescent compounds, DCF and E^+, respectively that could be detected by flow cytometry. For GSH analysis we used mercury orange as described in material and method section. Basal expression levels of ROS and GSH were expressed in MFI. When OSCC cells were incubated with drugs, ROS and GSH expressions were normalized to control.

The Figure 24 shows the basal expression levels of reactive oxygen species, (a) H_2O_2 and (b) O_2^-, and the (c) anti-oxidant defense GSH in BICR-10 and HSC-3 cell lines. We observed that HSC-3 cells expressed higher basal ROS levels (H_2O_2: 45 ± 7,781 MFI; O_2^-: 57,4 ± 1,738 MFI) than BICR-10 cells (H_2O_2: 21,18 ± 8,175 MFI; $O_2^{-:}$ 40,86 ± 5,52 MFI). Basal expression levels of GSH did not differ significantly in both OSCC cell line populations (BICR-10 cells: 61,44 ± 10,41; HSC-3 cells: 71,14 ± 8,401).

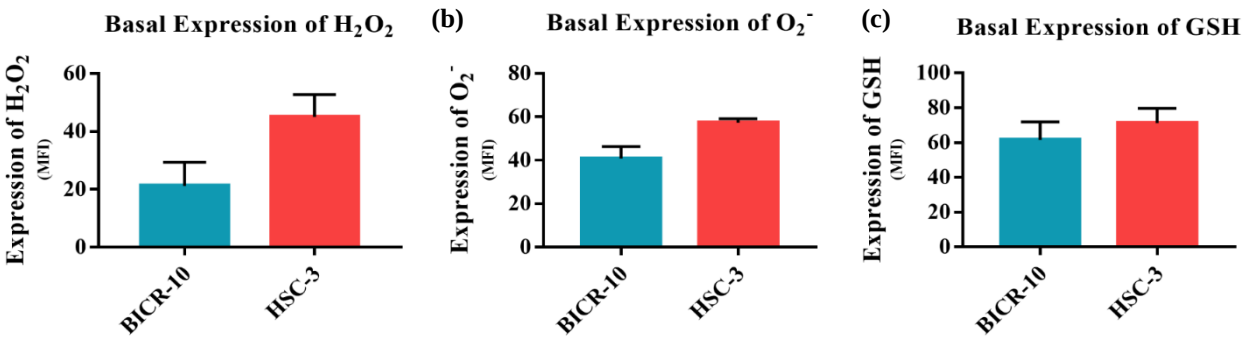

Figure 24 – Basal expression levels of (a) H_2O_2, (b) O_2^- and (c) GSH in BICR-10 and HSC-3 cell lines, by flow cytometry. The basal expression of H_2O_2, O_2^- and GSH was determined by flow cytometry, using the probes, H_2DCF-DA, DHE and Mercury Orange, as described in material and methods section. The results represent mean ± SEM of 2 to 5 independent experiments, and are expressed in MFI. MFI, Mean Fluorescence intensity.

In general, only in BICR-10 cells we observed a decrease in peroxides levels, while an increase in superoxide anion is detected. In HSC3 cells we observe an increase in both ROS (Figure 25).

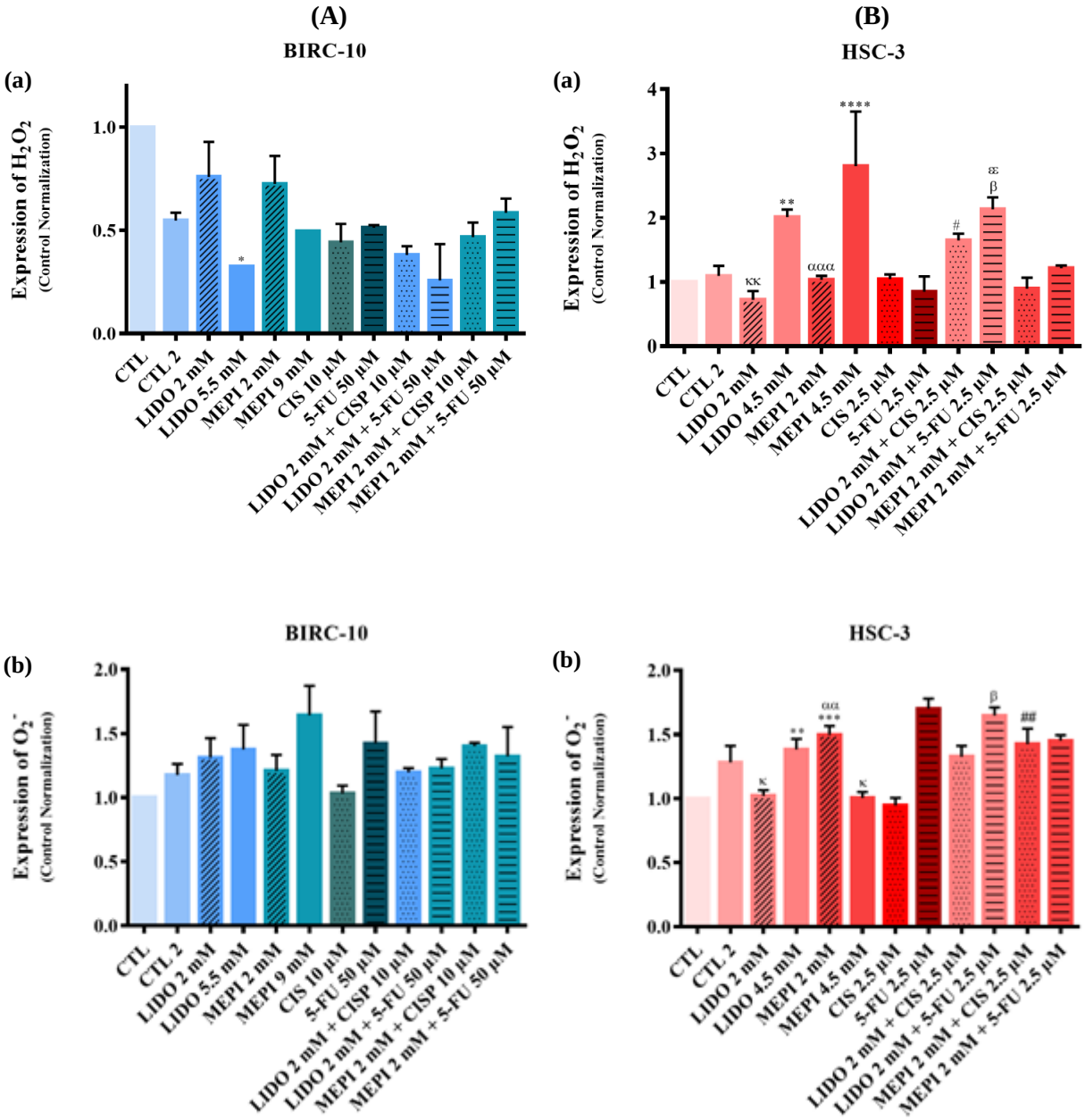

Figure 25 – ROS expression levels in BICR-10 (A) and HSC-3 (B) cell lines incubated with Lidocaine and Mepivacaine in monotherapy and in combination with Cisplatin and 5-Fluorouracil. ROS levels were determined by flow cytometry through the expression levels of H_2O_2 **(a)** and $O_2^{\cdot-}$ **(b)**. For these determinations we used the H_2DCF-DA and DHE probes, respectively, as described in material and methods section. The results represent mean ± SEM of 1 to 2 independent experiments in BICR-10 cells and 2 to 4 independent experiments in HSC-3 cells in conditions represented in figure. The results are expressed normalized to control. CTL, Control; CTL 2, Control 2 (Sodium Chloride + Dimethyl Sulfoxide, NaCl + DMSO); LIDO, Lidocaine; MEPI, Mepivacaine; CIS, Cisplatin; 5-FU, 5-Fluorouracil. *, Statistical difference relative to Control (* $p < 0,05$, ** $p < 0,01$, **** $p < 0,0001$); β, Statistical difference relative to Control 2 (β $p < 0,05$); κ, Statistical difference relative to Lidocaine at 4,5 mM (κκ $p < 0,01$); α, Statistical difference relative to Mepivacaine at 4,5 mM (ααα $p < 0,001$); #, Statistical difference relative to Cisplatin at 2,5 µM (# $p < 0,05$); ε, Statistical difference relative to 5-Fluorouracil at 2,5 µM (εε $p < 0,01$)

As represented in Figure 25-A, in BICR-10 cell line treated with Lidocaine at 5,5 mM and Mepivacaine at 9 mM (IC_{50} concentrations) a decreased intracellular H_2O_2 levels relative to control is observed (in almost 30% for lidocaine and 50% for Mepivacaine) (Figure 25-Aa); however only the results obtained with Lidocaine had statistical significance ($p<0,05$). More experiments with these conditions are running to confirm these results. The reduction in H_2O_2 intracellular production revealed to be dose-dependent. Simultaneously, in these conditions, we observe a tendency increase in superoxide anion levels (for Lidocaine at 5,5 mM about 1,375x and for Mepivacaine at 9 mM 1,643x) (Figure 25-Ab). Associations of Lidocaine and Mepivacaine with Cisplatin showed similar results in intracellular production of H_2O_2, but a tendency to increase in O_2^- expression levels, when compared with Cisplatin alone, with the association with Mepivacaine showing the highest level (1,401x) (Figure 25-Aa and Ab). The association of Lidocaine with 5-Fluorouracil induced a reduction in H_2O_2 and O_2^- production, as opposed to the association of Mepivacaine with the same chemotherapeutic drug, which had a tendency to increase H_2O_2 production in BICR-10 cells. To note that Control 2 condition (NaCl + DMSO) presented an important effect in H_2O_2 reduction in BICR-10 cells, probably due to DMSO. Conditions where Cisplatin and 5-Fluorouracil were present contained DMSO as vehicle, so any comparison with these conditions should be made relatively to control 2 and not to control condition.

The H_2O_2 and O_2^- intracellular production in HSC-3 cell line incubated with the drugs tested in this study is represented in Figure 25-Ba and Bb. Local anesthetics, Lidocaine and Mepivacaine at IC_{50} doses (4,5 mM), induced an increase in production of peroxides when compared to control (about 2x and 2,8x, for Lidocaine and Mepivacaine at 4,5 mM, respectively), being the differences statistically significant ($p < 0,01$ and $p < 0,0001$, respectively). At the IC_{50} concentrations, the increase in superoxide anion is only observed in cells treated with Lidocaine. This effect in ROS production was dose-dependent. Although,

control 2 condition did not presented a substantial effect in HSC-3 cells in ROS production, as with BICR-10 cells, any comparison with conditions which have Cisplatin or 5-Fluorouracil, should be made relatively to control 2 and not to control condition. Thereby, we observed a statistical significant augment in H_2O_2 production ($p < 0,05$) when we compare Lidocaine associated with 5-Fluorouracil with control 2 (2,132 ± 0,186 *vs* 1,097 ± 0,154). The association of Lidocaine with Cisplatin, but not the association of the same chemotherapeutic drug with Mepivacaine, resulted in an increase in H_2O_2 expression levels in HSC-3 cells, when compared with Cisplatin by itself (1,646 ± 0,107 *vs* 1,047 ± 0,073), being this result statistically significant ($p < 0,05$). These drug associations induced an increment in O_2^- levels, being the association with Mepivacaine which induced the highest level of this ROS ($p < 0,01$). Both associations of Lidocaine and Mepivacaine with 5-Fluorouracil led to a rise in H_2O_2 and a decrease in $O_2^{-\cdot}$ intracellular production when compared with 5-Fluorouracil alone, presenting the association with Lidocaine an increase statistically significant about 2x in H_2O_2 levels ($p < 0,01$).

Figure 26 represents the expression levels of GSH in BICR-10 and HSC3 cells incubated with LA in monotherapy and in combination with Cisplatin and 5-Flourouracil. As we can observe, in general, we detected a tendency to an increase in this antioxidant defense, being the differences particularly significant in BICR-10 cells treated with Lidocaine and Mepivacaine in combination with Cisplatin. In fact, the association of Cisplatin with Lidocaine and Mepivacaine showed an important increase in GSH expression levels in BICR-10 cells (1,489 ± 0,055 and 1,645 ± 0,029) relative to Cisplatin alone. These two associations presented differences with statistical significance relative to control 2 condition ($p < 0,05$, and $p < 0,01$, respectively). Relative to 5-Fluorouracil alone (1,109 ± 0,021, $n = 2$), we assisted to an increase in GSH levels for association of 5-Fluorouracil and Mepivacaine (1,3 ± 0,124) and no influence in GSH expression with association of 5-Fluorouracil with Lidocaine. NaCl + DMSO condition (control 2) induced reduction in GSH expression levels relative to control, so conditions with

Cisplatin and 5-Flourouracil (that had DMSO as vehicle) were compared with control 2 and not to control.

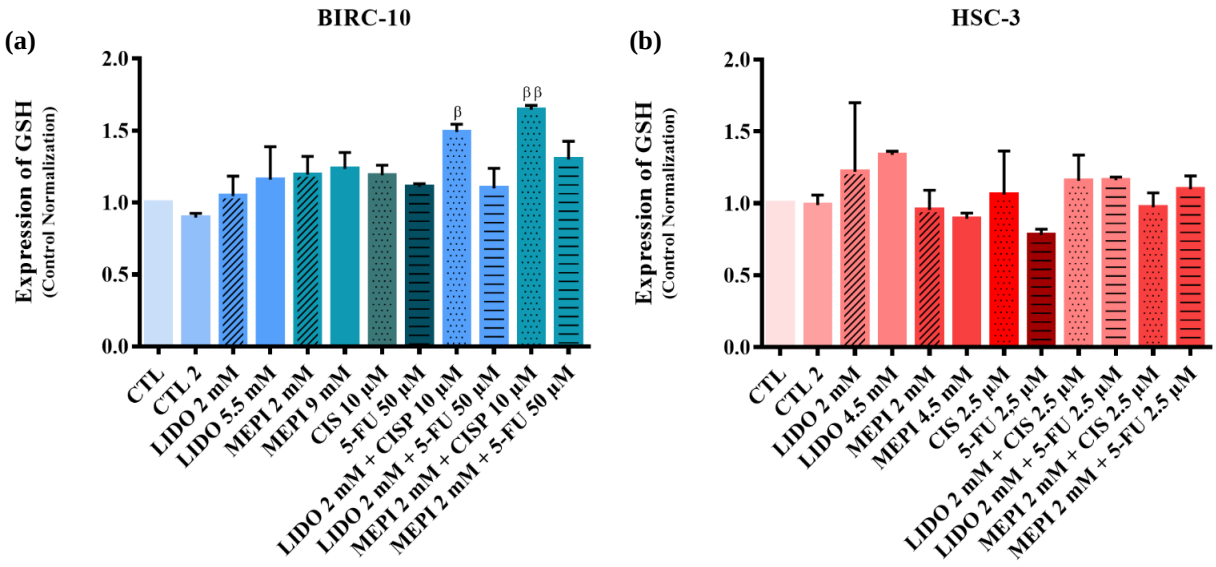

Figure 26 – Expression levels of GSH in (a) BICR-10 and (b) HSC-3 cell lines incubated with Lidocaine and Mepivacaine in monotherapy and in combination with Cisplatin and 5-Fluorouracil. The expression levels of GSH was determined by flow cytometry, using Mercury Orange, as described in material and methods section and in conditions represented in Figure. The results represent mean ± SEM of 2 to 3 independent experiments in BICR-10 and HSC-3 cells. They are expressed normalized to control. CTL, Control; CTL 2, Control 2 (Sodium Chloride + Dimethyl Sulfoxide, NaCl + DMSO); LIDO, Lidocaine; MEPI, Mepivacaine; CIS, Cisplatin; 5-FU, 5-Fluorouracil. β, Statistical difference relative to Control 2 (β $p < 0,05$; ββ $p < 0,01$).

3.2.1.3. Evaluation of mitochondrial membrane potential

To clarify if mitochondrial dysfunction was present in OSCC cell lines when submitted to Lidocaine and Mepivacaine at IC_{50} concentration, and in association with Cisplatin and 5-Fluorouracil, the mitochondrial membrane potential ($\Delta\psi_{mit}$) was analyzed by flow cytometry, using the fluorescent probe JC-1. The results of basal $\Delta\psi_{mit}$ in OSCC cell lines were expressed as the ratio between JC-1 Monomers and JC-1 Aggregates (JC-1 M/A) expressed in MFI and then normalized to control (Figure 27).

As we can observe in Figure 27, BICR-10 cells showed a higher JC-1 M/A ratio than HSC-3 cells, being the difference statically significant ($p < 0,0001$).

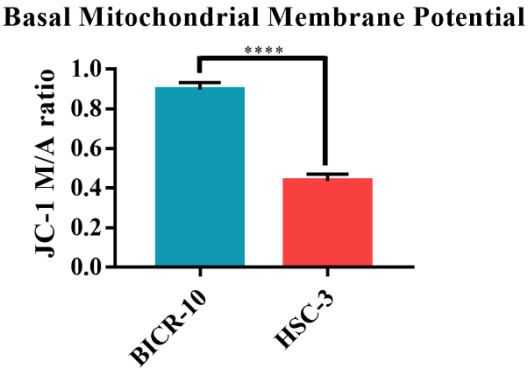

Figure 27 – Basal mitochondrial membrane potential of BICR-10 and HSC-3 cells. The basal mitochondrial membrane potential was determined by flow cytometry, using JC-1 probe, as described in material and methods section. The results represent the mean ± SEM of 3 independent experiments, and are expressed in JC-1 M/A MFI ratio. JC-1, 5,5´, 6, 6´- tethracloro-1, 1´, 3, 3´-tetraethylbenzimidazolcarbocyanine iodide; M/A, Monomers/Aggregates; MFI, Mean Fluorescence intensity. *, Statistical significance (**** $p < 0,0001$).

The $\Delta\psi_{mit}$ alterations induced by local anesthetics at IC_{50} doses in monotherapy and in association with chemotherapeutic drugs, in BICR-10 and HSC-3 cells, are drug, dose and cell line dependent, as represented in Figure 28.

In fact, in HSC-3 cells, the increase in JC-1 M/A ratio is statistically significant in these cells treated with Lidocaine in monotherapy (1,775 ± 0,138, $p < 0,001$) and in the associations of Lidocaine and Mepivacaine with Cisplatin and 5-Fluorouracil. In the association with Cisplatin the increase is about 2,112 and 2,396 times, while in the combination with 5-Fluorouracil the increase is about 1,342 and 2,242 times, when compared with the conventional chemotherapeutic drugs administered alone ($p< 0,01$, $p < 0,0001$ and $p < 0,05$, respectively). In BICR-10 cells, only in cells incubated with Mepivacaine at 2 mM in monotherapy and with Mepivacaine in combination with Cisplatin a significant increase is observed (1,459 ± 0,035 and 2,302 ± 0,256).

Note that control 2 (NaCl + DMSO) condition presented a substantial decrease in JC-1 M/A ratio in HSC-3 cells, so conditions were DMSO was vehicle (where Cisplatin and 5-Fluorouracil were present) were compared to it, and not to control condition.

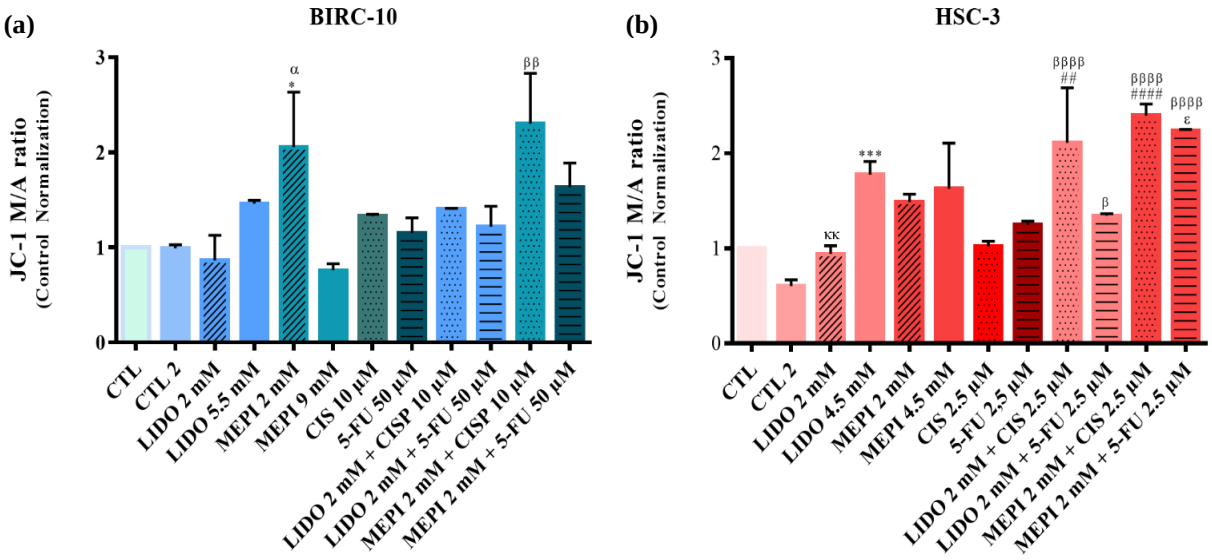

Figure 28 – Mitochondrial membrane potential in (a) BICR-10 and (b) HSC-3 cell lines when incubated with Lidocaine and Mepivacaine in monotherapy and associated with Cisplatin and 5-Fluorouracil. The mitochondrial membrane potential was determined by flow cytometry, using JC-1 probe, as described in material and methods section. The results represent mean ± SEM of 2 to 3 independent experiments in BICR-10 cells and 2 to 7 independent experiments in HSC-3 cells. The results were normalized to control. JC-1, 5,5´, 6, 6´- tethracloro-1, 1´, 3, 3´-tetraethylbenzimidazolcarbocyanine iodide; M/A, Monomers/Aggregates; CTL, Control; CTL 2, Control 2 (Sodium Chloride + Dimethyl Sulfoxide, NaCl + DMSO); LIDO, Lidocaine; MEPI, Mepivacaine; CIS, Cisplatin; 5-FU, 5-Fluorouracil. *, Statistical difference relative to Control (* $p < 0,05$, *** $p < 0,001$); β, Statistical difference relative to Control 2 (β $p < 0,05$; ββ $p < 0,01$; ββββ $p < 0,0001$); κ, Statistical difference relative to Lidocaine at 4,5 mM (κκ $p < 0,01$); α, Statistical difference relative to Mepivacaine at 9 mM (α $p < 0,05$); #, Statistical difference relative to Cisplatin at 2,5 µM (## $p < 0,01$; #### $p < 0,0001$); ε, Statistical difference relative to 5-Fluorouracil at 2,5 µM (ε $p < 0,05$).

3.3. Cell cycle analysis

To verify the anti-proliferative effect in BICR-10 and HSC-3 cells cultured with local anesthetics and chemotherapeutic drugs (as described in material and method section), we analyzed distribution of cells for the different phases of cell cycle (G1, S and G2/M phases), by flow cytometry. Also, with this technique, we were able to identify apoptotic cells, as they display a sub-G1 peak in cell cycle analysis.

Figure 29 is representative of the effect of local anesthetics at IC_{50} doses in cell cycle of BICR-10 and HSC-3 and, in Tables 2 and 3, we represented all the results obtained.

In both cell lines and for both Lidocaine and Mepivacaine, we observed an increase in pre-G1 peak relative to control, indicative of apoptosis. In BICR-10 cells, we observed an increment of cells in G0/G1 phase, which could be indicative of a modest blockade in this phase induced by local anesthetics (Figure 29). However, this results are not statistically significant in this cell line, as we can observed in Table 1. In HSC-3 cells, Lidocaine at 4,5 mM, induced an increase of cells in G0/G1 phase, while in this cell line incubated with Mepivacaine at 4,5 mM, we noticed an increase in S and G2/M phase relative to control (Figure 29) .

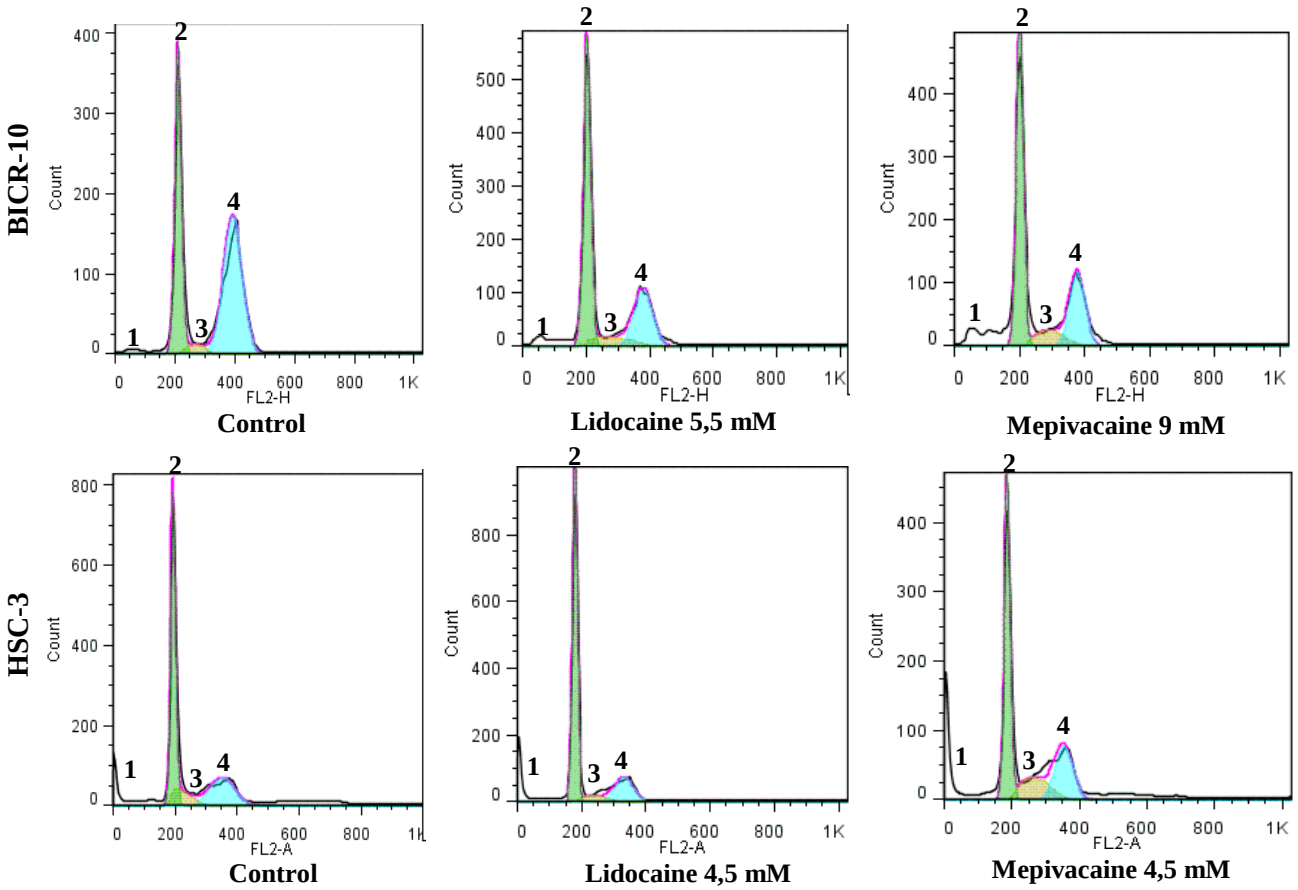

Figure 29 – Cell cycle analysis of BICR-10 and HSC-3 cells when incubated with local anesthetics at IC_{50} doses. Cell cycle analysis was performed by flow cytometry, using PI as described in material and methods section. **1,** Pre-G1 peak (apoptotic peak); **2**, G0/G1 phase; **3**, S phase; **4**, G2/M phase.

Table 2 – Distribution of BICR-10 cells by different phases of cell cycle and sub-G1 peak when incubated with local anesthetics in monotherapy and in association with Cisplatin and 5-Fluorouracil.

BICR-10	G0/G1 phase	S phase	G2/M phase	Pre-G1 peak
CTL	58,4 ± 3,72	15,47 ± 3,866	26,13 ± 6,997	0,754 ± 0,425
CTL 2	58,33	1,997	39,67	18,77
LIDO 2 mM	53,29 ± 5,71	13,9 ± 9,609	32,82 ± 15,32	8,488 ± 6,275
LIDO 5,5 mM	61,73	10,2	28,05	4,858
MEPI 2 mM	54,73	9,354	35,92	3,555
MEPI 9 mM	63,9 ± 3,588	11,72 ± 0,882	24,38 ± 4,47	13,69 ± 0,668
CIS 10 µM	63,83 ± 6,894	8,225 ± 0,431	27,94 ± 6,461	2,2 ± 0,792
5-FU 50 µM	43,32	15,43	41,26	7,233
LIDO 2 mM + CIS 10 µM	51,26	14,55	34,2	1,068
LIDO 2 mM + 5-FU 50 µM	48,9	17,21	33,9	2,102
MEPI 2 mM + CIS 10 µM	52,28	11,53	36,19	4,156
MEPI 2 mM + 5-FU 50 µM	51,26	21,19	27,55	2,291

The analysis of cell cycle was performed by flow cytometry, using PI, as described in material and methods section. Results expressed the percentage of cells presented in each cell cycle phase and represented the mean ± SEM of 1 to 5 independent experiments. Any conditions with Cisplatin and 5-Fluorouracil (with DMSO as vehicle) were compared to control 2 condition. CTL, Control; CTL 2, Control 2 (Sodium Chloride + Dimethyl Sulfoxide, NaCl + DMSO); LIDO, Lidocaine; MEPI, Mepivacaine; CIS, Cisplatin; 5-FU, 5-Fluorouracil.

As seen in Table 3, in HSC-3 cells, both Lidocaine and Mepivacaine induced mainly an increase in pre-G1 peak, that is dose dependent, being the differences statistically significant ($p < 0,01$) when cells are incubated with the drugs at 4,5 mM. In this conditions an increase approximately of 23% and 25% relative to control is observed. Otherwise, we didn´t observed any statistically influence in the percentage of cells in the different phases of cell cycle. However, when local anesthetics are in combination with chemotherapeutic drugs, a blockage

of cell cycle predominates, relatively to the drugs administered alone, instead of an increase in pre-G1 peak.

In HSC-3 cells treated with Lidocaine associated with Cisplatin an increase in percentage of cells in G2/M phase is observed (34,69% ± 10,12) compared with Cisplatin or Lidocaine alone (13,16% ± 2,52, 13,02% ± 4,405). When Mepivacaine is added to the cells in combination with Cisplatin an increase in G2/M phase is also observed (26,72% ± 12,69), but predominantly an increase in S phase is also detected (45,26% ± 18,26) which is statistically significant ($p<0,01$) compared with drugs administered alone (9,9% and 20,9%, respectively). Associations of both local anesthetics with 5-Fluorouracil induced mainly an increase in percentage of cells in S phase (Lidocaine: 57,15% ± 2,889; Mepivacaine: 58,01% ± 10,59) relative to 5-Fluorouracil alone (12,27% ± 4,251), being the difference statistically significant ($p < 0,001$).

Table 2 – Distribution of HSC-3 cells by different phases of cell cycle and sub-G1 peak when incubated with local anesthetics at IC_{50} dose and local anesthetics in association with Cisplatin and 5-Fluorouracil.

HSC-3	G0/G1 phase	S phase	G2/M phase	Pre-G1 peak
CTL	73,17 ± 3,116	9,993 ± 1,709	16,84 ± 2,904	2,758 ± 0,135
CTL 2	71,73 ± 4,782	12,87 ± 3,492	15,41 ± 4,44	4,943 ± 1,446
LIDO 2 mM	76, 16 ± 5,841	10,82 ± 3,144	13,02 ± 4,405	5,317 ± 0,802
LIDO 4,5 mM	77,98 ± 4,327	9,062 ± 2,092	12,96 ± 2,775	25,76 ± 10,24 **
MEPI 2 mM	72,75 ± 6,877	9,915 ± 3,514	17,34 ± 6,187	4,171 ± 0,755
MEPI 4,5 mM	54,51 ± 7,413	23,29 ± 5,495	22,19 ± 3,431	27,17 ± 9,688 **
CIS 2,5 µM	65,9 ± 1,857	20,94 ± 0,663	13,16 ± 2,52	4,741 ± 0,387
5-FU 2,5 µM	69,96 ± 16,51	12,27 ± 4,251	17,77 ± 12,26	6,52 ± 0,577
LIDO 2 mM + CIS 2,5 µM	58,49 ± 11,4	6,822 ± 1,279	34,69 ± 10,12	7,158 ± 1,406
LIDO 2 mM + 5-FU 2,5 µM	31,11 ± 4,325 ββββ; εε	57,15 ± 2,889 βββ; εεε	11,74 ± 7,214	5,861 ± 2,456
MEPI 2 mM + CIS 2,5 µM	28,02 ± 5,866 ββββ	45,26 ± 18,26 β	26,72 ±12,69	4,728 ± 1,358
MEPI 2 mM + 5-FU 2,5 µM	30,42 ± 7,341 ββββ; εε	58,01 ± 10,59 βββ; εεε	11,57 ± 3,249	6,044 ± 1,174

The analysis of cell cycle was performed by flow cytometry, using PI, as described in material and methods section. Results expressed the percentage of cells presented in each cell cycle phase and represented the mean ± SEM of 2 to 6 independent experiments. Any conditions with Cisplatin and 5-Fluorouracil (with DMSO as vehicle) were compared to control 2 condition. CTL, Control; CTL 2, Control 2 (Sodium Chloride + Dimethyl Sulfoxide, NaCl + DMSO); LIDO, Lidocaine; MEPI, Mepivacaine; CIS, Cisplatin; 5-FU, 5-Fluorouracil. *, Statistical significance relative to Control (** $p < 0,01$); β, Statistical significance relative to Control 2 (β $p < 0,05$, βββ $< 0,001$, ββββ $< 0,0001$); ε, Statistical significance relative to 5-Fluorouracil (εε $p < 0,01$, εεε $p < 0,001$).

3.4. Analysis of the effect of local anesthetics in cell adhesion and migration in OSCC cell lines

After studied the cytotoxic and anti-proliferative effects of local anesthetics in monotherapy and in association with conventional chemotherapeutic drugs in OSCC cells, we aimed to clarify their effect in cell adhesion and migration. For these proposes, in BICR-10 and HSC-3 cell lines, we analyzed the expression levels of adhesion molecules, like E-cadherin by flow cytometry, and β1-Integrins and β-catenins by western blot. By flow cytometry we also evaluated the expression levels of metalloproteinases and monitored their proteolytic activity by zymography assay. The effect in migration was analyzed by wound healing assay.

3.4.1. Analysis of E-Cadherins expression levels

E-cadherin expression levels were analyzed in OSCC cell lines cultured at conditions described above by flow cytometry, using Intracell kit with monoclonal antibody anti-E-Cadherin-PE, as described in material and methods section. The basal expression of E-cadherins in both cell lines were expressed in MFI and normalized to control.

The Figure 30 represents basal expression of E-cadherins in BICR-10 and HSC-3 cell lines. We verified that HSC-3 cells had a higher expression level of this adhesion molecule relative to BICR-10 cells.

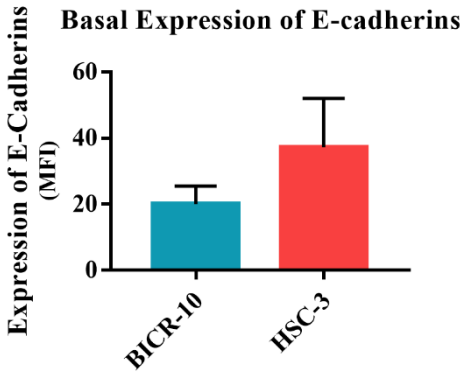

Figure 30 – Basal expression of E-cadherin adhesion molecule in BICR-10 and HSC-3 cells. The basal E-cadherin expression was determined by flow cytometry, using Intracell kit, as described in material and methods section. The results represent mean ± SEM of 2 independent experiments, and are expressed in MFI. MFI, Mean Fluorescence intensity.

In Figure 31 we can see the expression levels of E-cadherins in BICR-10 and HSC-3 cell lines after treatment with the drugs in the conditions referred in the Figure. As we can observe, only in the BICR-10 cells treated with the association of Cisplatin with Lidocaine and 5FU with Mepivacaine, we assisted to a significant increase in E-cadherins expression levels ($p<0,01$ and $p<0,05$, respectively). In HSC-3 cells we didn't detected any significant difference

in the expression levels of E-cadherins, when cells are treated with both LA in monotherapy or in association with Cisplatin and 5-Fluorouracil.

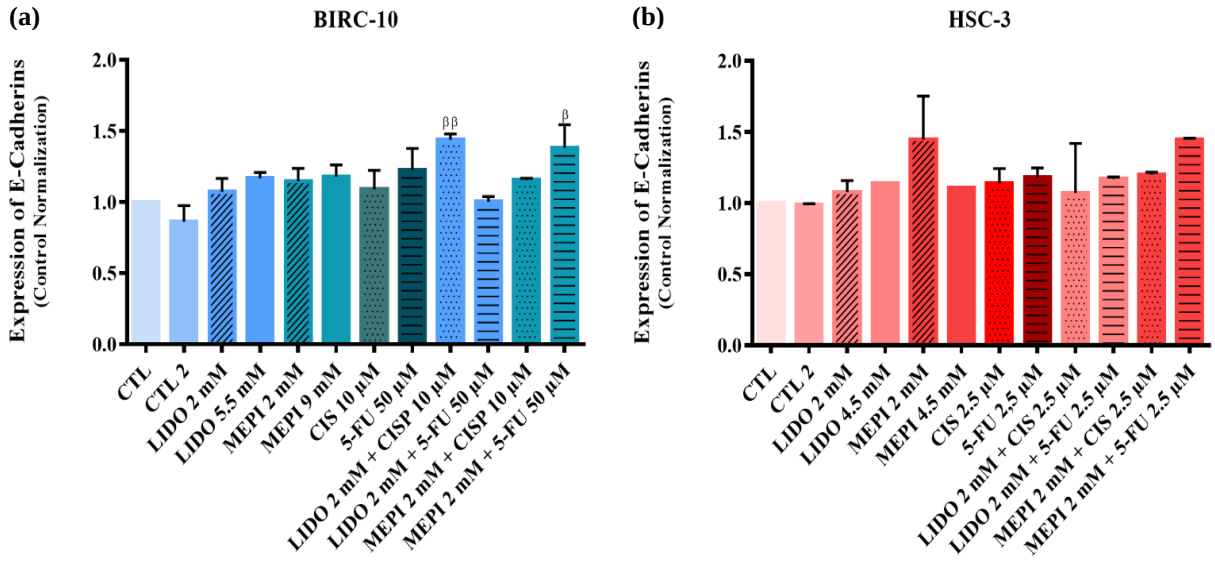

Figure 31 – Expression levels of E-cadherin in (a) BICR-10 and (b) HSC-3 cell lines incubated with Lidocaine and Mepivacaine in monotherapy and associated with Cisplatin and 5-Fluorouracil. Expression of E-cadherin was determined by flow cytometry, using Intracell kit, as described in material and methods section. The results represent mean ± SEM of 2 independent experiments in BICR-10 cells and 1 to 2 independent experiments in HSC-3 cells. The results were normalized to control. CTL, Control; CTL 2, Control 2 (Sodium Chloride + Dimethyl Sulfoxide, NaCl + DMSO); LIDO, Lidocaine; MEPI, Mepivacaine; CIS, Cisplatin; 5-FU, 5-Fluorouracil. β, Statistical difference relative to Control 2 (β $p < 0,05$; ββ $p < 0,01$).

3.4.2. Evaluation of β1-Integrins and β-Catenins by Western Blot

For complete the adhesion molecules profile of OSCC cell lines when incubated with local anesthetics associated with chemotherapeutic drugs, we evaluated the expression of the cell-cell adhesion protein, β-catenin, and the expression of the cell-matrix adhesion protein, β1-Integrin, by western blot. Results represented mean ± SEM and were expressed in percentage of adhesion molecule expression relative to control 2 (NaCl + DMSO) condition as shown in Figure 32. In Figure 33 we can see an image representative of the gel obtained in the western blot analysis.

In generally, in Figure 32 we observe a tendency to a decrease in the expression levels of these adhesion proteins, namely in HSC-3 cells treated with LA alone and in combination with conventional chemotherapeutic drugs, however the results are not statistically significant.

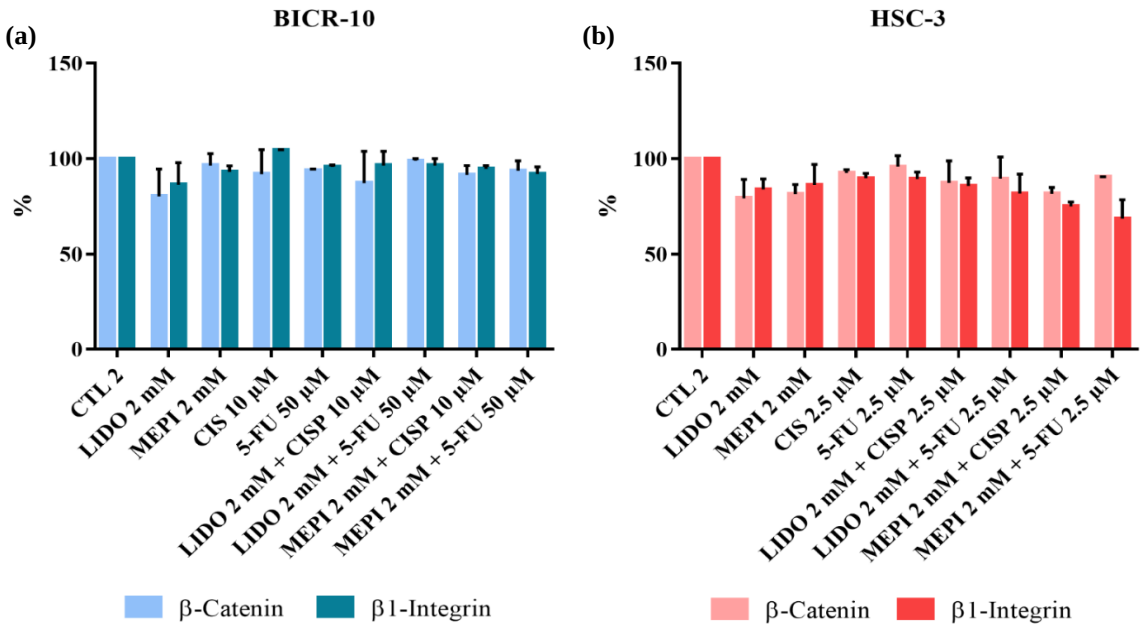

Figure 32 – Expression levels of β-Catenin and β1-Integrin in (a) BICR-10 and (b) HSC-3 cell lines treated with Lidocaine and Mepivacaine in combination with Cisplatin and 5-Fluorouracil. The expression was detected by western blot analysis using specific antibodies. Results represent mean ± SEM of 2 independent experiments and are expressed in percentage of adhesion molecules relative to control 2 condition. CTL 2, Control 2 (Sodium Chloride + Dimethyl Sulfoxide, NaCl + DMSO); LIDO, Lidocaine; MEPI, Mepivacaine; CIS, Cisplatin; 5-FU, 5-Fluorouracil.

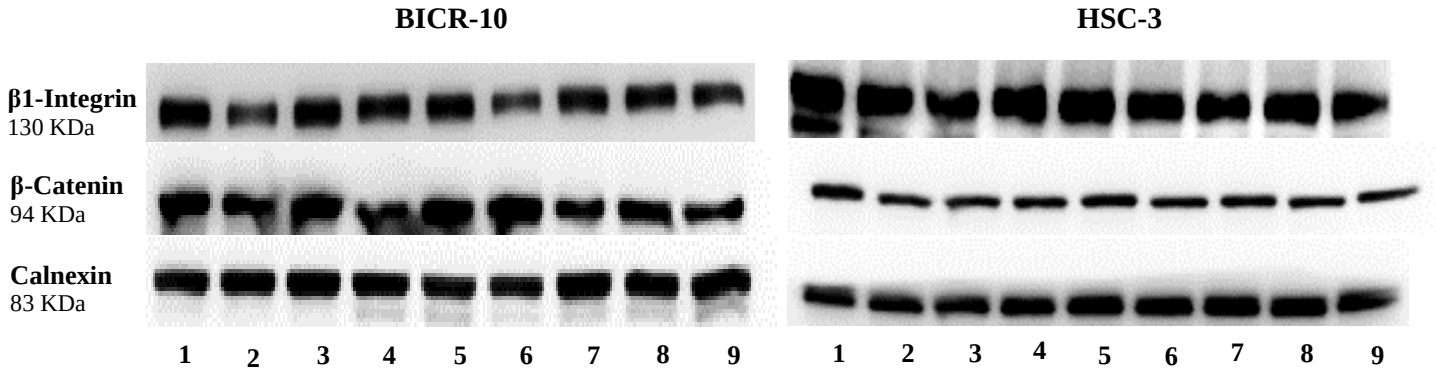

Figure 33 – Gel representative of β-Catenin and β1-Integrin band intensity by Western Blot analysis, in OSCC cell lines treated with local anesthetics in combination with chemotherapeutic drugs. The expression was detected by western blot analysis using specific antibodies. **1**, Control 2 (Sodium Chloride + Dimethyl Sulfoxide, NaCl + DMSO); **2**, Cisplatin at 10 µM for BICR-10 cells and 2,5 µM for HSC-3 cells at 10 µM for BICR-10 cells and 2,5 µM for HSC-3 cells; **3**, 5-Fluorouracil at 50 µM for BICR-10 cells and 2,5 µM for HSC-3 cells; **4**, Lidocaine at 2 mM; **5**, Lidocaine at 2 mM + Cisplatin at 10 µM for BICR-10 cells and 2,5 µM for HSC-3 cells; **6**, Lidocaine at 2 mM + 5-Fluorouracil at 50 µM for BICR-10 cells and 2,5 µM for HSC-3 cells; **7**, Mepivacaine at 2 mM; **8**, Mepivacaine at 2 mM + Cisplatin at 10 µM for BICR-10 cells and 2,5 µM for HSC-3 cells; **9**, Mepivacaine at 2 mM + 5-Fluorouracil at 50 µM for BICR-10 cells and 2,5 µM for HSC-3 cells.

3.4.3. Evaluation of expression levels and proteolytic activity of matrix metalloproteinases 2 and 9 (MMP-2 and MMP-9)

MMP-2 and MMP-9 basal expression levels in OSCC cell lines were analyzed by flow cytometry, using monoclonal antibodies (anti-hMMP-2-FITC and anti-hMMP-9-PE, respectively) labelled with fluorescent probes (Figure 34). The results were expressed in MFI, and represents the mean ± SEM.

The effect in proteolytic activity of MMP-2 and MMP-9 in OSCC cell lines incubated with associations of local anesthetics and chemotherapeutic drugs were analyzed by gelatin zymography, technique that identifies gelatinolytic activity in biological samples (Figure 35). The results were normalized to control and represents mean ± SEM.

In Figure 34 we saw that BICR-10 cells had a basal expression level of both MMP-2 and MMP-9 superior to HCS-3 cells.

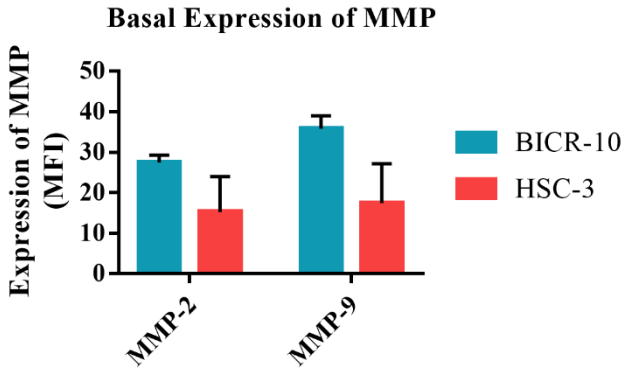

Figure 34 – Basal expression levels of MMP-2 and MMP-9 in BICR-10 and HSC-3 cells. The basal MMP expression was determined by flow cytometry, as described in material and methods section. The results represent mean ± SEM of 2 independent experiments, and are expressed in MFI. MMP, Metalloproteinases; MFI, Mean Fluorescence intensity.

The Figure 35 is representative of a gelatin zymography assay obtained in both OSCC cell lines. It was well perceived the difference of digestion pattern between both cell lines.

BICR-10 cells arrived to that digestion pattern in 24 hours of incubation with drugs, being noticed two different bands, one with molecular weight between 75 and 100 KDa, which correspond to MMP-9 (molecular weight of 82 KDa) and another with molecular weight of 65 KDa, corresponding to molecular weight of MMP-2. The band corresponding to MMP-9 had a lower density when compared with the band corresponding to MMP-2 in BICR-10 cells. The HSC-3 reached to that digestion pattern in 48 hours of drugs incubation. We observed three different bands corresponding to molecular weight of MMP-9 and pro-MMP-2 and MMP-2. Pro-MMP2 and MMP-2 bands had higher density than MMP-9 band.

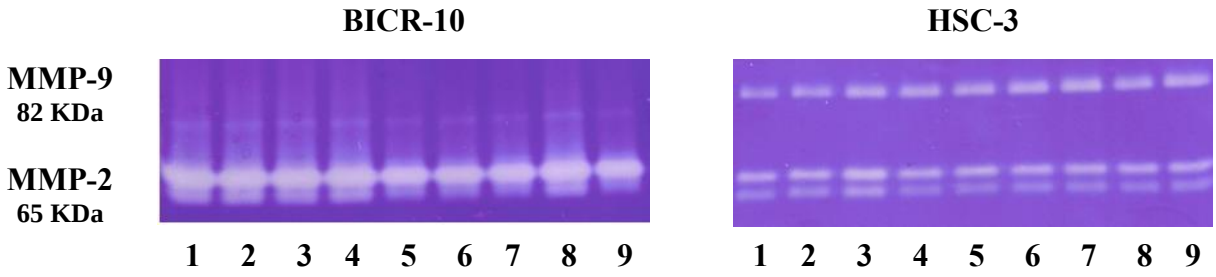

Figure 35 – Gel of zymography assay for evaluation of proteolytic activity of MMP-2 and MMP-9 in BICR-10 and HSC-3 cells incubated with local anesthetics associated with chemotherapeutic drugs. After incubation of BICR-10 cells for 24 hours, and HSC-3 cells for 48 hours, with drugs referred below, the supernatant was collected for analysis, as described in material and methods section. MMP, Metalloproteinases; Conditions: **1**, Control 2 (Sodium Chloride + Dimethyl Sulfoxide); **2**, Cisplatin at 10 µM for BICR-10 cells and at 2,5 µM for HSC-3 cells; **3**, 5-Fluorouracil at 50 µM for BICR-10 cells and at 2,5 µM for HSC-3 cells; **4**, Lidocaine at 2 mM; **5**, Lidocaine at 2 mM + Cisplatin at 10 µM for BICR-10 cells and at 2,5 µM for HSC-3 cells; **6**, Lidocaine at 2 mM + 5-Fluorouracil at 50 µM for BICR-10 cells and at 2,5 µM for HSC-3 cells; **7**, Mepivacaine at 2 mM; **8**, Mepivacaine at 2 mM + Cisplatin at 10 µM for BICR-10 cells and at 2,5 µM for HSC-3 cells; **9**, Mepivacaine at 2 mM + 5-Fluorouracil at 50 µM for BICR-10 cells and at 2,5 µM for HSC-3 cells.

The Figure 36 represented the band intensity of MMP-2 obtained by zymography assay and analyzed by Quantity One software, for both OSCC cell lines incubated with conditions described above. In both OSCC cell lines, only these MMP showed a reduction of activity when incubated with these drug conditions. However the results didn´t show statically significance.

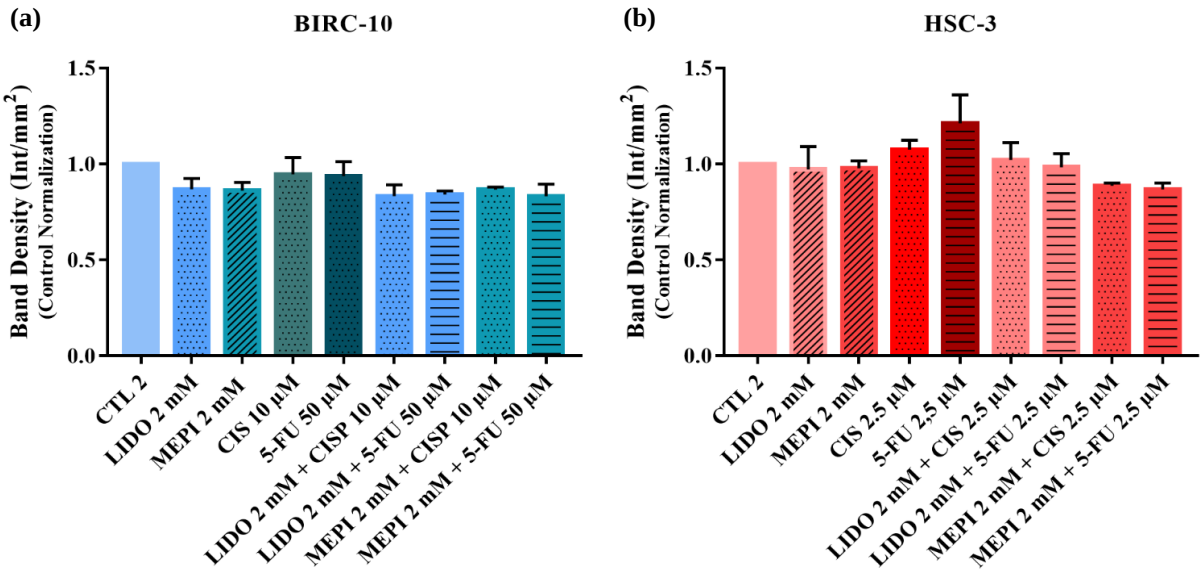

Figure 36 – Detection of MMP-2 proteolytic activity by gelatin zymography in (a) BICR-10 and (b) HSC-3 cell lines incubated with Lidocaine and Mepivacaine associated with Cisplatin and 5-Fluorouracil. After zymography, the gel was analyzed by Quantity One software for determination of band density expressed in Intensity (Int)/mm^2. The results were normalized to control and represents the mean ± SEM of 3 independent experiments in both cell lines. CTL 2, Control 2 (Sodium Chloride + Dimethyl Sulfoxide, NaCl + DMSO); LIDO, Lidocaine; MEPI, Mepivacaine; CIS, Cisplatin; 5-FU, 5-Fluorouracil.

3.4.4. Evaluation of cell migration by Wound Healing Assay

Following the results described above, we aimed to observe the effect of local anesthetics (in monotherapy at IC_{50} dose and in association with cisplatin and 5-fluorouracil) in OSCC cell lines migration capacity using wound healing assay according with Liang *et al.*, 2007, as described in material and methods section. In our experiments we observed the cells capacity of migration before incubation with drugs referred above (0 hours), and after 8 and 24 hours for BICR-10 cell line and 8, 12 and 24 hours for HSC-3 cell line, of their administration (Figures 37 to 40). The results represent the open area of scratch. They were normalized to control and are expressed as mean ± SEM.

BICR-10 cells showed capacity of migration, being the open area at 24 hours in control condition of 0,432 ± 0,062. The open area of scratch was higher than control at 24 hours for IC_{50} dose of Lidocaine (5,5 mM) and Mepivacaine (9 mM), being the mean ± SEM of 0,754 ± 0,116 and 0,80 ± 0,256, respectively (Figures 37 and 38, and Table 4).

At 24 hours, associations of Lidocaine and Mepivacaine with Cisplatin, showed a higher open area of scratch (0,646 ± 0,086 and 0,735 ± 0,181, respectively) when compared with Cisplatin alone (0 ± 0), having the differences statistical significance ($p < 0,05$). The association of Lidocaine and Mepivacaine with 5-Fluorouracil at 24 hours, showed a higher open area of scratch than 5-Fluorouracil alone, although not statically significant.

At 24 hours, BICR-10 cells incubated with conditions where Mepivacaine was present showed a tendency to maintain a higher scratch open area than BICR-10 cells incubated with conditions prepared with Lidocaine.

Table 4 – Results of wound healing assay in BICR-10 cell line incubated with Lidocaine and Mepivacaine in monotherapy and in association with Cisplatin and 5-Flourouracil at 8 and 24 hours.

DRUG CONDITIONS	8 h	24 h
CTL	0,968 ± 0,087	0,432 ± 0,062
CTL 2	0,645	0,304 ± 0,153
LIDO 2 mM	0,836 ± 0,123	0,753 ± 0,1
LIDO 5,5 mM	0,712	0,754 ± 0,116
MEPI 2 mM	1,009 ± 0,028	0,768 ± 0,032
MEPI 9 mM	0,982	0,80 ± 0,256
CIS 10 µM	0,793 ± 0,253	0 ± 0
5-FU 50 µM	0,8256 ± 0,041	0,213 ± 0,135
LIDO 2mM + CIS 10 µM	0,915 ± 0,022	0,646 ± 0,086
LIDO 2 mM + 5-FU 50 µM	1,048 ± 0,122	0,629 ± 0,169
MEPI 2 mM + CIS 10 µM	0,964 ± 0,069	0,735 ± 0,181
MEPI 2 mM + 5-FU 50 µM	0,834 ± 0,020	0,689 ± 0,178

The wound healing assay were realized as described previously in material and methods section. The results represent the open area of scratch normalized to control. They are expressed as mean ± SEM of 1 to 3 independent experiments. CTL, Control; CTL 2, Control 2 (Sodium Chloride + Dimethyl Sulfoxide, NaCl + DMSO); LIDO, Lidocaine; MEPI, Mepivacaine; CIS, Cisplatin; 5-FU, 5-Fluorouracil.

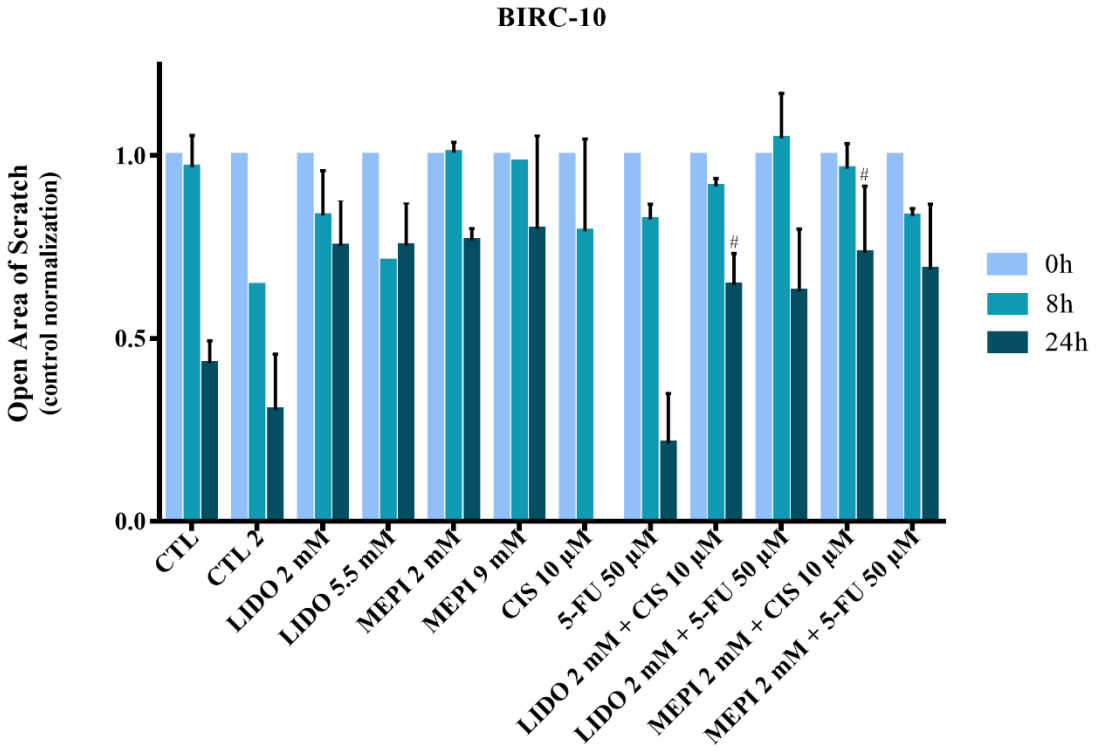

Figure 37 – Cell migration of BICR-10 cells at 0, 8 and 24 hours when incubated with Lidocaine and Mepivacaine in monotherapy and in association with Cisplatin and 5-Fluorouracil. The wound healing assay were realized as described previously in material and methods section. The results represents the open area of scratch normalized to control. They are expressed as mean ± SEM, and represents 2 or more independent experiments, with exception of conditions NaCl + DMSO, LIDO 5,5 mM and MEPI 9 mM at 8 hours. CTL, Control; CTL 2, Control 2 (Sodium Chloride + Dimethyl Sulfoxide, NaCl + DMSO); LIDO, Lidocaine; MEPI, Mepivacaine; CIS, Cisplatin; 5-FU, 5-Fluorouracil. # - Statistical difference relative to Cisplatin 10 µM (# $p < 0,05$).

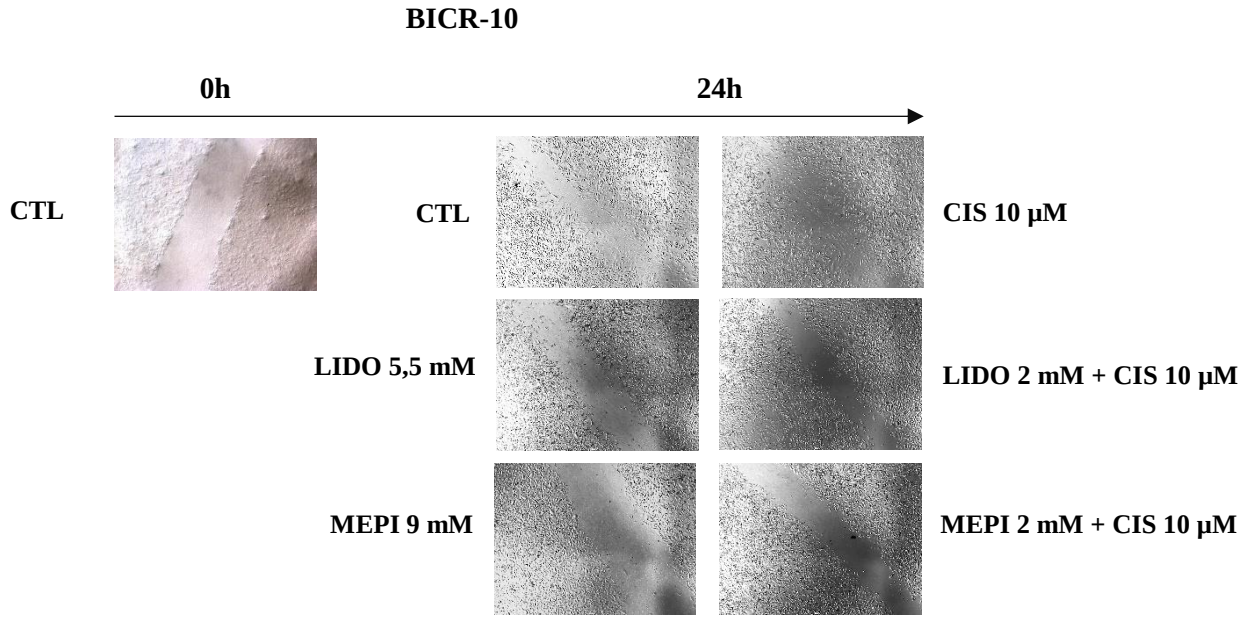

Figure 38 - Scratch wound healing assay images of BICR-10 cell lines incubated with local anesthetics in monotherapy and in association with Cisplatin, at 0 and 24 hours. The results are representative of optical microscopy images of BICR-10 cells scratch of control, Lidocaine, Mepivacaine, Cisplatin, and association of Lidocaine and Mepivacaine with Cisplatin conditions, at concentrations described in the figure, at 0 and 24 hours of drug incubation (40x magnification). CTL, Control; LIDO, Lidocaine; MEPI, Mepivacaine; CIS, Cisplatin.

HSC-3 cell line showed an important capacity of migration, being open area of scratch for control condition, at 24 hours, of 0,001 ± 0,001 (Figure 39 and 40).

At 12 hours of HSC-3 cells incubation with IC_{50} dose of local anesthetics, we observed a higher scratch open area for Mepivacaine at 4,5 mM than for Lidocaine at 4,5 mM, 0,674 ± 0,041 and 0,541 ± 0,230, respectively. At 24 hours, we observed that cells incubated with Mepivacaine at 4,5 mM had higher open area of scratch than cells incubated with Lidocaine at 4,5 mM, 0,796 ± 0,063 and $7{,}04 \times 10^{-6}$, respectively. However, the result obtained with Lidocaine at 4,5 mM was not expected, since open area of scratch for Lidocaine at 2 mM at same hour was 0,576 ± 0,070. Taking into account the result obtained for Lidocaine at 2 mM condition, and the fact of Lidocaine at 4,5 mM condition has only 1 independent experiment and the result was not concordant with expected, we will not proceed with this results analysis.

There are in progress more independent experiments to clarify this particular result. Mepivacaine at 4,5 mM showed an higher open area of scratch for 24 hours than for 12 hours, although not statistically significant.

Besides in cells in NaCl + DMSO condition (control 2) at 12 and 24 hours did not show differences relative to control, when we compare the results obtained at 12 and 24 hours for control 2 (12 hours: 0,248 ± 0,079; 24 hours: $2{,}75x10^{-5}$ ± $2{,}75x10^{-5}$) and Lidocaine associated with Cisplatin (12 hours: 0,841 ± 0,107; 24 hours: 0,593 ± 0,155) and 5-Fluorouracil (12 hours: 0,620 ± 0,051; 24 hours: 0,552 ± 0,011), we observed an important increase of open area of scratch in last conditions. For both associations, and relative to control 2 condition, the differences were statistically significant at 12 hours ($p<0{,}001$, and $p<0{,}05$, respectively), and 24 hours ($p< 0{,}001$, and $p< 0{,}01$, respectively).

Analyzing the results obtained at 12 and 24 hours for control 2 (NaCl + DMSO) condition, and Mepivacaine associated with Cisplatin (12 hours: 0,692 ± 0,066; 24 hours: 0,290 ± 0,082) and associated with 5-Fluorouracil (12 hours: 0,835 ± 0,093; 24 hours: 0,512 ± 0,105), the open area of scratch was higher for drugs associations. The differences were statistically significant at 12 hours for both associations ($p< 0{,}05$, and $p< 0{,}001$, respectively), and at 24 hours for Mepivacaine associated with 5-Fluorouracil ($p < 0{,}01$).

Furthermore, at 12 and 24 hours, associations of Lidocaine and Mepivacaine with Cisplatin showed a higher open area of scratch when compared with Cisplatin alone (12 hours: 0,435 ± 0,134; 24 hours: 0 ± 0), having statistical significance the association of Lidocaine with Cisplatin at two different hours ($p < 0{,}05$). The same was observed for Lidocaine and Mepivacaine in association with 5-Fluorouracil when compared with 5-Fluorouracil (12 hours: 0,551 ± 0,052; 24 hours: 0,0003 ± 0,0003). At 24 hours, the differences were statistically significant for both associations ($p < 0{,}05$, and $p < 0{,}01$, respectively).

The table 5 and the figure 39 are representative of results described above for HSC-3 cells.

Table 5 – Results of wound healing assay in HSC-3 cell line incubated with Lidocaine and Mepivacaine in monotherapy and in association with Cisplatin and 5-Flourouracil at 8, 12 and 24 hours.

DRUG CONDITIONS	8 h	12 h	24 h
CTL	0,75 ± 0,073	0,246 ± 0,053	0,001 ± 0.001
CTL 2	0,840 ± 0,079	0,248 ± 0,031	$2{,}75x10^{-5}$ ± $2{,}75x10^{-5}$
LIDO 2 mM	0,900 ± 0,091	0,796 ± 0,026	0,576 ± 0,070
LIDO 4,5 mM	0,772 ± 0,051	0,541 ± 0,230	$7{,}04x10^{-6}$
MEPI 2 mM	1,062 ± 0,159	0,584 ± 0,038	0,265 ± 0,040
MEPI 4,5 mM	0,964 ± 0,083	0,674 ± 0,041	0,796 ± 0,063
CIS 2,5 µM	0,731 ± 0,098	0,435 ± 0,134	0 ± 0
5-FU 2,5 µM	0,707 ± 0,089	0,551 ± 0,052	0,0003 ± 0,0003
LIDO 2mM + CIS 2,5 µM	0,972 ± 0,069	0,841 ± 0,107	0,593 ± 0,155
LIDO 2 mM + 5-FU 2,5 µM	0,861 ± 0,048	0,620 ± 0,051	0,552 ± 0,011
MEPI 2 mM + CIS 2,5 µM	0,974 ± 0,084	0,692 ± 0,066	0,290 ± 0,082
MEPI 2 mM + 5-FU 2,5 µM	0,895 ± 0,081	0,835 ± 0,093	0,512 ± 0,105

The wound healing assay were realized as described previously in material and methods section. The results represents the open area of scratch normalized to control. They are expressed as mean ± SEM of 1 to 6 independent experiments. CTL, Control; CTL 2, Control 2 (Sodium Chloride + Dimethyl Sulfoxide, NaCl + DMSO); LIDO, Lidocaine; MEPI, Mepivacaine; CIS, Cisplatin; 5-FU, 5-Fluorouracil.

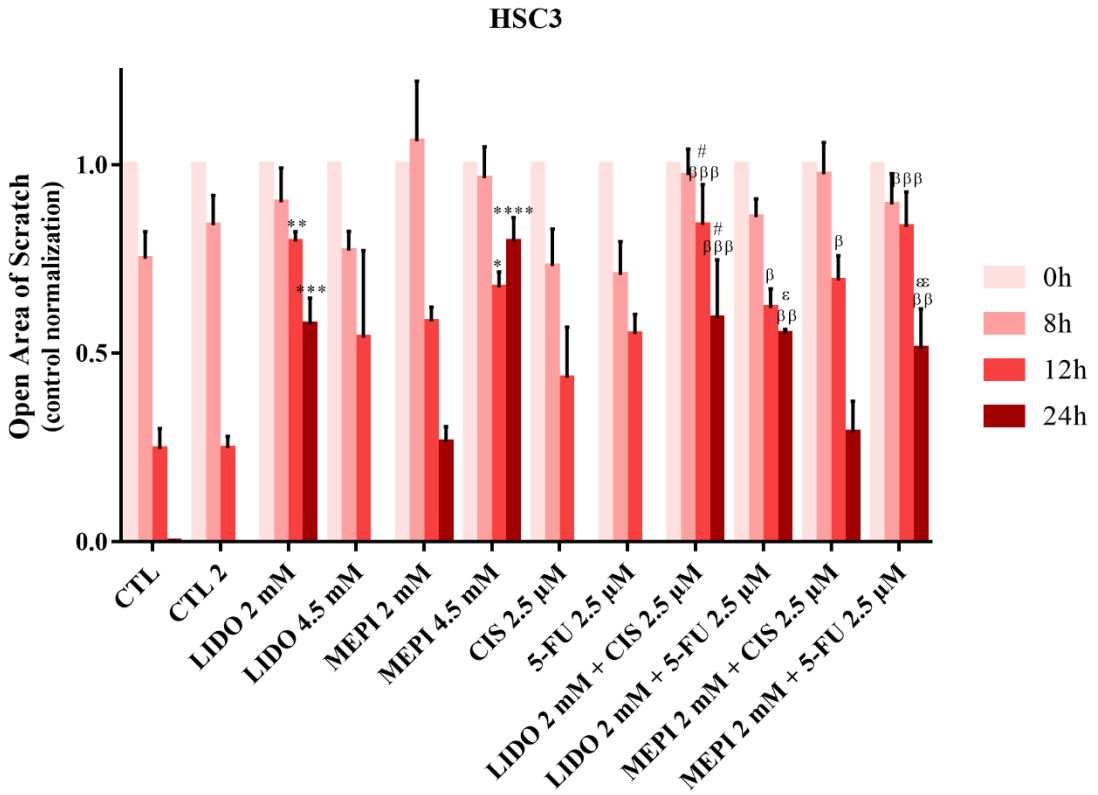

Figure 39 – Cell migration of HSC-3 cells at 0, 8, 12 and 24 hours when incubated with Lidocaine and Mepivacaine in monotherapy and in association with Cisplatin and 5-Fluorouracil. The wound healing assay were realized as described previously in material and methods section. The results represents the open area of scratch normalized to control. They are expressed as mean ± SEM, and represents 2 or more independent experiments, with exception of LIDO 4,5 mM condition, at 24 hours. CTL, Control; CTL 2, Control 2 (Sodium Chloride + Dimethyl Sulfoxide, NaCl + DMSO); LIDO, Lidocaine; MEPI, Mepivacaine; CIS, Cisplatin; 5-FU, 5-Fluorouracil. *, Statistical difference relative to Control (* $p < 0,05$; ** $p < 0,01$; *** $p < 0,001$; **** $p < 0,0001$); β, Statistical difference relative to Control 2 (β $p < 0,05$; ββ $p < 0,01$; βββ $p < 0,001$); #, Statistical difference relative to Cisplatin 2,5 µM (# $p < 0,05$); ε, Statistical difference relative to 5-Fluorouracil (ε $p < 0,05$; εε $p < 0,01$).

The figure 40 represents optical microscopy images, for 0 and 12 hours of incubation of HSC-3 cells with local anesthetics in monotherapy at IC_{50} dose, and in association with Cisplatin.

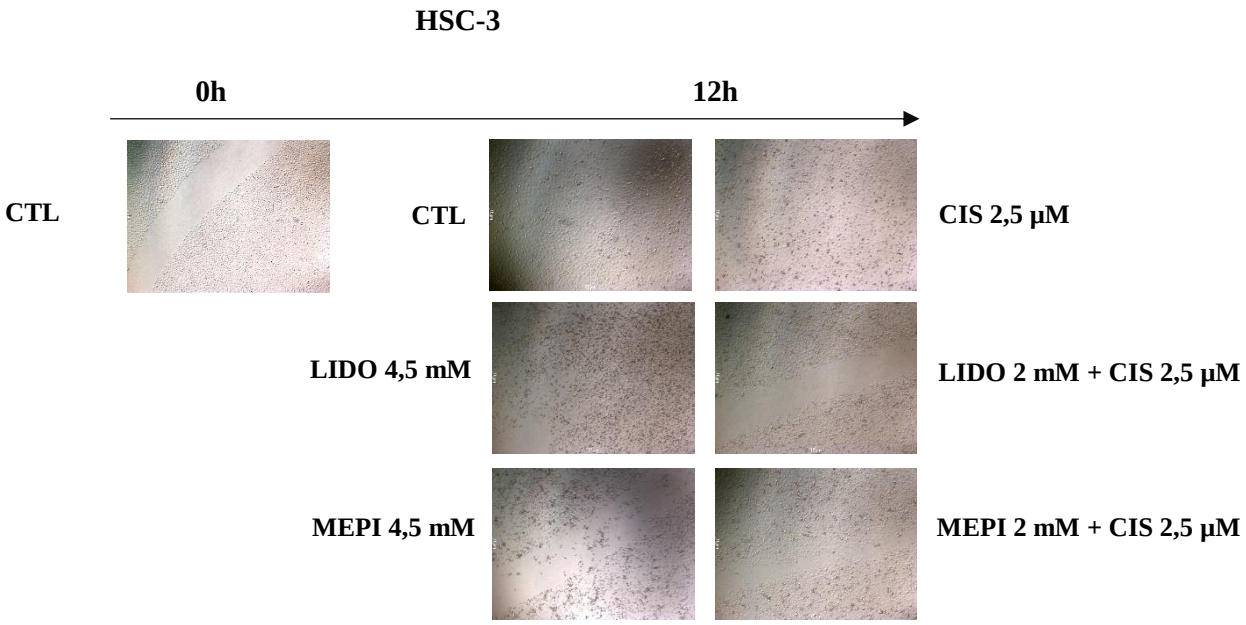

Figure 40 - Scratch wound healing assay images of HSC-3 cell lines incubated with local anesthetics in monotherapy and in association with Cisplatin, at 0 and 12 hours. The results are representative of optical microscopy images of HSC-3 cells scratch of control, Lidocaine, Mepivacaine, Cisplatin, and association of Lidocaine and Mepivacaine with Cisplatin conditions, at concentrations described in the figure, at 0 and 12 hours of drug incubation (40x magnification). CTL, Control; LIDO, Lidocaine; MEPI, Mepivacaine; CIS, Cisplatin.

4. DISCUSSION

Oral cancer (OC) is estimated to be the sixth most common cancer and the eighth most frequent cause of cancer related deaths worldwide, being a major public health problem (Nema R *et al.*, 2016). Its incidence in Europe ranges from 2% to 6% among all cancer patients (Tsantoulis PK *et al.*, 2007). In 2008, oral and pharyngeal cancer in Portugal represented the sixth most common cancer in men and the sixteenth in women. In a recent review Monteiro LS et al. 2013 observed an increase incidence trend in both sex of 3,49% per year. Oral squamous cell carcinoma (OSCC) correspond to 90% of cancer of head and neck region (Nema R *et al.*, 2016; Tsantoulis PK *et al.*, 2007; Lippman SM *et al.*, 2005; Hsu S *et al.*, 2004).

The development of OSCC is a complex multistep process. Transformation of normal keratinocytes through cytogenetic and epigenetic processes lead to alteration of cell cycle, DNA repair mechanisms, cell differentiation and apoptosis, with consequently mutations that ends in a malignant neoplasia. Microenvironment tumor alterations, including modifications in adhesion and extracellular matrix molecules, contributes to proliferation, invasion, migration and metastasis (Rivera C, 2015).

OSCC patients have an average 5-year survival rate of 50%. Despite therapeutic advances over the past three decades the survival rate has not increased (Nema R *et al.*, 2016; Rivera C, 2015; Lippman SM *et al.*, 2005; Ziober BL *et al.*, 2001).

Surgical resection and adjuvant therapies are the mainstay treatment for solid tumors, as OSCC. Adjuvant therapies for OSCC are radiotherapy and chemotherapy, with agents such as Cisplatin and 5-Fluorouracil (Rivera C, 2015). However, tumor cells can be released on circulation, increasing the risk of metastatic disease. Other per-operative factors implicated in tumorigenesis are metabolic, neuroendocrine and inflammatory alterations, and compromise immunological response, which determine upregulation of major malignant molecular pathways (Xuan W *et al.*, 2015; Fodale V *et al.*, 2014; Mao L *et al.*, 2013;Yeager MP *et al.*, 2010)

There are many recent studies that discuss the role of anesthesia on cancer surgery and outcomes, including the effect of local anesthetics. Adding to analgesic, antiarrhythmic, anti-inflammatory and antimicrobial properties, local anesthetics appear as protective against tumor growth and metastasis in many in vitro and in vivo studies, performed in different cancer types. They act via several mechanisms, including direct cytotoxicity and induction of apoptosis; inhibition of proliferation, migration, and invasion. They also can modulate gene expression via methylation (Tedore T, 2015; Chang YC, Hsu YC *et al.*, 2014)

In our investigation we studied the effect of local anesthetics, namely Lidocaine and Mepivacaine, in proliferation, adhesion and migration potential of two OSCC cell lines, BICR-10 (in situ carcinoma) and HSC-3 (metastatic carcinoma). With the objective to improve outcomes and/or reduce dose of conventional drug administrated, and so decrease potential adverse side effects, we also studied if the association of low doses of the local anesthetics with conventional chemotherapeutic drugs, Cisplatin and 5-Fluorouracil, have synergic effect. Briefly, we began to study in BICR-10 and HSC-3 cell lines, the effect of Lidocaine and Mepivacaine in cell viability, the type of cell death and its mechanisms, and their anti-proliferative effect. In the next step, we evaluated its influence in adhesion molecules expression and cell migration potential.

In the present study, we verified that both Lidocaine and Mepivacaine induced a reduction in OSCC cell lines viability in a dose, time and cell type dependent manner. HSC-3 showed more sensitive than the BICR-10 cells, probably due to its pronounced proliferative potential relative to BICR-10 cells. These results are in concordance with Kamiya M *et al.*, (2006) that showed that Lidocaine in human histiocytic lymphoma reduced cell viability in dose- and time-dependent manner. These same results were verified in thyroid and breast cancer cell lines (Chang YA, Hsu YC *et al.*, 2014; Chang YA, Liu CL *et al.*, 2014). Chang YA, Liu

CL *et al.*, (2014) noticed that malignant breast cancer cells were the more susceptible to local anesthetics effects.

In our study, the daily administration of lower doses of local anesthetics did not show any advantage in reduction of BICR-10 and HSC-3 cells viability relative to administration of a single dose. These results suggests that the highest benefit in reduction of OSCC cell lines viability may be achieved by unique administration of higher concentrations of local anesthetics, with the concentrations tested being used in clinical practice.

In HSC-3 cells the association of lower doses of Lidocaine and Mepivacaine (2 mM) with Cisplatin and 5-Fluorouracil showed a tendency to reduction in cell viability relative to cells treated with conventional chemotherapeutic drugs in monotherapy. These results favor the hypothesis of a synergic effect of these drugs suggesting its potential role in the treatment of metastatic OSCC. For *in situ* OSCC (BICR-10 cells), the synergic effect in cell viability of local anesthetics plus conventional chemotherapeutic drugs is only seen with Lidocaine.

So, in this study we observed a reduction in OSCC cell lines viability with local anesthetics Lidocaine and Mepivacaine in monotherapy in a dose-, time-, type cellular- and schedule-dependent manner. These results may justify intra-operative use of Lidocaine and Mepivacaine (namely tissue infiltration), not only for analgesic proposes, but to potentially reduce cancer cell viability. Combination of local anesthetics with chemotherapeutic drugs, Cisplatin and 5-Fluorouracil at lower doses showed a synergic effect relative to conventional treatment, which may led to new therapeutic options with less adverse effects, namely in metastatic OSCC cell lines.

After observing the effects of local anesthetics and its associations with chemotherapeutic drugs in OSCC cells viability, we proceed to evaluate their effects in cell death (cytotoxic effect) and cell cycle (anti-proliferative effect).

Results in this study showed that, both Lidocaine and Mepivacaine had cytotoxic effects in metastatic OSCC cells, without inducing arrest in cell cycle. The type of cell death predominantly seen in cells treated with these two drugs was late apoptosis/necrosis, which was corroborated by typical morphological characteristics observed at optical microscopy and by the pre-G1 peak observed in cell cycle analysis. In in situ OSCC cells, we observed a tendency to local anesthetics induce cytotoxic effects, especially Mepivacaine, without alteration of cell cycle profile.

In the literature the cytotoxic effect or anti-proliferative effect induced by local anesthetics differs with the dose of local anesthetic used and the type of cancer cell line studied. Our results were supported by some studies, like Sakaguchi M *et al.,* (2006) that observed in human tongue cancer cells, that Lidocaine induced anti-proliferative effect in concentrations of 400 µM and a cytotoxic effect at 4000 µM. Kobayashi K *et al.,* (2012) showed that Lidocaine and Mepivacaine induced cytotoxicity toward OSCC cell lines (including HSC-3) at similar doses used in our study, and that dibucaine had cytotoxic but not cytostatic effects in OSCC cells. In thyroid cancer cells and human histiocytic lymphoma cells, Lidocaine induced cell death by apoptosis at lower doses and necrosis in higher doses, without inducing the arrest of cell cycle. In Jurkat Wild-type cells and in neuroblastoma cells, Lidocaine also induced apoptosis at lower doses and necrosis at higher doses. (Werdehausen R *et al.,* 2007 and 2009) Sakaguchi M *et al.,* (2006) reports that Lidocaine suppresses the proliferation of human tongue squamous cell carcinoma with inhibition of the tyrosine kinase activity of the Epidermal Growth Factor Receptor (EGFR).

Comparing HSC-3 cell line treated with chemotherapeutic drugs in monotherapy and with association of these drugs with local anesthetics, we observed a significant increase in anti-proliferative effect for combined treatment. Association of Lidocaine with Cisplatin resulted in cell cycle blocking in G2/M phase, while association of Mepivacaine with Cisplatin and

associations of both local anesthetics with 5-Fluorouracil resulted in cell cycle arrest in S phase. Only the association of Mepivacaine with Cisplatin showed an increase in cytotoxic effect (with predominance of late apoptosis/necrosis) relative to Cisplatin in monotherapy. In BICR-10 cell line was not visible any anti-proliferative effect with combined therapy, with no alteration of cell cycle profile. Association of Mepivacaine and Cisplatin as in metastatic cell line showed a tendency to higher cytotoxic effect (with increase in late apoptosis/necrosis and necrosis) when compared with cells treated with Cisplatin alone.

This anti-proliferative effect, seen at lower doses of local anesthetics associated with Cisplatin and 5-Fluorouracil, is probably related with induction of a blockade in MAPK/ERK signaling pathways, which regulate cell cycle progression involving cyclin and cyclin-dependent kinases. That signaling pathways were described as involved in molecular mechanism of apoptosis of local anesthetics at higher doses (Chang YC, Hsu YC *et al.*, 2014).

So, in metastatic OSCC cells local anesthetics induced cytotoxic effects, with late apoptosis/necrosis being the type of cell death more prevalent. When associated with conventional chemotherapeutic drugs, we observed a pronounced cytostatic effect relative to chemotherapeutic drugs in monotherapy.

Furthermore, in BICR-10 cells Lidocaine and Mepivacaine at IC_{50} doses led to an increase in caspase activity and O_2^- production. Mitochondrial dysfunction occurred mainly with Mepivacaine and not with Lidocaine. This result confirms apoptosis as the main mechanism of cytotoxicity in in situ OSCC cells, although through different mechanisms: Lidocaine through mitochondrial pathway and Mepivacaine probably through extrinsic pathway.

Our results showed that in metastatic OSCC cells (HSC-3 cells), both Lidocaine and Mepivacaine induced apoptosis through increasing caspase activity, mitochondrial dysfunction and production of ROS (H_2O_2) that is dose-dependent, which suggest that in HSC-3 cells

apoptosis is caspase and mitochondrial-dependent, probably with activation of intrinsic apoptosis pathway. We supposed that HSC-3 cells were more susceptible to local anesthetic cytotoxicity because they have lower GSH levels relative to BICR-10 cells.

In other experiments, as observed in our study, Lidocaine proved to induce apoptosis through mitochondria and caspase-dependent pathways, mainly by intrinsic apoptotic pathway. This had been referred in human histiocytic lymphoma, in Jurkat wild-type, in neuroblastoma, in cancer thyroid and in breast tumor cell lines (Chang YC, Liu CL *et al.*, 2014; Chang YC, Hsu YC *et al.*, 2014; Werdehausen R *et al.*, 2007; Kamiya Y *et al.*, 2005). These aspects are reinforced by the fact that in various types of cancer cell lines local anesthetics, and mainly Lidocaine, induced mitochondrial dysfunction with loss of membrane mitochondrial potential, release of cytochrome c and activation of caspase-3 and -9 (Chang YC, Hsu YC *et al.*, 2014; Lucchinetti E *et al.*, 2012; Werdehausen R *et al.*, 2007; Kamiya Y *et al.*, 2005). Johnson ME et al., 2004 observed that Lidocaine led to blockade of respiratory chain function of mitochondria in neurons with neurotoxicity mediated by a direct effect on mitochondria. However, there are some studies that implicate extrinsic apoptotic pathway activation by local anesthetics in cancer cells (Chang YC, Liu CL *et al.*, 2014; Chang YC, Hsu YC *et al.*, 2014), which could not be excluded in our study. There are some reports that observed an increase in ROS production with local anesthetics (Lucchinetti E *et al.*, 2012)

In BICR-10 cells, associations of local anesthetics with Cisplatin led to an increase in caspase activity and ROS (O_2^-) production, which was balanced with a higher increase in GSH anti-oxidant defense. We supposed that the difference between cytotoxicity related with two different associations is that association of Cisplatin with Mepivacaine showed a great increase in mitochondrial dysfunction associated to a higher O_2^- production, which may be the cause of activation of mitochondria-dependent apoptosis and higher cytotoxicity effect.

Our results also showed that in HSC-3 cells the associations of local anesthetics with Cisplatin induced an increase in caspase activity, mitochondrial dysfunction and intracellular ROS production comparative to cells treated only with Cisplatin. The higher cytotoxic effect observed previously with Mepivacaine plus Cisplatin may be due to a reduction in GSH expression levels induced by this association. Associations with 5-Fluorouracil led to a reduction in caspase activity relative to this drug in monotherapy, and to a decrease in membrane mitochondrial potential. We also observed an increase in intracellular ROS production and GSH expression. These results suggests that in metastatic OSCC cells the anti-proliferative effect and, at lesser extent, cytotoxic effect observed with associations of local anesthetics with conventional chemotherapeutic drugs may be due to mitochondrial dysfunction.

Ohara T *et al.*, (2009) shows that OSCC patients with higher expression levels of α3, α6, and β1-integrins has better prognosis than those with lower expression levels, showing β1-integrin expression the highest correlation with clinical and pathological characteristics.

Then, we proposed to study the influence of local anesthetics and its association with Cisplatin and 5-Fluorouracil in cell adhesion and migration in OSCC cell lines.

With regard to adhesion molecules β1-Integrin and β-Catenin our results showed a tendency to a decreased expression in both adhesion molecules when comparing OSCC cell lines treated with conventional chemotherapeutic drugs and with associations of local anesthetics and chemotherapeutic drugs, namely in HSC-3 cells. In in situ and metastatic OSCC cells we observed a tendency to increase expression levels of E-cadherin with association of Mepivacaine with 5-Fluorouracil, which suggest an increase in cell-cell adhesion, with consequently decrease in invasion and migration potential.

The immunohistochemical expression of MMP-2 and -9 is related to the invasive potential of OSCC (PK Tsantoulis *et al.*, 2007). Several studies in oral cancer show an

association of MMP-2 expression with local invasiveness, cervical nodal and occult metastasis and prognosis and MMP-9 expression with cervical nodal and distant metastasis and survival rates (Sei Young Lee *et al.,* 2011). However, MMP-2 expression seems to be more prominent than MMP-9 in OSCC samples (PK Tsantoulis *et al.*, 2007).

Our study showed that both OSCC cells expressed MMP-2 and MMP-9. When treated with combined therapy (local anesthetics and chemotherapeutic drugs) both BICR-10 and HSC-3 cells showed a decrease in MMP-2 proteolytic activity compared with treatment with chemotherapeutic drugs in monotherapy, with HSC-3 having the highest reduction. These results suggest that the association of both local anesthetics with Cisplatin or 5-Fluorouracil may have an important effect in reduction of invasion and migration, and consequently in the metastization potential, namely of metastatic OSCC cells, by reducing proteolytic activity of MMP-2.

Lucchinetti E *et al.*, (2012) observed that local anesthetic Ropivacaine (amide-type local anesthetic, as Lidocaine and Mepivacaine) has an inhibitory effect on cell migration.

Our results corroborate the same conclusion, suggesting that Lidocaine and Mepivacaine in BICR-10 and HSC-3 cells led to a significantly reduction in cell migration. The same could be affirmed when comparing OSCC cells treated in monotherapy with Cisplatin or 5-Fluorouracil and treated with these drugs associated with Lidocaine or Mepivacaine. We propose that local anesthetics have an important role in decrease migration in OSCC cells, and consequently in invasion and metastization, namely in HSC-3 cells, presenting a synergic effect with Cisplatin and 5-Fluorouracil.

5. CONCLUSION

In OSCC cells lines LA induce a decrease in cell viability and an increase in cell death namely by apoptosis which is dependent on the dose, cell type and scheme of drug administration. Furthermore, the inhibition on cell invasion could be a good therapeutic approach in metastatic cancer

The synergistic effect observed between the LA and conventional cytostatics could contribute to the decrease in the adverse effects mediated by chemotherapeutic drugs.

These results suggests a new clinical therapeutic approach, namely for metastatic OSCC, with association of local anesthetics with conventional chemotherapies agents showing higher decrease in cancer cells viability and in the metastatic potential.

6. REFERENCES

Borgeat A, Aguirre J. Update on local anesthetics. *Current Opinion in Anaesthesiology*, 2010; 23: 466-471.

Boselli E, Duflo F, Debon F, Allaouchiche B, Cassard D, Thomas L, Portoukalian J. The Induction of Apoptosis by Local Anesthetics: A Comparison Between Lidocaine and Ropivacaine. *Anesthesia & Analgesia*, 2003; 96: 755-756.

Bruin EC, Medema JP. Apoptosis and non-apoptotic deaths in cancer development and treatment response. *Cancer Treatment Reviews*, 2008; 34: 737-749.

Chaabane W, User SD, El-Gazzah M, Jaksik R, Sajjadi E, Rzeszowska-Wolny J, Los MJ. Autophagy, Apoptosis, Mitoptosis and Necrosis: Interdependence Between Those Pathways and Effects on Cancer. *Archivum Immunologiae et Therapiae Experimentalis*, 2013; 61: 43-58.

Chaffer CL, Weinberg RA. A perspective on cancer Cell Metastasis. *Science*, 2011; 331: 1559-1564.

Calatayud J, González A. History of the Development and Evolution of Local Anesthesia Since the Coca Leaf. *Anesthesiology*, 2003; 98: 1503-1508.

Chang YC, Hsu YC, Liu CL, Huang SY, Hu MC, Cheng SP. Local Anesthetics induce Apoptosis in Human Thyroid Cancer Cells through the Mitogen-Activated Protein Kinase Pathway. *PLOS ONE*, 2014; 9(2):1-11.

Chang YC, Liu CL, Chen MJ, Hsu YW, Chen SN, Lin CH, Chen CM, Yang FM, Hu MC. Local Anesthetics induce Apoptosis in Human Breast Tumor Cells. *Anesthesia & Analgesia*, 2014; 118(1):116-124.

Chiang AC, Massagué J. Molecular Origins of Cancer - Molecular Basis of Metastasis. *The New England Journal of Medicine*, 2008; 359: 2814-23.

Cox B, Durieux ME, Marcus MAE. Toxicity of local anaesthetics. *Best Practice & Research Clinical Anaesthesiology*, 2003; 17 (1): 111-136.

Dacie J, Lewis S. Preparation and Staining methods for blood and bone-marrow film. *Pratical Haemathology*. 8th Edition. Churchill Livingstone. Chapter 6: 83-102.

Deegan CA, Murray D, Doran P, Moriarty DC, Daniel I. Sessler, Mascha E, Kavanagh BP, Buggy DJ. Anesthetic Technique and The Cytokine and matrix Metalloproteinase response to Primary Breast Cancer Surgery. *Regional Anesthesia and Pain Medicine*, 2010; 35(6):490-495.

Dourado M, Sarmento AB, Pereira SV, Alves V, Silva T, Pinto AM, Rosa MS. CD26/DPPIV expression and 8-azaguanine response in T-acute lymphoblastic leucemia cell lines in culture. *Pathophysiology*, 2007; 14(1):3-10.

Fodale V, D´Arrigo MG, Triolo S, Mondello S, La Torre D. Anesthetic Techniques and Cancer Recurrence after Surgery. *The Scientific World Journal*, 2014; 1-10.

Gebäck T, Schulz MMP, Koumoutsakos P, Detmar M. A novel and simple software tool for automated analysis of monolayer wound healing assays. *BioTechniques*, 2008.

Gomes A, Fernandes E, Lima JLFC. Fluorescence probes used for detection of reactive oxygen species. *Journal of Biochemical and Biophysical Methods*, 2005; 65:45-80.

Gonçalves AC, Alves V, Silva T, Carvalho C, Oliveira CR, Sarmento-Ribeiro AB. Oxydative stress mediates apoptotic effects of ascorbate and dehydroascorbate in human Myelodysplasia cells in vitro. *Toxicology in Vitro*, 2013; 27:1542-1549.

Gonçalves AC, Barbosa-Ribeiro A, Alves V, Silva T, Sarmento-Ribeiro AB. Selenium Compounds Induced ROS-Dependent Apoptosis in Myelodysplasia Cells. *Biological Trace Element Research*, 2013; 154:440-447.

Hadzic A, Carrera A, Clark T, Gadsden J, Karmakar M, Sala-Blanch X, Vandepitte C, Xu D. *Hadzic´s Peripheral Nerve Blocks and Anatomy for Ultrasound-Guided Regional Anesthesia.* 2th Edition. Mc Graw Hill Medical, 2012; Chapter 2:29-40.

Halliwell B, Whiteman M. Measuring reactive species and oxidative damage in vivo and in cell culture: how should you do it and what do the results mean?. *British Journal of Pharmacology*, 2004; 142: 231-255.

Hanahan D, Weinberg RA. Hallmarks of Cancer: The Next Generation. *Cell*, 2011; 144, March 4: 646-674.

Hedley DW, Chow S. Evaluation of Methods for Measuring Cellular Glutathione Content Using Flow Cytometry. *Cytometry*, 1994; 15:349-358.

Howen B. Blood Film Preparation and Staining Procedures. *Laboratory Hematology*, 2000; 6(1):1-7.

Hsu S, Singh B, Schuster G. Induction of apoptosis in oral cancer cells: agents and mechanisms for potential therapy and prevention. *Oral Oncology*, 2004; 40:461-473.

Hu X, Beeton C. Detection of Functional Matrix Metalloproteinases by Zymography. *Journal of Visualized Experiments*, 2010; 45:1-4.

Jain MV, Paczulla AM, Klonisch T, Dimgba FN, Rao SB, Roberg K, Schweizer F, Lengerke C, Davoodpour P, Palicharla VR, Maddika S, Los M. Interconnections between apoptotic, autophagic and necrotic pathways: implications for cancer therapy development. *Journal of Cellular and Molecular Medicine*, 2013; 17(1):12-29.

Jemal A, Bray F, Center MM, Ferlay J, Ward E, Forman D. Global Cancer Statistics. *CA: A Cancer Journal for Clinicians*, 2011; 61:69-90.

Johnson ME, Uhl CB, Spittler KH, Wang H, Gores GJ. Mitochondrial Injury and caspase Activation by the Local Anesthetic Lidocaine. *Anesthesiology*, 2004; 101:1184-94.

Kamiya Y, Ohta K, Kaneko Y. Lidocaine-induced apoptosis and necrosis in U937 cells depending on its dosage. *Biomedical Research*, 2005; 26(6):231-239.

Kobayashi K, Ohno S, Uchida S, Amano O, Sakagami H, Nagasaka H. Cytotoxicity and Type of Cell death induced by Local Anesthetics in Human Oral Normal and Tumor cells. *Anticancer Research*, 2012: 32: 2925-2934.

Lee SY, Park SY, Kim SH, Choi EC. Expression of Matrix Metalloproteinases and Their Inhibitors in Squamous Cell Carcinoma of the Tonsil and Their Clinical Significance. *Clinical and Experimental Otorhinolaryngology*, 2011; 4 (2): 88-94.

Liang CC, Park AY, Guan JL. In vitro scratch assay: a convenient and inexpensive method for analysis of cell migration in vitro. *Nature Protocols*, 2007; 2(2):329-333.

Lippman SM, Sudbo J, Hong WK. Oral Cancer Prevention and the Evolution of Molecular-Targeted Drug Development. *Journal of Clinical Oncology*, 2005; volume 23, number 2, 10:346-356.

Lirk P, Hollmann MW, Fleischer M, Weber NC, Fiegl H. Lidocaine and ropivacaine, but not bupivacaine, demethylate deoxyribonucleic acid in breast cancer cells in vitro. *British Journal of Anaesthesia*, 2014; 113(S1):i32-i38.

Lucchinetti E, Awad AE, Rahman M, Feng J, Lou PH, Zhang L, Ionescu L, Lemieux H, Thébaud B, Zaugg M. Antiproliferative Effects of Local Anesthetics on Mesenchymal Stem Cells – Potential Implications for Tumor Spreading and Wound Healing. *Anesthesiology*, 2012; 166(4):841-856.

Mammoto T, Higashiyama S, Mukai M, Mammoto A, Ayaki M, Mashimo T, Hayashi Y, Kishi Y, Nakamura H, Akedo H. Infiltration Anesthetic Lidocaine Inhibits Cancer Cell invasion by Modulating Ectodomain Sheeding of Heparin-Binding Epidermal Growth Gactor-Like Growth factor (HB-EGF). *Journal of Cellular Physiology*, 2002; 192:351-358.

Mao L, Lin S, Lin J. The effects of anesthetics on tumor progression. *International Journal of Pathology, Pathophysiology and Pharmacology*, 2013; 5(1):1-10.

Mendes F, Sales T, Domingues C, Schugkl S, Abrantes AM, Casalta-Lopes J, Rocha C, Laranjo M, Simões PC, Ribeiro ABS, Botelho MF, Rosa MS. Effects of X-radiation on lung cancer cells: the interplay between oxidative stress and P53 levels. *Medical Oncology*, 2015; 32:266.

Miller RD, Eriksson LI, Fleisher L, Wiener-Kronish JP, Cohen NH, Young WL. *Miller´s Anesthesia.* 8th Edition. Churchill Livingstone, 2014. Chapter 36:1028-1154.

Monteiro LS, Antunes L, Bento MJ, Warnakulasuriya S. Incidence rates and trends of lip, oral and oro-pharyngeal cancers in Portugal. *Journal of Oral Pathology & Medicine*, 2013; 42:345-351.

Nema R, Vishwakarma S, Agarwal R, Panday RK, Kumar A. Emerging role of sphingosine-1-phosphate signaling in head and neck squamous cell carcinoma. *Journal of Onco Targets and Therapy*, 2016; 9:3269-3280.

O´Brien J, Wilson I, Orton T, Pognan F. Investigation of the Alamar Blue (resazurin) fluorescent dye for the assessment of mammalian cell cytotoxicity. *European Journal of Biochemistry*, 2000; 267:5421-5426.

O´Connor JE, Kirnler BF, Morgan MC, Tempas KJ. A Flow Cytometric Assay for Intracellular Nonprotein Thiols Using Mercury Orange. *Cytometry*, 1988; 9:529-532.

Ohara T, Kawashiri S, Tanaka A, Noguchi N, Kitahara H, Okamune A, Kato K, Hase T, Nakaya H, Yoshizawa K. Integrin Expression Levels Correlate with Invasion, Metastasis and prognosis of Oral Squamous Cell Carcinoma. *Pathology & Oncology Research*, 2009; 15: 429-436.

Perrot S, Dutertre-Catella H, Martin C, Warnet JM, Rat P. A New nondestructive Cytometric Assay Based on Resazurin Metabolism and an Organ Culture Model for the Assessment of Corneal Viability. *Cytometry Part A*, 2003; 55A:7-14.

Ram H, Sarkar J, Kumar H, Konwar R, Bhatt ML, Mohammad S. Oral Cancer: Risk Factors and Molecular Pathogenesis. *Journal of Maxillifacial and Oral Surgery*, 2011; 10 (2): 132-137.

Riccardi C, Nicoletti I. Analysis of apoptosis by propidium iodide staining and flow cytometry. *Nature Protocols*, 2006; 1(3):1458-1461.

Rivera C. Essentials of oral cancer. *International Journal of Clinical and Experimental Pathology*, 2015; 8(9):11884-11894.

Safdari Y, Khalili M, Farajnia S, Asgharzadeh M, Yazdani Y, Sadeghi M. Recent advances in head and neck squamous cell carcinoma — A review. *Clinical Biochemistry*, 2014, 47:1195–1202.

Sakagushi M, Kuroda Y, Hirose M. The Antiproliferative Effect of Lidocaine on Human Tongue Cancer Cells with Inhibition of the Activity of Epidermal Growth factor Receptor. *Anesthesia & Analgesia*, 2006; 102:1103-1107.

Santos K., Laranjo M, Abrantes M, Brito AF, Gonçalves C, Sarmento-Ribeiro AB, Botelho MF, Soares MIL, Oliveira ASR, Pinho e Melo TMVD. Targeting triple-negative breast cancer cells with 6,7-bis(hydroxymethyl)-1*H*,3*H*-pyrrolo[1,2-*c*]thiazoles, *European Journal of Medicinal* Chemistry, 2014; 1:35.

Smith PK, Krohn RI, Hermanson GT, Mallia AK, Gartner FH, Provenzano MD, Fujimoto EK, Goeke NM, Olson BJ, Klenk DC. Measurement of protein using bicinchoninic acid. *Analytical Biochemistry*, 1985; 150(1):76-85.

Snyder GL, Greenberg S. Effect of anaesthetic technique and other perioperative factors on cancer recurrence. *British Journal of Anaesthesia*, 2010; 105(2):106-115.

Thomas GJ, Speight PM. Cell Adhesion Molecules and Oral Cancer. *Critical Reviews in Oral Biology & Medicine*, 2001; 12 (6): 479-498.

Toth M, Fridman R. Assessment of Gelatinases (MMP-2 and MMP-9) by Gelatin Zymography. *Methods in Molecular Medicine*, 2001; 57:1-9.

Tsantoulis PK, Kastrinakis NG, Tourvas AD, Laskaris G, Gorgoulis VG. Advances in the biology of oral cancer. *Oral Oncology*, 2007; 43: 523-534.

Vecchia CL, Tavani A, Franceschi S, Levi F, Corrao G, Negri E. Epidemiology and Prevention of Oral Cancer. *Oral Oncology*, 1997; 33 (5): 302-312.

Werdehausen R, Braun S, Essmann F, Schulze-Osthoff K, Walczak H, Lipfert P, Stevens MF. Lidocaine Induces Apoptosis via the Mitochondrial Pathway Independently of Death Receptor Signaling. *Anesthesiology*, 2007; 107:136-43.

Werdehausen R, Fazeli S, Braun S, Hermanns H, Essmann F, Hollmann, Bauer I, Stevens MF. Apoptosis induction by different local anesthetics in neuroblastoma cell line. *British Journal of Anaesthesia*, 2009; 103(5):711-18.

Wong RSY. Apoptosis in cancer: from pathogenesis to treatment. *Journal of Experimental & Clinical Cancer Research*, 2011; 30: 87-100.

Yao J, Jiang Z, Duan W, Huang J, Zhang L, Hu L, He L, Li F, Xiao Y, Shu B, Liu C. Involvement of Mitochondrial Pathway in Triptolide-Induced Cytotoxicity in Human Normal Liver L-02 Cells. *Biochemical and Pharmaceutical Bulletin*, 2008; 31(4):592-597.

Yeagger MP, Rosenkranz KM. Cancer Recurrence After Surgery – A Role for Regional Anesthesia?. *Regional Anesthesia and Pain Medicine*, 2010; 35(6):483-484.

Xuan W, Hankin J, Zhao H, Yao S, Ma D. The potential benefits of the use of regional anesthesia in cancer patients. *International Journal of Cancer*, 2015: 137:2774-2784.

Ziober BL, Silverman SS, Kramer RH. Adhesive Mechanisms Regulating Invasion and Metastasis in Oral Cancer. *Critical Reviews in Oral Biology & Medicine*, 2001; 12(6):499-510.